

**Blue, Green and Orange-Red Light Emitting Polymers:
Synthesis, Characterization and Prospects of
Applications in Optoelectronic Devices**

Thesis submitted to

Cochin University of Science and Technology

in partial fulfilment of the requirements

for the award of the degree of

DOCTOR OF PHILOSOPHY

in

Polymer Chemistry

Under the Faculty of Technology

By

Vidya G.

Department of Polymer Science and Rubber Technology

Cochin University of Science and Technology

Kochi – 682022, Kerala, INDIA

October 2012

Blue, Green and Orange-Red Light Emitting Polymers: Synthesis, Characterization and Prospects of Applications in Optoelectronic Devices

Submitted by : ***Vidya G.***

Department of Polymer Science and Rubber Technology

Cochin University of Science and Technology

Kochi – 682 022, Kerala, India

vidyagopi5@gmail.com

Research Supervisors

Prof. Rani Joseph

Professor

Department of Polymer Science and Rubber Technology

Cochin University of Science and Technology

Kochi – 682 022

rani@cusat.ac.in

Dr. S. Prathapan

Associate Professor

Department of Applied Chemistry

Cochin University of Science and Technology

Kochi – 682 022

prathapan@cusat.ac.in

Prof. V. P. N. Nampoori

Emeritus Professor

International School of Photonics

Cochin University of Science and Technology

Kochi – 682 022

nampoori@cusat.ac.in

Cover page : Front cover- Synthesized polymer TBPV1, Back cover- RGB color model

Kochi- 682 022
October, 2012

Declaration

I hereby declare that the work presented in this thesis is based on the original research work done by me under the guidance of Prof. Rani Joseph (Department of Polymer Science and Rubber Technology), Dr. S. Prathapan (Department of Applied Chemistry) and Prof. V. P. N. Nampoori (International School of Photonics), Cochin University of Science and Technology, Kochi, India- 682 022, and that it has not been included in any other thesis submitted previously for the award of any other degree/diploma.

Vidya G.

Dedicated to my beloved Ammachi and Achan
==== *Their encouragement and love have been a constant force* ====
of making me move forward.

"Humble yourselves, therefore, under God's mighty hand, that he may lift you up in due time. Cast all your anxiety on him because he cares for you": 1 Peter 5:6-7

Acknowledgement

"All praises to God for the strengths and His warm blessings in completing my Ph.D."

This thesis would not have been possible without encouragement and support from many people including my Guides, my well wishers, my friends and colleagues. It is a pleasurable task to express my gratitude to all those who contributed in many ways to the success of my work.

At this moment first of all I am gratefully thanks to my guide Dr. Rani Joseph for her supervision and constant support. Her immense courage and conviction will always inspire me; during the inevitable ups and downs of my research work she often reminded me life's true priorities by what could be the influence of God Almighty. Equivalently my heartfelt respect to my co-supervisor Dr. S. Prathapan, he opened the window to the world of light emitting polymers for me. I am very greatly thankful to him for picking me up as a student at the critical stage of my Ph.D and providing me all the facilities at organic lab for the successful completion of my research work. I express my deep sense of gratitude for all the constructive criticism, encouragement, his valuable advice, his extensive discussions around my work and constant support he rendered to me.

I am also extremely indebted to my co-supervisor Dr. V. P. N. Nampoori for his advice, support and help. I take this opportunity to sincerely acknowledge Dr. Jayalakshmi, Professor, Department of Physics, for her timely support, valuable suggestions, encouragement and providing the necessary facilities in the Department. I am also grateful to my research committee member, Dr. Philip Kurian, Department of PS & RT.

I would like to also thank Dr. Sunil K. Narayanankutty, Head, Department of PS&RT, Prof. K. E. George, Dr. Thomas Kurian, Dr. Eby Thomas Tachil and Ms. Jayalatha for their support during my research. I would also like to extend warm thanks to office staff and technical staff of PS & RT for their co-operation.

I take this opportunity to sincerely acknowledge University Grand Commission (UGC), for providing financial assistance in the form of Senior Research Fellowship which support me to perform my work comfortably.

My special thanks to Dr. Gopi Das (NIIST, TVM) for providing me permission to carry out cyclic voltammetry analysis in his lab. I would also thank Mr. Tony (NIIST) for his support.

I would like to express my sincere thank to Mr. Sreekanth J. Varma, Department of Physics, for his huge support and caring. Thank you for sharing your experiences and opinions with me.

I am gratefully acknowledged Sophisticated Test and Instrumentation Centre, Cochin for all spectral analysis. I would like to thank Mr. Saji (STIC, CUSAT) for his constant support during my NMR analysis. I would also thank Ms. Sreelekha. G (ISP) for giving me experimental part of LASER. I would also extend my gratitude to Mr. Kashbir (CUSAT) for experimental facility.

My special appreciation goes to organic lab (DAC) friends, Jomon, Sajitha, Sandhya, Reshma, Eason, Rakesh, Nithya, Soumya and Liji for their encouragement and moral support during my study. Thanks for the friendship and memories. I am much indebted to Dr Mahesh Kumar for his valuable suggestions in my work.

I am also thankful to Sobha teacher and Denny teacher for their constant support and encouragement. I would thanks to all FIP teachers Jabin teacher, Preetha teacher, Zeena teacher, Jessy teacher, pramila teacher, Jolly sir, Newly teacher, Juli teacher and Jasmine teacher. My special thanks goes to my roommate Asha Krishnan and my friends Misha Hari, Reni George and Saisy K, Esthappan. My special thanks to Anand and Sajimol teacher (Dept of Physics) for their support. My special thanks goes to my new friends Vineesh, Shaji chettan, Babitha and Theresa (VAST)

I would also like to thank some people from early days of my research, Dr. Anna Dilli, Mercy Anna Philip, Dr. Leny Mathew, Dr. Saritha, Dr Elizabeth, Dr. Vijayalakshmi, Dr. Dhanya, Neena George, Murali, Jenish and Elizabeth were among those who kept me going at the beginning. I am indebted to Dr. Suma.K.K and Dr. Sinto, for their valuable help and constant support. My special thanks to my PS&RT friends Sona, Ajilesh, Reshmi, Aiswarya, Vidya, Sreejesh, Nisha, Renju, Shadiya, Teena and all juniors. I wish to thank Bipin Sir and Abhilash chettan for their advice.

It's my pleasure to gratefully acknowledge the support of some special individuals. Words fail me to express my appreciation to Madhu Sir (Scientist, RRI) for his constant support, prayers and motivation. I convey my thanks to Dr Nimmi Sarath for her fruitful friendship and support. I would like to thank Dr Tintu R for her huge support and lovely friendship. I convey my deepest thanks to Cimi. A. Daniel, she is always beside me during the happy and hard moments.

Last but not least, I would like to pay high regards to my Ammachi and Achan and my sister Vrinda for their sincere inspiration and prayers throughout my research work and lifting me uphill this phase of life.

Vidya G.

Preface

Light emitting polymers (LEPs) are considered as the second generation of conducting polymers. A Prototype LEP device based on electroluminescence emission of poly(*p*-phenylenevinylene) (PPV) was first assembled in 1990. LEPs have progressed tremendously over the past 20 years. The development of new LEP derivatives are important because polymer light emitting diodes (PLEDs) can be used for the manufacture of next-generation displays and other optoelectronic applications such as lasers, photovoltaic cells and sensors. Under this circumstance, it is important to understand thermal, structural, morphological, electrochemical and photophysical characteristics of luminescent polymers. Our goal was to synthesize a series of light emitting polymers that can emit three primary colors (RGB) with high efficiency.

Three major objectives of the present study are listed hereunder:

- To synthesis and characterize blue, green, orange-red light emitting polymers
- To study structural and physical properties of synthesized polymers
- To explore the suitability of these polymers in the field of optoelectronic devices

The thesis is divided into **six chapters**.

A concise introduction to the subject is presented in the **first chapter**. Chapter begins with a short review on conducting polymers, followed by a review on light emitting polymers. After the introductory section, different synthetic techniques used for the preparation of light emitting polymers such as poly(phenylenevinylene)s and poly(thiophene)s are explained. It includes brief

notes on fully-conjugated PPV derivatives, segmented block PPV copolymers and light emitting hybrid polymers. Optoelectronic applications of light emitting polymers with special emphasis on organic semiconductor lasers (polymer laser) and PLEDS (polymer based light emitting diodes) are also included in this chapter. This chapter concludes with identification and outline of scope and objectives of the research problem selected by us.

Chapter 2 is focussed on the synthesis, characterization and photophysical studies of low polydispersity index orange-red light emitting MEH-PPV. MEH-PPV was purified by using sequential extraction method. Fluorescent quantum yield of the purified MEH-PPV in different organic solvents is discussed in this chapter. Preliminary LASER emission studies (ASE studies) in tetrahydrofuran (THF) solvent using Nd:YAG laser (532 nm, 10 Hz) is also presented.

Substituent effects on two new segmented PPV block copolymers are presented in **Chapter 3**. Two new well defined segmented block copolymers consisting of substituted distyrylbenzene (DSB) block containing bulky side groups with different kind of steric characteristics were synthesized in good yields. Copolymers were synthesized by Horner-Emmons condensation polymerization reaction and purified by using sequential extraction method. Structure of the synthesized copolymers was confirmed by elemental analysis (CHN), ^1H NMR, ^{13}C NMR and FT-IR spectroscopy. Molecular mass of the copolymers was determined by gel permeation chromatography (GPC). Glass transition temperature, thermal transitions and thermal stability were studied using DSC and TGA analysis. The lowest unoccupied molecular orbital (LUMO) and highest occupied molecular orbital (HOMO) of the copolymers were evaluated by using cyclic voltammetry. XRD studies disclose the structural characteristics of both copolymers. Photophysical properties such as UV-Vis absorption and photoluminescence characteristics are included

herein. Surface smoothness of spin coated films of the newly synthesized polymers was analyzed by using AFM. Current-voltage measurements (I-V characteristics) and their corresponding band structure diagrams are also presented.

Chapter 4 deals with the synthesis and characterization of a new blue light emitting bulky ring substituted segmented PPV block copolymer. Copolymer was synthesized by Horner-Emmons condensation polymerization reaction and purified by using sequential extraction method. Structure of the synthesized copolymer was confirmed by elemental analysis (CHN), ^1H NMR, ^{13}C NMR and FT-IR spectroscopy. Molecular weight of the copolymer was determined by gel permeation chromatography (GPC). Thermal behaviour of the copolymer was studied by using DSC and TGA analysis. Electrochemical behaviour of the copolymer was investigated by cyclic voltammetry analysis. Optical studies were done by using UV-Vis spectra and photoluminescence spectra. Semi crystalline nature of the copolymer was revealed by using XRD. Surface smoothness of the spin coated film was analyzed by AFM. Schottkey diode characteristics were determined by using current- voltage measurements and its energy band diagram also presented.

Chapter 5 deals with the synthesis and characterization of novel intense green light emitting thienylene- biphenylenevinylene hybrid polymers. Polymers were synthesized by Stille coupling polymerization reaction and purified by using sequential extraction method. Structure of the freshly synthesized polymers was confirmed by elemental analysis (CHN), ^1H NMR, ^{13}C NMR and FTIR spectroscopy. Molecular weight of the polymers was determined by gel permeation chromatography (GPC). Thermal properties of the polymers were investigated by thermogravimetric analysis (TGA) and differential scanning calorimetry (DSC). Electrochemical properties of the polymers were studied by using cyclic voltammetry. Structural and morphological studies were done by

using XRD and SEM techniques. UV-Vis absorption spectra and PL spectra provide information on the electronic structures of these new polymers. Surface smoothness of the spin coated film was analyzed by using AFM. Schottky diode formation has been confirmed from the I-V characteristics of the two polymers synthesized. The corresponding band structure diagrams have also been presented.

Important findings drawn from our investigations are presented in **Chapter 6**. Conclusions and references are given towards the end of each chapter.

Contents

Chapter 1 Introduction to Semi-Conducting Light Emitting Polymers for Optoelectronic Applications.....	1
1.1 Conducting Polymers.....	1
1.2 Light Emitting Polymers (LEP's) - The Second Generation Conducting Polymers.....	5
1.2.1 Chemistry Behind Light Emitting Polymers.....	8
1.2.2 Chemical Structures of Light Emitting Polymers.....	11
1.3 Chemical Synthesis of Light Emitting Polymers.....	15
1.3.1 Soluble Precursor Route.....	15
1.3.2 Dehydrohalogenation reactions.....	16
1.3.2.1 Glich Polymerization Route.....	17
1.3.3 Transition Metal-Catalyzed Coupling Polymerizations.....	17
1.3.3.1 The Heck Reaction.....	18
1.3.3.2 Stille Coupling Reaction.....	18
1.3.3.3. Kumada Coupling.....	19
1.3.3.4 McCullough Method.....	20
1.3.3.5 Reike Ni - Catalyzed Polymerization.....	21
1.3.3.6 Suzuki Coupling Reaction.....	21
1.3.4 Condensation Polymerizations.....	22
1.3.4.1 Wittig Reaction.....	22
1.3.4.2 Horner-Emmons Condensation.....	23
1.3.4.3 Knoevenagel Coupling Route.....	23
1.4 Fully-Conjugated PPV Derivatives.....	24
1.5 Segmented Block PPV Copolymers.....	27
1.6 Light Emitting Hybrid Polymers.....	29
1.7 Light Emitting Polymers for Optoelectronic Applications.....	31
1.7.1 Organic Semiconducting Lasers (Polymer Lasers).....	31
1.7.2 Semi Conducting Polymer Light Emitting Diodes.....	33
1.8 Aim and Scope of the Thesis.....	35
1.9 References.....	36

Chapter 2 Orange-Red Light Emitting MEH-PPV with Narrow MWD: Synthesis, Characterization and Photophysical studies	43
2.1 Introduction and Motivation	43
2.2 Results and Discussion	45
2.2.1 Monomer and Polymer Synthesis	45
2.2.2 Thermal Analysis	48
2.2.3 X-ray diffraction data (XRD)	49
2.2.4. Photophysical studies	50
2.2.4.1 Absorption and fluorescence studies	50
2.2.4.2 Fluorescence Quantum Yield Studies of MEH-PPV in Different Organic Solvents	51
2.2.4.3 Amplified spontaneous emission (ASE)	53
2.3. Conclusions	56
2.4 Experimental Section	57
2.4.1 General Techniques	57
2.4.2 Experimental procedure for Amplified Spontaneous Emission (ASE)	58
2.4.3 Materials	58
2.4.4 Synthesis of monomer and polymer	58
2.4.4.1 Synthesis of 1-Methoxy-4-(2-ethylhexyloxy) benzene (1)	58
2.4.4.2 Synthesis of 1,4-bis(bromomethyl)-2-(2'-ethylhexyloxy)-5-methoxy benzene (2)	59
2.4.4.3 Synthesis of Poly[2-methoxy-5-(2'-ethyl-hexyloxy)-1,4-phenylenevinylene] {MEH-PPV}	60
2.5 References	60
Chapter 3 Substituent Effects on Light-Emitting Segmented Block PPV Copolymers: Synthesis, Characterization and Photophysical Studies	63
3.1 Introduction and Motivation	63
3.2 Results and Discussion	66
3.2.1 Synthesis of Monomers	66
3.2.2 Synthesis of Copolymers	67
3.2.3 Thermal Analysis of Segmented Block Copolymers	73

Chapter 4 Synthesis and Characterization of a New Intense Blue-Light Emitting Ring Substituted Segmented PPV Block Copolymer	97
4.1 Introduction and Motivation	97
4.2 Results and Discussion	100
4.2.1 Monomer and Polymer Synthesis	100
4.2.2 Thermal Analysis	105
4.2.3 X-ray diffraction Analysis (XRD).....	106
4.2.4 Scanning electron microscopy (SEM)	107
4.2.5. Photophysical studies.....	107
4.2.6. Electrochemical studies	109
4.2.7. Measurement of I-V characteristics.....	111
4.3 Conclusions	112
4.4 Experimental Section.....	113
4.4.1 Materials and Instruments	113
4.4.2 Synthesis of Monomers	114
4.4.2.1. 1,6-Bis(4-formyl-2,6-dimethoxyphenoxy)hexane (3).....	114
4.4.3 Synthesis of Polymer.....	114
4.4.3.1 Synthesis of Poly[1,6-hexanedioxy-(2,6-dimethoxy-1,4-phenylene)-1,2-ethenylene-(2,5-dicyclohexylmethoxy-1,4-phenylene)-1,2-ethenylene-(3,5-dimethoxy-1,4-phenylene)] (P3).....	114
4.5 References	115

Chapter 5 Two Novel Intense Green Light Emitting Thienylene-Biphenylenevinylene Hybrid Polymers: Synthesis, Characterization and Photophysical Studies.....	117
5.1 Introduction and Motivation	117
5.2 Results and Discussion	121
5.2.1 Monomer Synthesis	121
5.2.2 Polymer Synthesis.....	124
5.2.3 Thermal Properties.....	128
5.2.4 X-ray diffraction analysis (XRD).....	130

5.2.5 Scanning electron microscopy (SEM)	130
5.2.6 Photophysical studies.....	131
5.2.6.1 Absorption and photoluminescence (PL) studies of monomers.....	131
5.2.6.2 Absorption and photoluminescence (PL) studies of polymers.....	132
5.2.6.3 Fluorescence quantum yield of polymers	134
5.2.7 Electrochemical studies	135
5.2.8 Measurement of Schottky diode characteristics	137
5.3 Conclusions	140
5.4 Experimental Section.....	141
5.4.1 General Techniques	141
5.4.2 Materials	142
5.4.3 Synthesis of monomers M1 and M2.....	142
5.4.3.1: Synthesis of 4,4'-Dioctyloxy -1,1'-biphenyl (1a).....	142
5.4.3.2: Synthesis of 2,2'-Dioctyloxy-1,1'-biphenyl (2a).....	143
5.4.3.3: Synthesis of 3,3'-bis(bromomethyl)-4,4'-di(octyloxy)-1,1'- biphenyl (1b).....	143
5.4.3.4: Synthesis of 5,5'-bis(bromomethyl)-2,2'-di(octyloxy)-1,1'- biphenyl (2b).....	144
5.4.3.5: Synthesis of 3,3'-bis(diethylphosphonate)-4,4'(dioctyloxy)- 1,1'-biphenyl (1c).....	144
5.4.3.6: Synthesis of 5,5'-bis(diethyl phosphonate)-2,2'- (dioctyloxy)-1,1'-biphenyl (2c).....	145
5.4.3.7: Synthesis of monomer 5,5'-(1E,1'E)-2,2'-(4,4'- bis(octyloxy)biphenyl-3,3'-diyl)bis(ethene- 2,1- diyl)bis(2-bromothiophene) (M1)	145
5.4.3.8: Synthesis of monomer 5,5'-(1E,1'E)-2,2'-(6,6'- bis(octyloxy)biphenyl-3,3'-diyl)bis(ethane-2,1-diyl)bis(2- bromothiophene)(M2).....	146
5.4.4 Synthesis of polymers Using Stille Coupling Reaction.....	147
5.4.4.1 Synthesis of polymer TBPV1	147
5.4.4.2 Synthesis of polymer TBPV2.....	148

5.5 References	149
Chapter 6 Summary and Conclusion	153
Publications	157

List of Abbreviations

ASE	:	Amplified Spontaneous Emission
AFM	:	Atomic Force Microscopy
CB	:	Conduction Band
CRTs	:	Cathode Ray Tube
CDT	:	Cambridge Display Technology
DMF	:	Dimethylformamide
DSC	:	Differential Scanning Calorimetry
DTA	:	Differential Thermal Analysis
E_g	:	Band Gap
EA	:	Electron Affinity
EL	:	Electroluminescence
Φ_F	:	Fluorescence Quantum Yield
GRIM	:	Grignard Metathesis Polymerization
GPC	:	Gel permeation Chromatography
HOMO	:	Highest Occupied Molecular Orbitals
I-V curve	:	Current-Voltage curve
ITO	:	Indium-Tin oxide
IP	:	Ionization Potential
K ^t OBu	:	Pottassium tert- butoxide
LASER	:	Light Amplification by Stimulated Emission of Radiation
LCDs	:	Liquid Crystal Displays
LDA	:	Lithium Diisopropylamine
LUMO	:	Lowest Unoccupied Molecular Orbitals
LEP	:	Light emitting polymer
MEH-PPV	:	Poly[2-methoxy-5-(2'-ethyl-hexyloxy)-1,4-phenylenevinylene]
Ni	:	Nickel
Ni(dppp)Br ₂	:	[1,3-Bis(diphenylphosphino)propane]dibromonickel(II)

Ni(dppp)Cl ₂	:	[1,3-Bis(diphenylphosphino)propane]dichloronickel(II)
NMR	:	Nuclear magnetic resonance
OLED	:	Organic light emitting diode
Pd	:	Palladium
PPV	:	Poly(phenylenevinylene)
PT	:	Polythiophene
PPP	:	Poly(μ -phenylene)
PPS	:	Poly(μ -phenylene sulphide)
PFU	:	Polyfuran
PF	:	Polyflourene
PPy	:	Polypyrrole
PLED	:	Polymer light emitting diode
PL	:	Photoluminescence
PATs	:	Poly(3-alkylthiophene)s
PPE	:	Poly(phenyleneethynylene)
PDI	:	Polydispersity index
RGB	:	Red, Blue, Green
SBC	:	Segmented Block Copolymer
SEM	:	Scanning electron microscopy
TGA	:	Thermal Gravimetric Analyzer
THF	:	Tetrahydrofuran
UV-Vis	:	Ultraviolet – Visible
VB	:	Valence band
XRD	:	X-Ray Powder Diffractometer

Chapter 1

Introduction to Semi-Conducting Light Emitting Polymers for Optoelectronic Applications

Contents

- 1.1 Conducting Polymers
- 1.2 Light Emitting Polymers (LEP's) - The Second Generation Conducting Polymers
- 1.3 Chemical Synthesis of Light Emitting Polymers
- 1.4 Fully-Conjugated PPV Derivatives
- 1.5 Segmented Block PPV Copolymers
- 1.6 Light Emitting Hybrid Polymers
- 1.7 Light Emitting Polymers for Optoelectronic Applications
- 1.8 Aim and Scope of the Thesis
- 1.9 References

1.1 Conducting Polymers

Traditionally, polymers have been considered as insulators of electricity. Polymeric materials find widespread application as passive dielectrics. 40 years ago nobody would have guessed that polymers could conduct electricity as efficiently as metals. But now such feats have been achieved. Metal-like conductivity in polyacetylene doped with various electron donors or electron acceptors was discovered in 1977 by Alan J Heeger, Alan MacDiarmid and Hideki Shirakawa.¹ They were awarded Nobel Prize in Chemistry in 2000 for the ground-breaking discovery of electrically conducting polymers. These materials combine the electrical properties of metals together with the advantages of polymers such as light weight, corrosion resistance, greater workability, resistance to chemical attack, lower cost etc. Conducting polymers have enriched our day to day life with a wide range of products. Their applications extend from most common consumer goods to highly specialized electronic components, non-linear optics, aeronautics etc. Therefore, no wonder these electrically conducting polymers are known as “materials of the twenty-first century”. The invention of highly conducting polyacetylene led to a rapid spurt in research activity directed towards the study of novel conducting polymeric materials. At present many novel

conducting polymer systems are known, and these include polyaniline (PANI), polypyrrole (PPy), polyphenylenevinylene (PPV), polythiophene (PT), Poly(*p*-phenylene) (PPP), Poly(*p*-phenylenesulphide) (PPS), polyfuran (PFU), polyfluorene (PF) etc. These conducting polymers share many structural features such as a conjugated backbone, planarity and large anisotropy ratio i.e. the intrachain conductivity is much larger than the interchain conductivity. Also, the conductivity of the polymers depend upon doping percent, alignment of polymer chains, conjugation length and purity of the sample. Figure 1.1 illustrates some examples of conducting polymers.

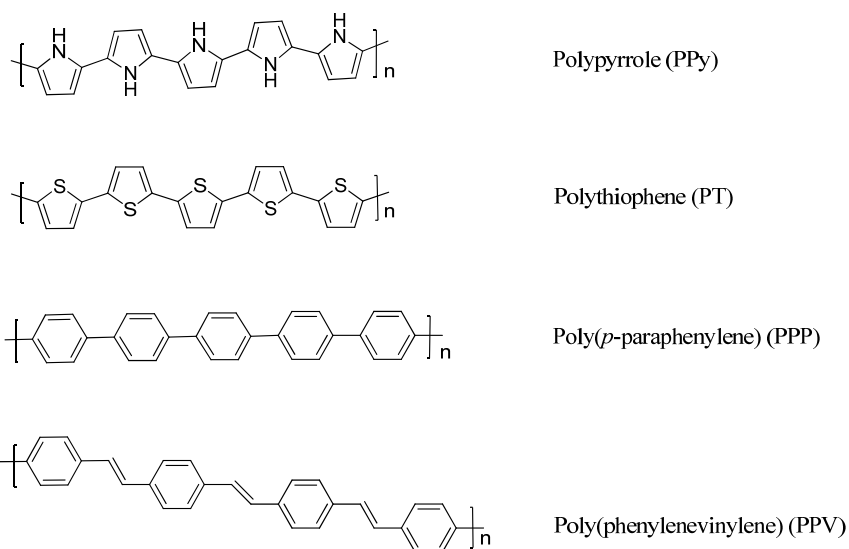


Figure 1.1 Structures of some popular conducting polymers

The conjugated structure with alternating single and double bonds or conjugated segments coupled with atoms providing *p*-orbitals for a continuous orbital overlap (e.g. N, S) seem to be necessary for polymers to become electrically conductive. Therefore the semiconducting property is obtained from π -delocalization of single $2p_z$ valence electrons at each carbon atom along the polymer chain. The electron is accessible as only three sp^2 electrons are required for bonding through σ -orbitals and each $2p_z$ electron overlaps outside the skeleton of the macromolecule to give a delocalized π -band.² The electronic structure of the conducting polymers depend on the energy levels of the constituent repeating

units. The molecular orbitals in which π and π^* are distributed in the highest occupied molecular orbitals (HOMO) and lowest unoccupied molecular orbitals (LUMO), otherwise termed bonding (VB-the highest filled band) and antibonding (CB-the lowest empty or partially occupied) states respectively as shown in Figure 1.2. Energy levels of these HOMO- LUMO bands are also dependent on the length of the conjugated segment.³ Each unit carries a HOMO and LUMO, and they are brought together by extending the chain and collectively combine to form the VB and CB, respectively. These linear combinations results not only in the formation of bands but also in an alternating structure of single and double bond. This effect is called as Peierls effect that stabilizes the chain but also the full valence band is separated from the upper empty conduction band by a distinct amount of energy.² This energy gap determines the conductivity of the polymers; therefore the electrons should overcome this barrier to move. The energy gap is usually called the band gap (E_g) and can be large or small, essentially depending on the structure of the polymer.⁴

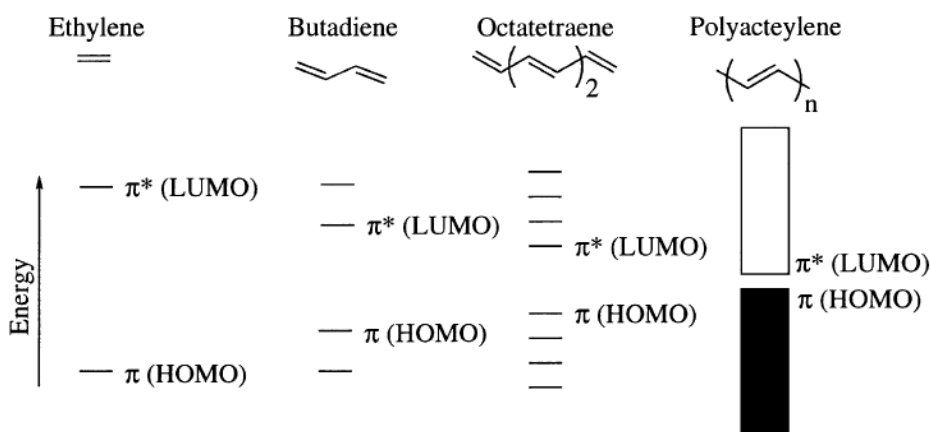


Figure 1.2 Molecular orbital diagram (π -levels) with the number of monomer units.
(Adapted from Ref. 3)

The energy band gap (E_g) of conducting polymers are generally of the order of 0.8eV to 4.0eV and it is particularly correlated with the energy of visible light enabling electrons to interact with light and this property is exploited in many

optoelectronic applications.⁵ In the case of insulators their band structure is similar to that of semiconductors but their energy gap is much greater than 4eV leading to inefficient electron transfer between bands. Polyacetylene has two mesomeric structures that are energetically equal, and the system is called degenerate state. Majority of conjugated polymers consist of their mesomeric structures that are energetically unequal, so these energy levels are termed non-degenerate.³ Conductivity of conducting polymers is enhanced by doping, that effectively results in a material that combine the high conductivities of metals with good mechanical properties associated with polymers. Doping is based on a charge transfer redox reaction of electron-withdrawing (*p*-type doping) or electron-donating (*n*-type doping) impurities with the polymer.⁶ Doping is generally achieved by chemical or electrochemical means. Conducting polymers do not easily undergo controllable and reversible doping. Doping introduces charges into the polymeric chain that locally modifies the alternation of single and double bonds giving rise to localized electronic states with electrons and holes in the forbidden gap. Quasi-particles such as solitons and polarons are formed depending on whether or not the ground state of the polymer is degenerate.⁷ During doping of the system, soliton is present at a degenerate ground state and it shows charge $q = \pm e$ and exhibit zero spin, whereas for a neutral soliton $q = 0$ and spin $S = \frac{1}{2}$. Polarons and bipolarons are positive or negative charges connected with a local deformation of a polymer chain that is changing from one form to another. Polarons are totally different from solitons i.e. polarons are present in non-degenerate state as they are simultaneously charge ($q = \pm e$) and spin carriers ($S = \frac{1}{2}$). The hopping of polarons along or between the polymer chains contributes to the bulk electronic transport of the material. Thus the addition and removal of an electron to the existing polarons forms a new charge carrier known as bipolaron and it consist of zero spin.⁸

Optical properties of conducting polymers are controlled by fundamental electronic structure of the material. Therefore specific electronic properties of conducting polymers are obtained by proper molecular designing. Almost all

conducting polymers are insoluble in common organic solvents. This limitation has detrimental effect on the processability of these polymers. To overcome these shortcomings, long flexible alkyl or alkoxy side chains are attached onto the polymeric backbone.⁹ Versatility of organic chemistry offers a wide variety of appropriate reactions for facile access to target compounds optimized for smart materials with fine-tuned electro-optical properties. Thanks to their low cost, high processability, flexibility etc. Conducting polymers are very attractive when compared to their inorganic counterparts.

This introduction will not attempt to give a wide-ranging review of conducting polymers since many review articles have appeared in the literature.^{10,11} Herein, the primary focus is on the synthesis and development of light emitting polymers, called the second generation of conducting polymers. The introduction begins with a brief note on conducting polymers followed by short review on light emitting polymers. After that we shall highlight different synthetic techniques used for the preparation of light emitting polymers with special emphasis on poly(phenylenevinylene)s and poly(thiophene)s. We have also included a brief discussion on fully-conjugated PPV derivatives, segmented block PPV copolymers and light emitting hybrid polymer. Finally, we shall discuss light emitting polymers for optoelectronic applications such as organic semiconductor Lasers (Polymer Laser) and PLEDS (polymer based light emitting diodes).

1.2 Light Emitting Polymers (LEP's) - The Second Generation Conducting Polymers

Light emitting polymers (LEPs) constitute a unique class of conjugated organic compounds that exhibit semiconducting behaviour and emit light when electrically stimulated or by long wave ultraviolet irradiation. Consequently, they exhibit electroluminescent as well as photoluminescent characteristics. Development of advanced materials with simultaneous control over optical, electrical, and mechanical properties is essential for advancement of technology

for display and lighting industries based on novel concepts such as “plastic light” and “plastic electronics”.¹² This new technology offers many opportunities in modern electronic fields and it is likely to replace the conventional devices due to its various advantages. Special properties of light emitting polymers that make them potential candidates for application in light emitting devices include large non-linear optical range, amenable electronic structure, optimal energy band gap, color quality, ultrafast optical responses, viable life time at lower cost, less environment impact than traditional incandescent lamps, excellent processing advantages along with architectural flexibility and finally attractive mechanical properties of polymers.¹²

The historic development of electroluminescence started with the invention of light emission from organic molecules on the application of an electric field.¹³ In the early 1960s, scientists at Dow Chemical Company observed light emission from organic semiconductors. This was first reported for anthracene single crystals. The process of electroluminescence arises out of injection of electrons from one electrode and holes from the other electrode, followed by capture of oppositely charged charge carriers called as recombination. Finally the radiative decay of the excited electron-hole state (exciton) produced by recombination process results in electroluminescence. Tang and co-workers established an efficient electroluminescent in two-layer sublimed organic thin film devices.¹³ But making an organic light emitting diode (OLED) was not possible because these materials have very poor conductivity and required high operating voltage. Therefore the actual fabrication of an OLED device had to wait until the discovery of electroluminescence from light emitting conducting polymers. Shortly afterwards, in 1990 the Cambridge group under the leadership of Richard Friend observed green-yellow electroluminescence, when poly(*p*-phenylenevinylene) (PPV) prepared from solution processable precursor method was used as an active layer in LEDs.¹⁴ They reported that, the ease of fabrication, the combination of excellent structural properties, light emission in green-yellow

part of the emission spectrum and high efficiency suggest that this polymer can be used as a potential emissive layer in optoelectronic devices.

PPV was first synthesized by Wessling at Dow Chemicals in 1968 and has a π - π^* electronic energy gap at about 2.5 eV.¹⁵ Unsubstituted PPV is insoluble in common organic solvents; therefore it requires special processing steps to produce a conjugated thin film for emissive device applications. A soluble precursor polymer was first prepared, and then a film was prepared from its solution by spin casting which was thermally converted to the conjugated form in the final stage. In 1992, Cambridge Display Technology (CDT) received a key patent on light emission from conjugated polymers.¹⁵ Heeger and co-workers in 1991, at the University of California at Santa Barbara announced the electroluminescence in soluble derivative of PPV, namely poly[2-methoxy-5-(2'-ethylhexyloxy)-1,4-phenylenevinylene] (MEH-PPV).¹⁶ Dialkoxy substituent group in MEH-PPV offered good solution processability and its electronic band gap was 2.2 eV, which is red-shifted from that of PPV. Research groups from University of California at Santa Barbara and DuPont formulated optimal process manufacturing guidelines for the commercialization of PLED-based devices. The progress in the performance of PLED devices has been very impressive and several processable light emitting polymers have been introduced during the last 20 years. Figure 1.3 shows some examples of light emitting polymers based on PPV and polythiophene (PT) and their derivatives.

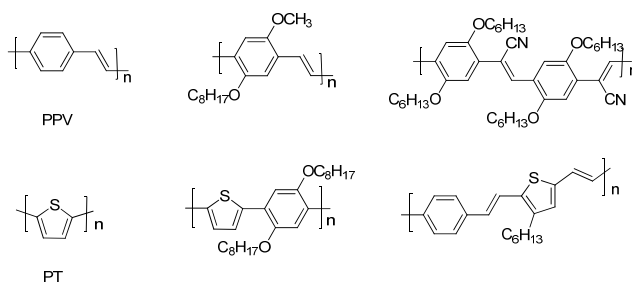


Figure 1.3 Examples of light emitting polymers based on PPV and Polythiophene (PT) and their derivatives

1.2.1 Chemistry Behind Light Emitting Polymers

Light emitting polymers are conducting polymers with π - molecular orbitals delocalized along the polymer chain, so the electronic charge transport differs from inorganic semiconductors. Light emitting polymers which emit light, when a voltage is applied to it; the property is called electroluminescence (EL). The band gap of the light emitting polymer determines wavelength region (color) of the emitted light. Polythiophenes, PPV and its derivatives, polyfluorenes, polyphenylenes, polypyridines and their copolymers are the most commonly used light emitting polymers. Worldwide research efforts about LEP's are on to enhance the lifetime, stability, improve efficiency of LEP device through modifying their configuration etc. In recent years, study of EL polymers is becoming an active research field, because whether the nature of initial photoexcitation is band-like (free carriers) as in semiconductors or excitonic as in molecular solids remains an open question. This has led to detailed study of the excited states and emission characteristics of emissive polymers. The amorphous and slight crystalline nature of polymer chain morphology results in inhomogeneous broadening present in the energies of the chain segments, consequently hopping type transport. And another effect is the distortion of the chain around charge carriers; therefore the charged excitations are usually described as polarons in emitting polymers.¹⁷

Besides the condition to be conducting polymers, additional requirements must be fulfilled for light emitting polymers.^{17,18} These include

- 1) σ bonds are stronger than π -bonds even when there are excited states in the π^* bonds.
- 2) π orbitals present on the adjoining polymer molecules should overlap with each other enabling three dimensional movement for electrons and holes between molecules
- 3) permit electrons and holes capture each other to form excitons
- 4) permit the excitons to emit photons

In order to understand the mechanism of light emission, it is instructive to start with the process behind photoluminescence. The absorption of emissive polymers are attributed to electronic excitation from π - π^* transition states and π^* - π for emission. Upon electronic excitation of a molecule, a number of photophysical processes has been occurred are shown in figure 1.4.

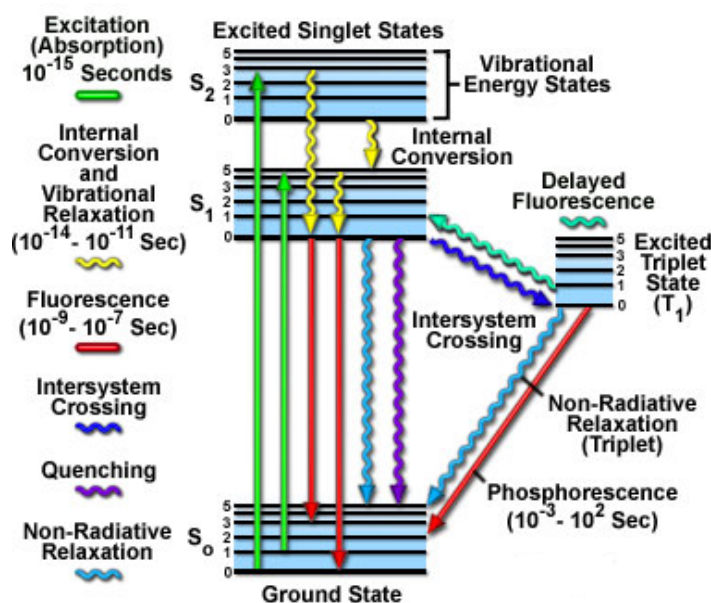


Figure. 1.4 The relationship between absorption, emission and non-radiative vibrational transition processes (general Jablonski energy diagram).

When a molecule is irradiated by light of appropriate wavelength, excitation of an electron from the highest occupied orbital state (S_0) to the lowest unoccupied orbital state generates an excited state (S_1) which can release the absorbed energy in the following ways,

- 1) Non-radiative transitions, such as internal conversion and intersystem crossing
- 2) Emission of radiation (fluorescence and phosphorescence)

Fluorescence is observed after singlet relaxation from the first excited state. If intersystem crossing occurred, a triplet excited state is generated whose

relaxation will result in phosphorescence. If emission does not occur a non-radiative pathway is produced. It is very exceptional when an organic compound emits all of its absorbed energy as back. Most commonly, when organic molecules emit light of lower energy than of light originally absorbed. The difference between absorption and emission maxima of the molecule is called Stokes shift and it occurs when emission from the lowest vibrational level of the excited state relaxes to various vibrational levels of the ground state. Fluorescence efficiency of a light emitting polymer is characterized by its fluorescence quantum yield (Φ_F).¹⁹ Fluorescence quantum yield is the ratio of photons emitted through fluorescence to photons absorbed.

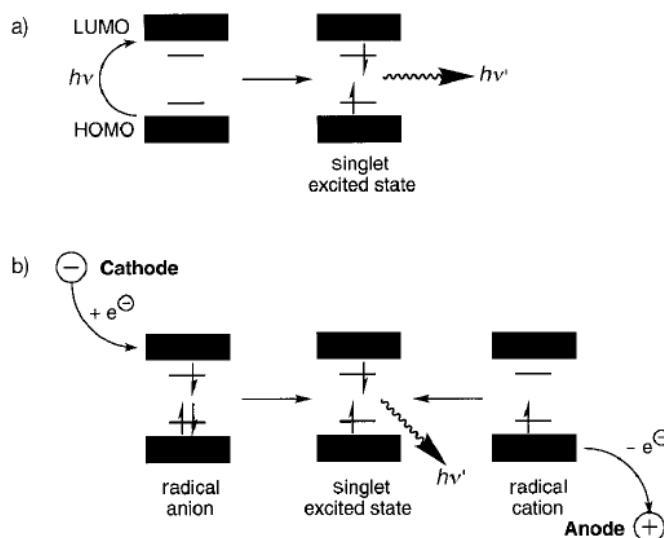


Figure 1.5 Illustration of photoluminescence and electroluminescence in light emitting polymers (adapted from ref: 20)

Figure 1.5 displays the similarities between photoluminescence and electroluminescence in light emitting polymers suggesting that same emitting species is involved in both cases. But the mechanism of formation of emission is much more complicated in electroluminescence. Irradiation of a light emitting polymer excites an electron from HOMO to LUMO, two new energy states are generated upon relaxation within the original HOMO-LUMO energy gap and are each filled with one electron of opposite spin (singlet excited state). The excited

state species then relax to the ground state with emission of light at a longer wavelength than that absorbed (photoluminescence). In a PLED device, electrons are injected into the LUMO (to form radical anions) and holes into the HOMO (to form radical cations) of the electroluminescent polymer. The resulting oppositely charged species move about from one polymer chain to another polymer chain under the influence of the applied electric field. When a radical anion and a radical cation combine on a single conjugated segment, singlet and triplet excited state are formed which can radiatively decay with the emission of visible light. The emission spectra of LEPs are very broad because of the presence of vibronic sublevels and structural inhomogeneity.²⁰ The close relationship between photoluminescence and electroluminescence suggest materials exhibiting high photoluminescence quantum efficiency will also exhibit high electroluminescence efficiency. Quantum efficiency of photoluminescence is defined as (number of photons emitted/number of photons absorbed) \times 100%. On the otherhand, efficiency of electroluminescence is defined as [number of photons emitted/number of charge (both holes and electrons) injected] \times 100%.²⁰

1.2.2 Chemical Structures of Light Emitting Polymers

In principle, several polymers such as polyacetylene and polypyrrole can act as LEPs. One of the major constraints for fabricating devices based on LEPs is their lack of processability. Unsubstituted polymers are infusible and insoluble due to presence of rigid backbone and strong intermolecular force of attraction between the chains. Mainly two synthetic methods are used for developing conducting polymers *viz* electrochemical polymerization and chemical polymerization method. Electrochemical polymerization¹⁰ produce a polymer film in very low yield. One of the advantage of this method is avoiding polymer isolation and purification. This method does not always produce materials with well defined structures. Therefore different types of chemical polymerization methods are routinely employed. Several strategies are included for the synthesis of light emitting polymers; they are highlighted in the next section. Light emitting

materials are mainly classified into four groups,²¹ these are schematically represented in Figure 1.6.

- 1) Conjugated polymeric systems
- 2) Main chain polymers with isolated chromophores
- 3) Side chain polymers with linked chromophores
- 4) Low molecular weight electroluminescence active compounds.

Luminescent behaviour of LEPs depends on three main factors *viz* nature of carbon skeleton, organization of building blocks present on the chains and the type and positions of the substituent groups present in the polymer backbone.

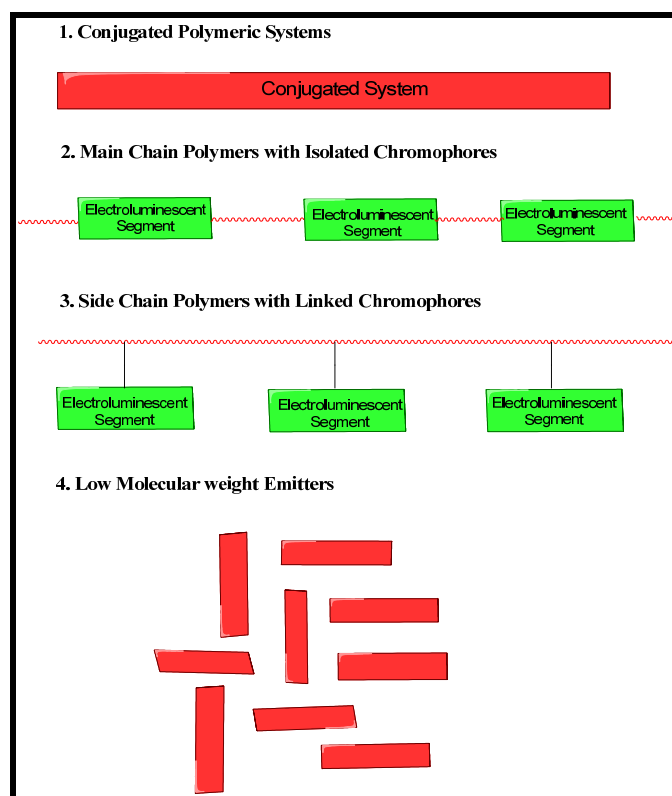
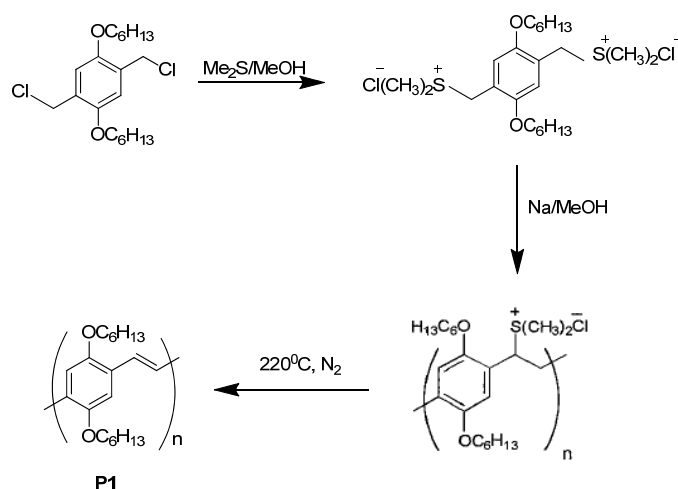


Figure 1.6 Concepts of light emitting polymers. (adapted from ref:21)

The substituent groups present in the conjugated system plays an important role on luminescence properties. In other words, substituents with improved π -

electron mobility will lead to good fluorescence efficiency and also the combination of electron donating substituent groups such as $-\text{NH}_2$, $-\text{OCH}_3$ and $-\text{OH}$, and electron withdrawing substituents such as $>\text{C}=\text{O}$, $-\text{CN}$, $-\text{SO}_3\text{H}$, $-\text{COOH}$ is used to get better fluorescence. Halogens like bromine and iodine will reduce fluorescence efficiency where ever they occur as substituent groups, due to heavy-atom induced non-radiative decay i.e increase in intersystem crossing. Photoluminescence is also improved by the introduction of large bulky groups into the polymeric backbone to weaken intermolecular interactions, and thereby enhancing the stiffness of the backbone.²² Introduction of bulky substituent groups as pendant groups enable dissolution of polymers in its conjugated form whereby processability of the material is improved. Wudl and coworkers in 1989 reported the synthesis and development of first soluble PPV derivative consisting of long dihexyloxy side chains, which makes the polymer soluble above 80°C .²³ Synthesis was carried out by following the sulfonium salt route depicted in Scheme 1.1.



Scheme 1.1 Sulfonium salt route to poly(2,5-dialkoxyphenylenevinylene)

Apart from the sulfonium salt route other synthetic routes are commonly used in C-C bond formation such as McMurray polymerization,²⁴ Wittig condensations,²⁵ Heck²⁶ coupling reaction etc have been applied for the preparation of light emitting polymers. Controlling the emission wavelength is achieved by adjusting of $\pi-\pi^*$ band gap by suitable choice of fluorescent conjugated homo-polymers. Fine-tuning of band

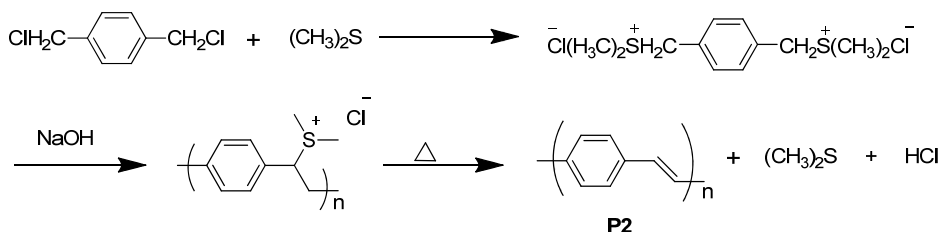
gap is achieved by shortening the effective conjugation length through substitution and co-polymerization using different emissive segments. Block copolymers in which the conjugation of one block is frequently interrupted by another block with a wider band gap results in precise control of luminescence from such a material. By trapping of excitons hindering their migration to quenching sites, conjugated/non-conjugated sequences provide improved electroluminescence efficiency and color tunability.²⁷ Low molecular weight materials used as emitters in optoelectronic devices are the oligomeric analogues of the light emitting polymers. Additionally, studies of oligomeric model compounds have been necessary for estimating structure–property relationships in LEPs. Low molecular weight organic compounds are used for the fabrication of LEDs made of multilayer devices; when the emitting layer acts simultaneously also as an electron transporting layer and hole transporting layer.²⁸ Short oligomers have larger optical gaps than longer oligomers. Electron affinity and ionization potentials of LEPs can be tuned by introduction of either electron withdrawing or by electron donating group. Electronic properties are modified by different type of structural modifications such as variation of structure through arylene building blocks, modification of vinylene linkage, constructing materials with defined conjugation lengths.^{29,30,31} Therefore, modification of the structure of LEPs with a view to fine-tuning electronic band gap could induce either blue-shift or red-shift. PPV and other delocalized polymers possess lowest singlet excited state with large transition dipole moment while linear polymer like polyacetylenes, such a state is above a singlet state in which the transition dipole moment is very small. The emissive species in the polymers are restricted due to chain rigidity and they have a tendency to undergo aggregation more particularly in the solid state. This results in the formation of weakly emissive interchain species in the excited state and reduces the luminescence efficiency. It is possible to control aggregation by controlling the environment of aggregation by the confinement of conjugation length and increasing interchain distances and thus to tune the optical gap of molecules.^{32,33,34}

1.3 Chemical Synthesis of Light Emitting Polymers

Several polymerization techniques used for the preparation of light emitting polymers. Synthesis of several light emitting polymers reported in literature exploited four different C-C bond forming schemes that continue to be important routes. These four methodologies *viz* i) soluble precursor polymer route, ii) dehydrohalogenation reactions, iii) transition metal-catalyzed coupling polymerizations and iv) condensation polymerizations; will be discussed in this section highlighting recent literatures. Polymerization methods discussed in the following section are primarily focused on the synthesis of poly(phenylenevinylene)s and polythiophenes.

1.3.1 Soluble Precursor Route

Precursor route polymerization strategy is the most extensively used method for the synthesis of PPV and its substituted derivatives. PPV itself is insoluble, intractable and difficult to process. During early 60's, Wessling and Zimmerman developed a general method for the synthesis of PPV. The method consists of thermo-conversion of a processable sulfonium intermediate (pre-polymer) into PPV in its film form. This pre-polymer is subjected to thermal elimination ultimately yielding the desired PPV derivative. The polymer produced by this method can be of very high molecular weight, and their films highly oriented by stretching during conversion of the precursor polymer to its conjugated form (Scheme 1.2).³⁵ Under suitable conditions, the thermo-conversion can give pin-hole free thin films of PPV suitable for PLED fabrication. The conversion temperature can be reduced to 100°C by using bromide derivatives instead of chlorides, thus enabling the fabrication of flexible devices.³⁶



Scheme 1.2 The Wessling-Zimmerman precursor route to PPV

Precursor polymer **P1** obtained as highly ordered free-standing film can then be converted into PPV with the elimination of gaseous dimethylsulfide and HCl at 200°C. The precursor polymer shows poor stability and extremely disagreeable odour of the mercaptane by-product can be resolved by substitution of the sulfonium leaving groups with a methoxy group under acidic catalysis. But the resulting PPV showed significantly improved optical properties due to high degree of order of the polymer backbone.³⁷ Different types of sulphide groups also used for the preparation of precursor polymers they are tetrahydrothiophene salts and other cyclic sulphide salts, respectively, in place of dimethylsulphide. Tetrahydrothiophene salts show some added advantages due to good stability of the pre-polymer at low temperatures and easiness of conversion to PPV.³⁸ The structure of tetrahydrothiophene monomer salt is shown in figure 1.7.

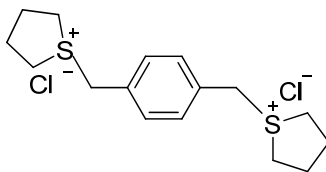
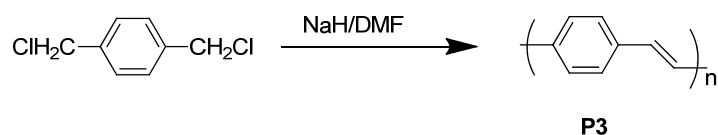


Figure 1.7 Structure of tetrahydrothiophene monomer salt

1.3.2 Dehydrohalogenation reactions

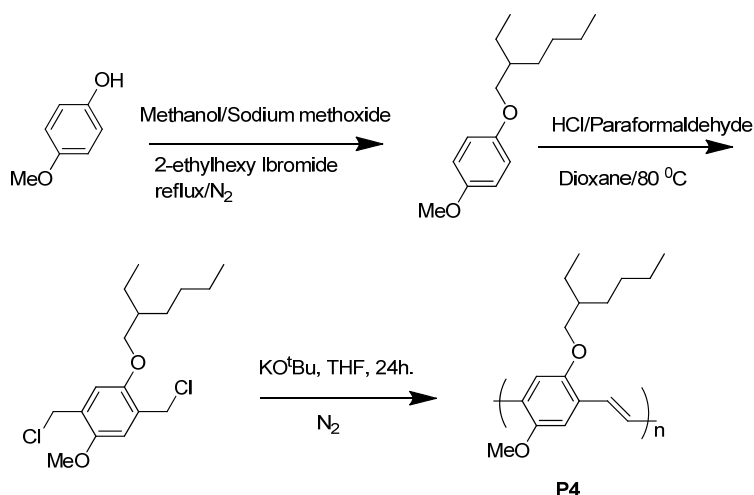
Dehydrohalogenation reactions are employed for the synthesis of different kinds of PPV derivatives. Polymerization is carried out by using strong bases such as potassium *tert*-butoxide, sodium hydride etc.³⁹ Dehydrohalogenation was carried out in dichloroethylene in the presence of sodium hydride and DMF solvent to give unsubstituted PPV is shown in Scheme 1.3.



Scheme 1.3 Dehydrohalogenation reaction

1.3.2.1 Gilch Polymerization Route

Gilch polymerization is most widely used for the synthesis of PPV derivatives. Mainly alkyl or alkoxy substituted PPV derivatives are synthesized using this method. The reaction is carried out by base-promoted 1,6-elimination of 1,4(bis-halomethylbenzene) but the mechanism of Gilch polymerization is still a subject of controversy.⁴⁰ It is generally accepted to proceed through a reactive quinodimethane intermediate produced by either a radical or a living chain anionic polymerization. Gilch route contain only two steps resulting in substantially increased yields. Scheme 1.4 shows the synthesis of the most studied dialkoxy-PPV derivative: MEH-PPV.⁴¹ Careful control of concentration of reagents is mandatory to avoid gelation. Molecular weight of the resulting polymer can be controlled by changing reaction parameters such as temperature, time, solvent, concentration of the monomer, and amount of base equivalent. Relatively high molecular weight and selective generation of trans double bonds led up wide usage of Gilch polymerization in the synthesis of PPV homopolymers and copolymers.



Scheme 1.4 Gilch polymerization of MEH-PPV

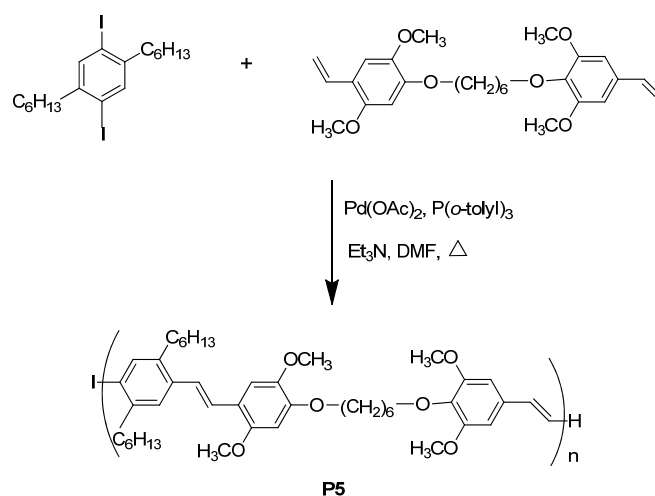
1.3.3 Transition Metal-Catalyzed Coupling Polymerizations

Metal catalyzed coupling reactions are the most popular routes to synthesize light emitting polymers. Emissive polymers with a defined structural

sequence of repeat units can be synthesized by metal catalyzed coupling reaction between two monomers with reactive sites. Metal catalyzed coupling methodology is an attractive alternative for the synthesis of heterocycles containing strongly electron-withdrawing groups as they generally tend to accelerate the reaction.

1.3.3.1 The Heck Reaction

Palladium mediated olefin arylation reaction (Heck coupling process) involves the reaction between an organic halide and a vinylbenzene derivative producing a carbon-carbon double bond, with remarkable *trans*-selectivity.⁴² Heck method is not suitable for the preparation of PPV homopolymers but this method is more useful for the preparation of PPV related block copolymers (Scheme. 1.5).⁴³ Heck reaction yields the same regular copolymer regiochemistry and double-bond configuration with a much higher yield, better purity and also high luminescence efficiency.

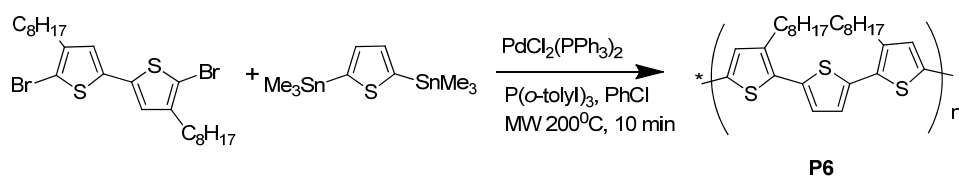


Scheme 1.5 Synthesis of PPV block copolymer by Heck coupling

1.3.3.2 Stille Coupling Reaction

The palladium-catalyzed Stille coupling reaction was used for preparing functionalized emissive polymers. This reaction has several advantages; it

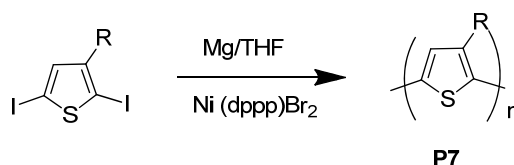
requires mild reaction conditions and produces high yields. Factors affecting polymerization include catalyst composition, concentration, different solvents, ligands and structures of monomers.⁴⁴ The Stille reaction involves the coupling of an organic halide, triflate, or carbonyl chloride with organo-tin compound catalyzed by a palladium (0) catalyst. Micro-wave assisted Stille coupling reaction is depicted in Scheme 1.6.⁴⁵ Highly electron rich thiophene containing monomers with stannyl groups are easily synthesized by using Stille reaction. Application of Stille reaction to synthesize functional and multifunctional light emitting polymers is given to demonstrate the versatility of this reaction.



Scheme 1.6 Pd catalyzed Stille coupling reaction

1.3.3.3. Kumada Coupling

The Kumada coupling is a special category of cross coupling reaction, useful for generating carbon-carbon bonds by the reaction of a Grignard reagent. The Kumada Coupling was the first Pd or Ni-catalyzed cross coupling reaction, developed in 1972. Presently, Ni or Pd catalyzed cross-coupling reaction of Grignard reagents with alkyl, vinyl or aryl in the presence of a suitable solvent most probably tetrahydrofuran (THF) termed as Kumada cross-coupling. Elsenbaumer and co-workers were the first to apply Kumada cross-coupling reaction to generate soluble and processable poly(3-alkylthiophene)s are shown in scheme 1.7.^{46, 47}



Scheme 1.7 Grignard synthesis of poly(3-alkylthiophene)

In this method, 2,5-diiodo-3-alkylthiophene was reacted with one mole equivalent of magnesium to form the mono Grignard species, Ni(dppp)Br₂ (dppp = diphenylphosphinopropane) catalyst was used to produce polymer by cross coupling. Since poly(3-alkylthiophene)s are non-centrosymmetric, regioregularity is a factor so these effects are important for its electronic properties. Poly(3-alkylthiophene)s (PATs) may couple as: head-to-head, head-to-tail, or tail-to-tail; as illustrated in Figure 1.8. The PATs prepared by Elsenbaumer and co-workers were regio-random in nature but later McCullough and co-workers synthesized regioregular PATs.^{48,49}

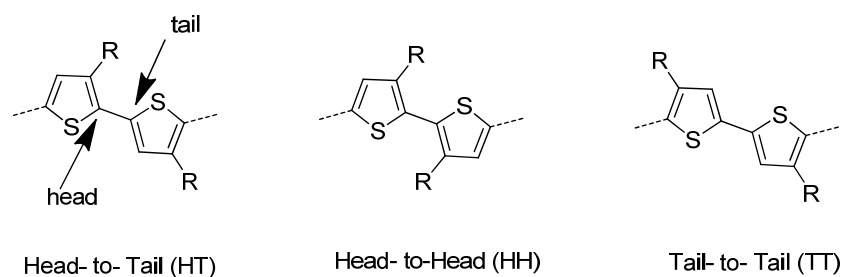
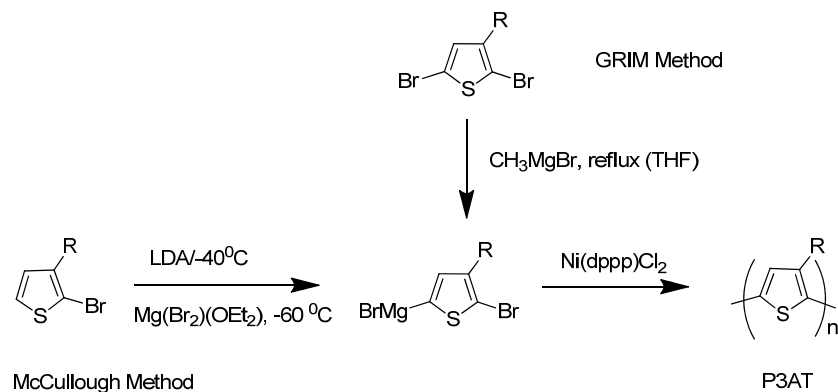


Figure 1.8 Possible linkages for 3-alkylthiophene

1.3.3.4 McCullough Method

McCullough and co-workers discovered two types of methods to synthesize poly(3-alkylthiophene)s (PATs); they are McCullough method and Grignard metathesis polymerization (GRIM).⁵⁰ Both methods are modified Kumada cross-coupling reaction and are depicted in Scheme 1.8.^{51,52}

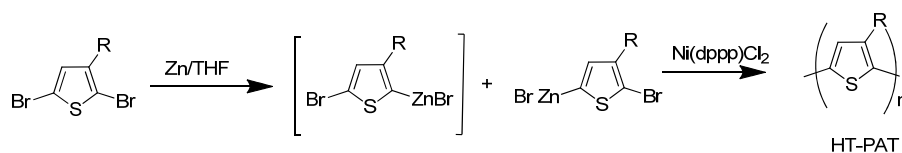


Scheme 1.8 Synthesis of Regioregular P3AT

In McCullough method highly pure 2-bromo-3-alkylthiophene is selectively lithiated with lithium diisopropylamide (LDA) at -40°C to afford 2-bromo-3-alkyl-5-lithiothiophene. This organolithium intermediate is subsequently converted to Grignard reagent by reacting with $\text{MgBr}_2 \cdot (\text{OEt})_2$ to yield 2-bromo-5-(magnesiobromo)-3-alkylthiophene. $\text{Ni}(\text{dppp})\text{Cl}_2$ catalyzed cross coupling of 2-bromo-5-(magnesiobromo)-3-alkylthiophene produced regio-regular poly(3-alkylthiophene). The GRIM method is a simpler route to make regioregular P3ATs. In this method, 2,5-dibromo-3-alkylthiophene monomer is used. The 2-bromo-5-(magnesiobromo)-3-alkylthiophene is easily formed by reacting 2,5-dibromo-3-alkylthiophene with Grignard reagent followed by cross coupling reaction in the presence of nickel catalyst to produce regio-regular poly(3-alkylthiophene) in high yields (60-70%).

1.3.3.5 Reike Ni - Catalyzed Polymerization

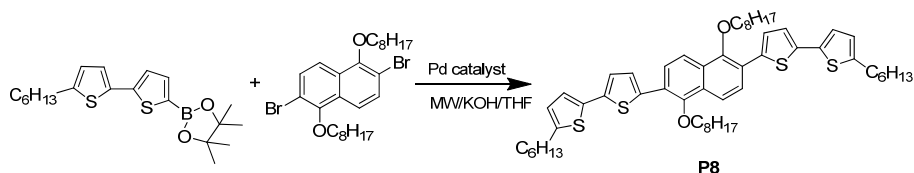
Reike and co-workers invented a new method for the preparation of regioregular thiophenes. This method is displayed in Scheme 1.9.⁵³ Basic difference between GRIM method and Reike method is in the generation of an organo-zinc intermediate that undergoes $\text{Ni}(\text{dppp})\text{Cl}_2$ catalyzed polymerization yielding regioregular PAT.



1.3.3.6 Suzuki Coupling Reaction

Suzuki coupling is yet another palladium catalyzed coupling reaction. Herein, reaction of organic halides with boronic acids is utilized to synthesize aryl derivatives. Suzuki coupling is effectively utilized for the preparation of poly(para-phenylenes), polyfluorenes and a great variety of light emitting polymers. Suzuki coupling has found extensive use for the preparation of

alternating copolymers. By using Suzuki coupling reaction, Sherf and co-workers synthesized thiophene/naphthalene oligomer is shown in Scheme 1.10.⁵⁴ This oligomer was prepared by using microwave assisted Pd catalyzed Suzuki coupling of the appropriate bromo derivative with corresponding boronic acid derivative.



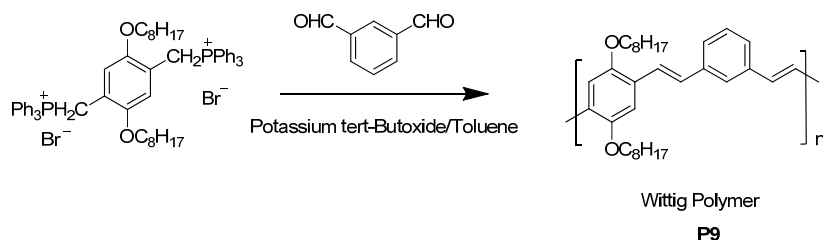
Scheme 1.10 Thiophene/naphthalene oligomer synthesized via Suzuki coupling

1.3.4 Condensation Polymerizations

In addition to various coupling methods listed above, several poly condensation reactions are also gainfully employed in the synthesis of useful LEPS. A brief discussion of such polymerization methods is presented in the following section.

1.3.4.1 Wittig Reaction

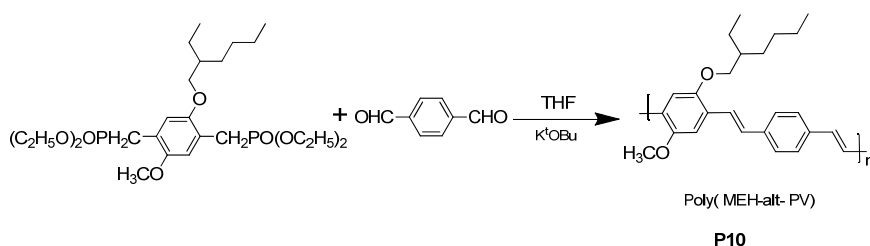
Wittig reaction is one of the most versatile methods for the synthesis of alkenes in which electrophilic carbonyl compounds such as aldehyde and ketone are attacked by a phosphorus ylide.⁵⁵ Phosphonium ylides are readily formed by the addition of a suitable base to the corresponding phosphonium salt. Wittig polycondensation route was used for the preparation of well-defined alternating copolymers. Here we present one of the example related to PPV, Werner J. Blau et al synthesized poly(*m*-phenylenevinylene-co-2,5-dioctyloxy-*p*-phenylenevinylene) by Wittig reaction.⁵⁶



Scheme 1.11 Synthesis of Poly(*m*-phenylenevinylene-co-2,5-dioctyloxy-*p*-phenylenevinylene) by Wittig reaction

1.3.4.2 Horner-Emmons Condensation

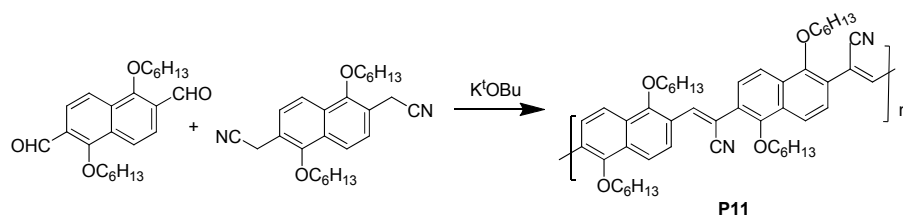
Horner-Emmons condensation is a practical modification of Wittig reaction that is used for the synthesis of PPV related alternating copolymers.⁵⁷ Wittig polymers have high molecular weight and it contain certain amount of *cis*-vinylene double bonds. Horner-Emmons condensation has some advantages over Wittig reaction such as, newly formed double bonds are purely *trans* in nature, it shows good regioselectivity, high degree of conversion and finally good yield.⁵⁸ Dong Uk Kim et al prepared poly (MEHPV-*alt*-PV) by using Horner-Emmons condensation is displayed in scheme 1.12.⁵⁹ The reaction consist of substituted phosphonate ester reacted with terephthalaldehyde under the presence of potassium *tert*-butoxide to produce alternating copolymer.



Scheme 1.12 Poly(MEH-*alt*-PV) synthesized by Horner-Emmons condensation

1.3.4.3 Knoevenagel Coupling Route

Emissive polymers containing vinylenes linkages are also prepared by using Knoevenagel coupling reaction, in which carbon-carbon double bonds are formed between respective monomers. Knoevenagel condensation based on the reaction between aldehyde groups with active methylene species requires strong electron withdrawing substituent groups (CN, for example).⁶⁰ Employing Knoevenagel condensation numerous PPV related homo and copolymers with CN containing vinylenes units have been synthesized.⁶¹ M. Hanack et al prepared cyano substituted poly(2,6-naphthylenevinylene) (CN-2,6-PNV) by using Knoevenagel condensation reaction between two monomers, namely 1,5-bis(hexyloxy)-2,6-naphthalenediacetonitrile and 1,5-bis(hexyloxy)-2,6-naphthalenedicarbaldehyde in the presence of a strong base is shown in Scheme 1.13.⁶²



Scheme 1.13 Knoevenagel condensation of poly(2,6-naphthylenevinylene) (CN-2,6-PNV)

1.4 Fully-Conjugated PPV Derivatives

Light emitting polymers possess extended π -system on their polymeric backbone. Therefore depending on its conjugation, electronic properties of the LEPS are varied i.e. fully conjugated polymers emit light in the longer wavelength region but interrupted conjugated polymers (not fully- conjugated) gives their emission at the shorter wave length region. In this section we shall try to explain the synthesis of some fully-conjugated PPV derivatives and their properties. PPV and its soluble derivatives can be made to give emission at both UV-Vis region and visible region by proper tuning of their band gap. Quantum efficiency for emission is very high for PPVs. Modifying the chemical structure of PPV offer various opportunities for tuning the opto-electronic properties of this material. The most suitable modification was introducing the substituents in the benzene ring including alkyl, alkoxy, silyl and electron releasing/withdrawing groups. Better processability and excellent film forming properties shows that PPV is a good candidate for light emitting diodes and Lasers.⁶³

Unsubstituted PPV is a fluorescent bright yellow polymer. It shows emission maximum in the green- yellow region at 551nm corresponding to a band gap estimated at 2eV. Unsubstituted PPV showed poor solubility, necessitating a modified Wessling route for the generation of PPVs having solubility inducing alkoxy groups attached on to the polymer backbone.^{63,64} Soluble electroluminescent PPV derivative prepared by substituting long alkyl or alkoxy

groups on to the polymer main chain such that the derivatization does not change the rod like character of the main chain. One of the first highly soluble, MEH-PPV derivatives was prepared by Santa Barbara group in California, which emitted a red-orange color.⁶⁵ But high molecular weight MEH-PPV does not dissolve properly, so the research related on light emitting polymers assumed different directions in order to increase solubility, fluorescence efficiency, color tuning etc. Another PPV derivative consist of bulky cholestanoxy side group, namely poly[2,5-bis(cholestanoxy)-1,4-phenylenevinylene] (BCHA-PPV) whose emission maximum is red shifted with respect to MEH-PPV.⁶⁶

Later, soluble PPVs were prepared by different polymerization reactions such as Gilch polymerization, Wittig condensation, Horner-Emmons condensation etc. H. H. Hörhold et al reported that Gilch-type polymer has marked shortage of regular vinylene groups (approximately 30%) that will leads to lack of long-range poly-conjugation.⁶⁷ In 2001 J. Jang et al reported improvement of photoluminescence efficiency by means of copolymerization with different bulky side ring substituents.⁶⁸ Jung Y. Huang et al demonstrated a new type of nanocrystalline TiO₂ doped MEH-PPV composite; electroluminescence of this composite is improved by the addition of TiO₂ nano-needles. Improved electroluminescence of the PPV derivatives is attributable to the decrease in hole barrier height and also leads to the increased hole mobility.⁶⁹

CN-PPV, a highly luminescent electron deficient PPV derivative with cyano groups in the vinylene units could be prepared by using Knoevenagel condensation reaction. CN-PPV is a highly fluorescent red material whose emission maximum at 590nm (2.1eV) is mainly determined by attached alkoxy/alkyl substituent groups. Some of the cyano substituted PPVs with their corresponding emission region are shown in Figure 1.9. Cyano groups contribute to enhance the electron affinity of the PPV and it is also used for multi layer devices.⁷⁰

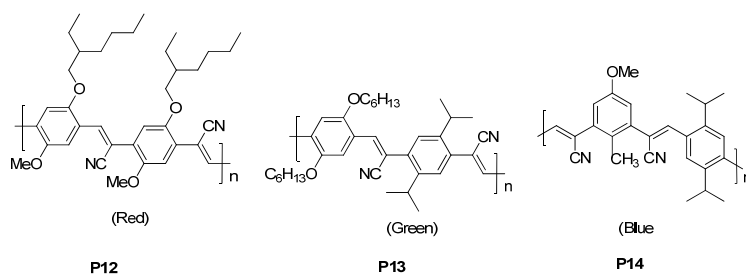


Figure 1.9 Cyano substituted PPV derivatives with their corresponding emission region

Solubility of the phenyl appended PPV derivatives is further improved by incorporating solubilizing groups onto the pendant phenyl group. The added bonus here is that such PPV derivatives showed good electroluminescence emission. Examples of biphenyl PPVs are shown in Figure 1.10. The twisted structure of the biphenyl unit decreases the effective conjugation length of the polymer and also limits the interchain interactions. Such structural features enhance their electroluminescence and photoluminescence quantum efficiencies.⁷¹

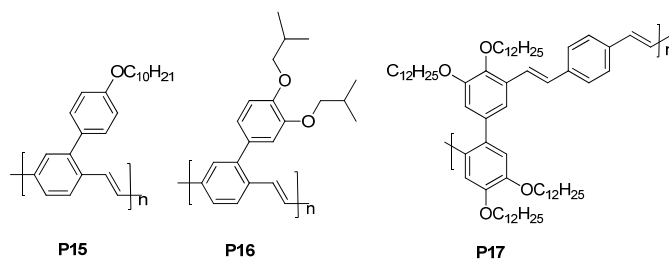


Figure 1.10 Biphenyl PPV derivatives

PPVs containing electron acceptor 2,5-diphenyl-1,3,4-oxadiazole group (**P18**), electron-donor carbazole group (**P19**), electron acceptor trifluoromethyl group (**P20**) attached directly to the phenylene units are depicted in Figure 1.11.⁷²

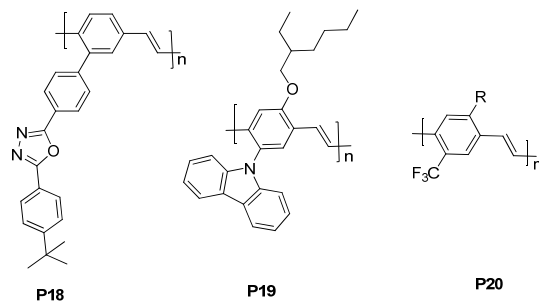


Figure 1.11 PPV derivative consist of electron-acceptor ((P18), electron-donor (P19) and trifluoromethyl substituted PPV derivative (P20)

1.5 Segmented Block PPV Copolymers

Segmented block copolymers (SBCs) otherwise known as conjugated/non-conjugated block copolymers are interesting molecules.⁷³ Upon increasing the chain length of light emitting polymers, noticeable red shift in emission wavelength is observed. In the case of fully conjugated polymers, chromophoric groups possess different energy gaps due to the difference in distribution of chain length among polymer units. Energy transfer is more dominant in fully conjugated derivatives that also exhibit lowering in energy band gap. Several synthetic approaches have been demonstrated recently, one of the approach is confinement of conjugation of the emitting polymers.⁷⁴ Examination of block copolymers in which a well-defined conjugating unit is intermixed with non-emitting blocks (aliphatic spacers) has confirmed that the emitted color is not affected by the length of the inert- aliphatic spacers. Those conjugated/non-conjugated copolymers exhibit excellent solubility in common organic solvents, homogeneity in terms of conjugation length, and can be intended to emit light in any part of the visible spectrum. In segmented polymers, energy transfer from higher band gap to lower band gap sequences will provide higher luminescence efficiency when compared to analogous structures of uniform conjugation.⁷⁴ Conjugated/non-conjugated polymers credited to decrease the interchain interactions with the help of interruption of the conjugation length, resulting in higher quantum efficiencies. Confinement of the effective conjugation leads to blue shifting the spectrum because the conjugated emitters can permit the formation of charge carriers but not to diffuse along the chain, thus limiting the transport of emitting species to the quenching sites.⁷⁵

Karasz et al reported the first highly soluble blue light emitting segmented block copolymer (P21) in 1993 that is shown in Figure 1.12.⁷⁶ Wittig reaction between 1,2-bis(4-formyl-2,6-dimethoxyphenoxy)octane and 1,4-xylylenebis (triphenylphosphoniumchloride) yielded **P21** in moderate yields.

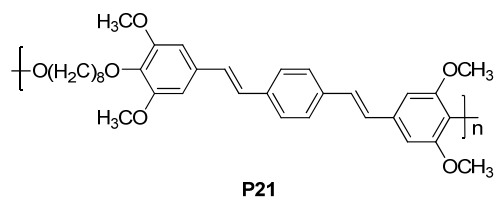
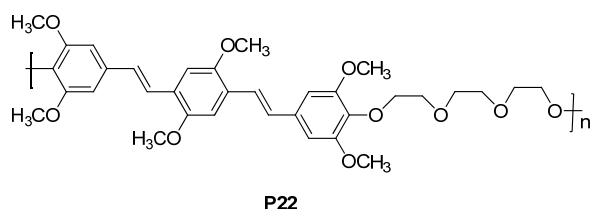
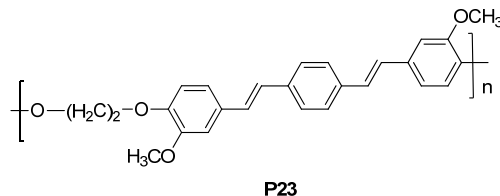


Figure 1.12 First soluble blue light emitting segmented copolymer

In 2002, Li et al demonstrated a new type of segmented block copolymer prepared by using Wittig polycondensation reaction.⁷⁷ This polymer named as TEO-MPV (**P22**) contains oligo-PPV segments as emitting chromophores and tri(ethylene oxide) segments as spacers. Furthermore, **P22** was used to fabricate a LED device showing lower turn-on time and operating voltage.

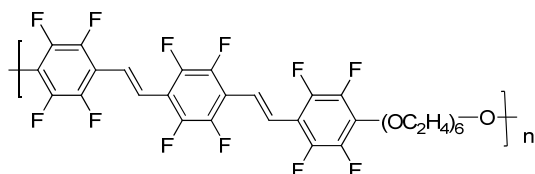


Conjugated/non-conjugated copolymers are commonly prepared by using Wittig condensation, Horner-Emmons condensation, Heck coupling etc. In these segmented copolymers, the flexible spacer provides solubility and also gives high molecular weight, and substituent groups present in the distyryl unit also enhances solubility.⁷⁸ Monkman et al prepared low molecular weight light emitting segmented copolymer (**P23**), that exhibited enhanced quantum yield originating from exciton confinement by the non-conjugated spacer groups, and also larger side groups that prevent aggregation and interchain interaction.⁷⁹



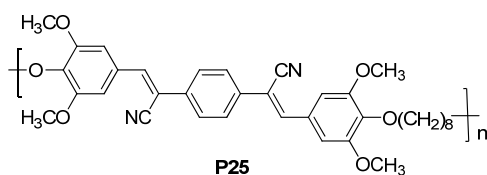
In 2002, Salaneck et al demonstrated a segmented block polymer (**P24**) consisting of fluorinated analogues with dodecafluorodistyrylbenzene as the

chromophoric group. Though this copolymer is a poor emitter, it could be used as an electron conducting layer.⁸⁰

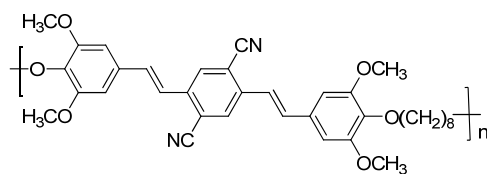


P24

Akcelrud et al reported cyano-group substituted light emitting segmented polymer synthesized by Wittig condensation and Knoevenagel condensation reactions.⁸¹ These Cyano group substituted segmented polymers (**P25 & P26**) show strong bathochromic effect when compared with those of a similar structure without cyano group. Furthermore, these polymers exhibited more pronounced red-shift and higher electroluminescence efficiency.



P25



P26

Due to space constraints, we have presented only a few of the most important advances in segmented block copolymer synthesis. Based on this short description, it is clear that advanced research is going on in the field of segmented block copolymers due to their excellent characteristics in the field of optoelectronic applications.

1.6 Light Emitting Hybrid Polymers

Hybrid conjugated- aromatic polymers are a new concept for the combinatorial material research. In the case of light emitting polymers, two

different conjugated polymers combine to form a new hybrid polymer exhibiting novel emitting properties and mechanical properties. Poly(phenylenevinylene) (PPV) and poly(phenyleneethynylene) (PPE) derivatives⁸² have been demonstrated to be valuable as active layers in polymer light-emitting diodes (PLEDs). In 2002, Bunz et al first introduced a concept about hybrid polymers; they prepared cross conjugated PPE-PPV hybrid synthesized by using $(\text{Ph}_3\text{P})_2\text{PdCl}_2/\text{CuI}$ catalyst. It should be of interest to have both polymers that combine the stability, electron affinity, and high emissive quantum yield of the PPEs with the excellent film forming property and hole injection capabilities of the PPVs.⁸³ Figure 1.13 shows the cross conjugated PPE-PPV hybrid polymer demonstrated by Bunz et al.

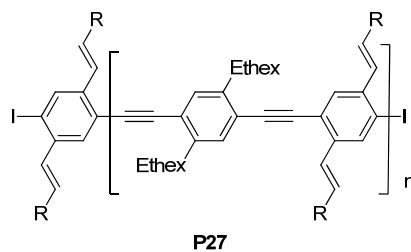
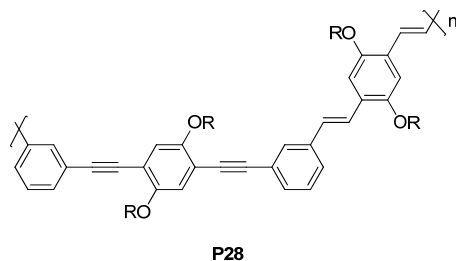
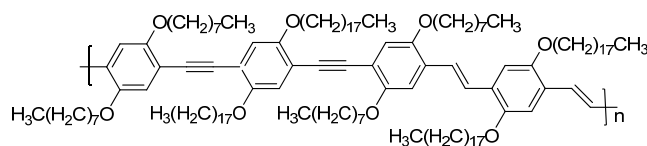
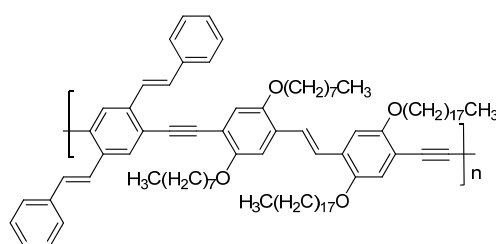


Figure 1.13 Cross conjugated PPE-PPV hybrid polymer

Karasz et al reported a new class of green-emitting PPE-PPV hybrid polymers (**P28**) containing different side chains that were synthesized by using a combination of Heck-type coupling and Horner-Wadsworth-Emmons condensation reactions. These hybrid polymers have well defined chemical structure consisting of phenyl rings linked alternatively at meta and para positions. Efficient energy transfer from PPE block to PPV block is possible and they demonstrated that PPV-PPE hybrid polymer emits light with the same wave length region as poly[*m*-phenylenevinylene)-*alt*-(*p*-phenylenevinylene)].⁸⁴



Egbe et al reported alkoxy substituted phenyleneethynylene (PE)/phenylenevinylene (PV) hybrid polymers (**P29** & **P30**) having the same structure as those reported by Bunz et al. They examined the influence of the conjugation pattern on the photophysical properties of the hybrid polymers. Styryl substituent groups in **P29** not only contribute to the red shift of the electroluminescence but also decrease the turn-on voltage of LEDs; in the case **P30** the conjugation pattern is more favourable to photoconductivity.^{85,86,87}



Hybrid conjugated aromatic polymers, having carbon-carbon double and triple bonds, could be of special interest, so PPE/PPV hybrid polymers are used for extensive studies.⁸⁸ Therefore research in this area also expanded along with research on other light emitting polymers due to the combined excellent characteristics of these polymers.

1.7 Light Emitting Polymers for Optoelectronic Applications

1.7.1 Organic Semiconducting Lasers (Polymer Lasers)

Among all kind of laser materials, conjugated semiconducting polymers are of foremost interest and form the rich family of so-called “organic lasers”, that also offer promise to the realization of electrically driven polymer injection laser devices. Lasers are composed of three essential building blocks: a gain medium, a

pump source and a resonator. The gain medium in a laser cavity can be a gas, a liquid or a solid where amplification of optical waves occurs by stimulated emission. Population inversion is carried out in pump source and resonator provides feedback and defines the spatial and spectral coherence of the beam.⁸⁹ Initially dyes were used for lasing action due to their high fluorescence quantum yield that enable them to be good emitters even at low concentrations. But dyes give less emission at high concentrations and also their emission wavelength cannot be tuned. On the other hand, light emitting polymers show high fluorescent quantum yield in the solid state. Recent advances in the application of conjugated light emitting polymers as laser materials has emerged as the direct outcome of active research effort worldwide in pursuit of this goal. Semiconducting polymers offer important advantages as potential laser active media based on their attributes listed below:⁸⁹

- 1) High photoluminescence efficiency and low self-quenching
- 2) Weak π - π stacking
- 3) Stimulated emission cross section is high
- 4) Combination of low inter-system crossing
- 5) Easily processed into optical quality thin films

Semiconducting polymers combine the particular advantages for lasing outlined above with the general characteristics of polymers applicable to all the applications in this regards, namely the scope for tuning the emission properties by changing the structure of the polymers, easy synthesis, and the possibility of fabricating flexible substrates. Excited states formed in light emitting polymers by charge injection or photoexcitation have photophysical characteristics analogous to laser dyes such as rhodamine, coumarin etc. High photoluminescence (PL) quantum yield and substantial Stokes shift make them semiconducting polymers promising candidates as laser media both in dilute solutions and solid state. The ultimate target is to make electrically pumped polymer lasers operating in the

visible wavelength region.⁹⁰ In 1992 Moses established lasing from conjugated polymers for the first time when he photopumped a cuvette that contained a solution of MEH-PPV.⁹¹ Subsequently, Rothberg et al reported that MEH-PPV exhibited stimulated emission only if it was in solution or diluted in a solid matrix such as polystyrene.⁹² Lasing action is found in other emissive polymers also. Graupner et al observed stimulated emission from films of a poly(*p*-phenylene) type ladder polymer using pump-probe techniques.^{93,94}

Hide et al and Frolov et al independently found line narrowing from PPV films due to amplified spontaneous emission (ASE).⁹⁵ ASE occurs even when the gain coefficient is small because the spontaneously emitted photons are wave guided and thus travel a large distance through the gain medium. The effective gain length of ASE is determined as a function of the exposed sample length.^{96,97} In 2006, Blubaugh et al observed aggregation effect in amplified spontaneous emission (ASE) spectra of MEH-PPV under different conditions such as thin film and solution in different types of solvent and different concentrations. Their results suggested that aggregation has a marked effect on ASE spectra.⁹⁸ Optically pumped polymer lasers and polymer laser diodes used in the field of integrated optics and optical computing. Based on their inherent advantages such as high nonlinear coefficients, high modulation frequencies and capacity to act as excellent waveguides, polymers are recommended for application as laser medium.⁹⁹ Polymer lasers can be electrically pumped indirectly to avoid problems of losses caused by charge absorption. These laser devices used for the development of industrial oriented laser application of emissive polymeric materials for data storage, optical computing, telecommunication, instrumentation and display technologies etc.¹⁰⁰

1.7.2 Semi Conducting Polymer Light Emitting Diodes

Electroluminescence (EL) can be defined as the emission of light as a result of the injection of charges of opposite sign. The basic structure of an organic EL device consists of a transparent organic film deposited in between two

electrodes. The simplest device configuration demands typical cathode/emitter/anode sandwich structure. Figure 1.14 shows the cross section of a simple polymer LED device (Fig. A) and an example of a basic band structure diagram is shown in Fig. B.^{21,101} Light emitting polymer devices exhibit impressive efficiency and brightness.¹⁰² Historical overview of a polymer light emitting diode has already been explained in Section 1.2.

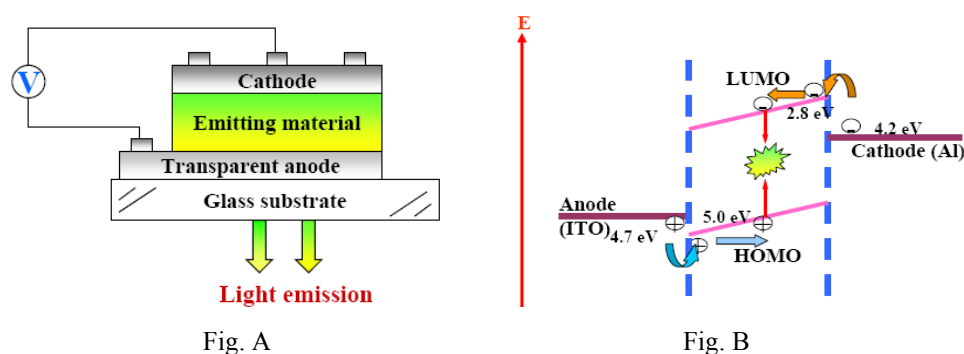


Figure 1.14 (Fig. A) Configuration of a simple PLED device. (Fig. B) Example of a basic band structure diagram of a simple PLED device.

Recently various research groups have reported a variety of light emitting polymer derivatives and also evaluated their efficiency in PLEDs.^{103,104,105} Shu et al developed efficient white light emitting polymers through the inclusion of green light emitting benzothiadiazole and red light emitting bithiophenylbenzothiadiazole moieties into the backbone of a blue light emitting polyfluorene copolymer.¹⁰⁶

In comparison to liquid crystal displays (LCDs), PLEDs displays offer many advantages such as greater power efficiency than all other flat panel displays, high brightness, long lifetime, wide view angle, fast moving images with optimum clarity, lower cost in comparison to CRTs or LCDs low power consumption, fast switching speeds and simple to use technology.¹⁷ One of the problems encountered was to stop the aging process of the device. The trickiest stage of device fabrication was the final soldering of the displays that is done clean rooms in an airtight environment because emissive molecules are labile

towards photo-oxidation. It is mandatory to use proper enclosures to protect the device from impurities and thereby to maintain a higher degree of quantum efficiency.¹⁰⁷

1.8 Aim and Scope of the Thesis

Polymeric electroluminescence (EL) was the major breakthrough in the field of conducting polymers. Light emitting polymers (LEPs) that emit light by applying an electric field have commanded increasing attention as potential materials for opto-electronic devices. Light emission from LEPs is a multidisciplinary field that challenges the skills of synthetic chemists, applied physicists, theoreticians and materials scientists. Synthesis of new emissive polymers is an important field of research to improve their performance in optoelectronic devices.

Poly(phenylenevinylene)s (PPVs) and polythiophenes (PTs) are selected for current studies due to their high luminescent characteristics and facile tunability of their band gaps with varying side groups. The thesis is mainly focused on the synthesis, characterization and optical properties of three classes of light emitting polymers; including fully-conjugated PPV derivative, segmented block PPV derivatives, and light emitting hybrid polymers based on biphenylenevinylene and thiophene. The main objectives of this work are as follows:

1. To synthesize Blue, Green and Orange-Red light emitting polymers utilizing suitable synthetic strategies.
2. Complete characterization of polymers using different spectroscopic techniques.
3. To alter the effective conjugation length, reduce aggregation (interchain π - π stacking), increase the photoluminescence intensity, increase the rigidity of the backbone, attain high purity, high thermal stability, high solubility, induce excellent film forming ability, effective band gap tuning (HOMO-LUMO), and low molecular weight distribution (MWD).

4. To study the structural, photophysical, electrochemical and morphological properties of currently synthesized polymers.
5. To investigate prospects of applications in polymer based optoelectronic devices mainly focused on the characteristics of PLED and Laser.

1.9 References

1. Nordén, B.; Krutmeijer, E.; The Nobel Prize in Chemistry, **2000**: Conductive polymers, *The Royal Swedish Academy of Sciences*.
2. Cuendias, A. D.; Hiorns, R. C.; Cloutet, E.; Vignauc, L.; Cramaila, H. *Polym Int.* **2010**, *59*, 1452.
3. Reddinger, J. L.; Reynolds, J. R. *Advances in Polymer Science* **1999**, *145*, 57.
4. Heeger, A. J. *Curr. Appl. Phys.* **2001**, *1*, 247.
5. Patil, A. O.; Heeger, A. J.; Wudl, F. *Chem. Rev.* **1988**, *88*, 183.
6. Wynne, K. J.; Street, G. B. *Ind. Eng. Chem. Prod. Res. Dev.* **1982**, *21*, 23.
7. Brédas, J. L.; Street, G. B. *Acc. Chem. Res.* **1985**, *18*, 309.
8. Moliton, A.; Hiorns, R. C. *Polym Int.* **2004**, *53*, 1397.
9. Choo, D. J.; Talaie, A.; Lee, Y. K.; Jang, J.; Park, S. H.; Huh, G.; Yoo, K. H.; Lee, J. Y. *Thin Solid Films* **2000**, *363*, 37.
10. Waltman, R. J.; Bargon, J. *Can. J. Chem.* **1986**, *64*, 76.
11. Bakhshi, A. K.; Bhalla, G. *J. Sci. Ind. Res. India.* **2004**, *63*, 715.
12. AlSalhi, M. S.; Alam, J.; Dass, L. A.; Raja, M. *Int. J. Mol. Sci.* **2011**, *12*, 2036.
13. Friend, R. H.; Gymer, R.W.; Holmes, A. B.; Burroughes, J.H.; Marks, R. N.; Taliani, C.; Bradley, D. D. C.; Dos Santos, D. A.; Brédas, J. L.; Lögdlund, M.; Salaneck, W. R. *Nature* **1999**, *397*, 121.
14. Burroughes, J. H.; Bradley, D. D. C.; Brown, A. R.; Marks, R. N.; Mackay, K.; Friend, R. H.; Burns, P.L.; Holmes, A. B. *Nature* **1990**, *347*, 539.
15. Friend, R.; Burroughes, J.; Bradley, D. *US Patent 5 247 190*, 1993.

16. Braun, D.; Heeger, A. *Appl. Phys. Lett.* **1991**, 58, 1982.
17. Patil, S. A.; Light emitting polymers: The revolutionary display technology, *Electronics for You.* **2002**.
18. Heeger, A. J. *Solid State Communications* **1998**, 107, 673.
19. Williams, A. T. R.; Winfield, S. A.; Miller, J. N. *Relative fluorescence quantum yields using a computer controlled luminescence spectrometer*, *Analyst.* **1983**, 108, 1067.
20. Kraft, A.K.; Grimsdale, A. C.; Holmes, A. B. *Angew. Chem. Int. Ed.* **1998**, 37, 402.
21. Segura, J. L. *Acta Polym.* **1998**, 49, 319.
22. Talaie, A.; Lee, Y. K.; Huh, G.; Kim, K. M.; Jeong, H. Y.; Choo, D. J.; Lee, J. Y.; Jang, J. *Materials Science and Engineering B.* **2001**, 85, 177.
23. Askari, S. H.; Rughooputh, S. D.; Wudl, F. *Synthetic Metals* **1989**, 29, E129.
24. Rehahn, M.; Schlütter, A. D. *Makromol. Chem. Rapid Commun.* **1990**, 375.
25. Hay, M.; Klavetter, F. L. *J. Am. Chem. Soc.* **1995**, 117, 7112.
26. Chan, W. K.; Yu, L. *Macromolecules* **1995**, 28, 6410.
27. Roncali. *J. Chem. Rev.* **1997**, 97, 173.
28. Scherf, U.; Müllen, K. *Synthesis* **1992**, 23.
29. Kim, Y.; Kwon, S.; Yoo, D.; Rubner, M, F.; Wrighton, M. S.; *Chem. Mater.* **1997**, 9, 2699.
30. Chang, C. P.; Wang, C. C.; Chao, C. Y.; Lin, M. S. *Journal of Polymer Research* **2005**, 12, 1.
31. Burn, P. L.; Kraft, A.; Baigent, D. R.; Bradley, D. D. C.; Brown, A. R.; Friend, R. H.; Cymer, R. W.; Holmes, A. B.; Jackson, R. W. *J. Am. Chem. Soc.* **1993**, 115, 10117.
32. Ramasesha, S. Lighting the World with Molecules. *Resonance* **2009**, 14, 798.

33. Kemerink, M.; Duren, J. J. K. V.; Jonkheijm, P.; Pasveer, W. F.; Koenraad, P. M.; Janssen, R. A. J.; Salemink, H. W. M.; Wolter, J. H. *Nano Lett.* **2003**, *3*, 1191.
34. Karastatiris, P.; Mikroyannidis, J. A.; Spiliopoulous, I. K.; Fakis, M.; Persephonis, P. *J. Polym. Sci.: Part A: Polym. Chem.* **2004**, *42*, 2214.
35. Wessling, R. A.; Zimmerman, R. G.; Polyelectrolytes from bis sulfonium salts, *U.S. Pat. No.3401152*, **1968**.
36. Garay, R. O.; Baier, U.; Bubeck, C.; Müllen, K. *Adv. Mater.* **1993**, *5*, 561.
37. Halliday, D, A.; Burn, P. L.; Bradley, D. D. C.; Friend, R. H.; Gelsen, O. M.; Holmes, A. B.; Kraft, A.; Martens, J. H. F.; Pichler, K. *Adv. Mater.* **1993**, *5*, 40.
38. Burn, P. L.; Bradley, D. D. C.; Brown, A. R.; Friend, R. H.; Holmes, A. B. *Synthetic Metals* **1991**, *261*, 41.
39. Hoeg, D. F.; Lusk, D. I.; Goldberg, E. P. *J. Polym. Sci. Part B, Polym. Lett.* **1964**, *2*, 697.
40. Neef, C. J.; Ferraris, J. P. *Macromolecules* **2000**, *33*, 2311.
41. Wudl, F.; Barbara, S.; Srdanov, G. *U.S. Pat. No.5189136*, **1993**.
42. Hilberer, A.; Brouwer, H, J.; van der Scheer, B, J.; Wildeman J.; Hadziioannou, G. *Macromolecules* **1995**, *28*: 4525.
43. Pasco, S, T.; Lahti, P. M.; Karasz, F. K. *Macromolecules* **1999**, *32*, 6933.
44. Bao, Z. B.; Chan, K. W.; Yu, L. *J. Am. Chem. Soc.* **1995**, *117*, 12426.
45. Carsten, B.; He, F.; Son, H. J.; Xu, T.; Yu, L. *Chem. Rev.* **2011**, *111*, 1493.
46. Jen, K. Y.; Oboodi, R.; Elsenbaumer, R. T. *Polym. Mater. Sci. Eng.* **1985**, *53*, 79.
47. Elsenbaumer, R. L.; Jen, K. Y.; Oboodi, R. *Synthetic Metals* **1986**, *15*, 169.
48. Loewe, R. S.; Ewbank, P. C.; Liu, J.; Zhai, L.; McCullough, R. D. *Macromolecules* **2001**, *34*, 4324.

49. Jeffries-El, M.; Sauve', G.; McCullough, R. D. *Macromolecules* **2005**, *38*, 10346.
50. Iovu, M. C.; Sheina, E. E.; Gil, R. R.; McCullough, R. D. *Macromolecules* **2005**, *38*, 8649.
51. Yokozawa, T.; Yokoyama, A. *Chem. Rev.* **2009**, *109*, 5595.
52. Loewe, R. S.; Khersonsky, S. M.; McCullough, R. D. *Adv. Mater.* **1999**, *11*, 250
53. Chen, T, A.; Wu, X.; Rieke, R. D. *J. Am. Chem. Soc.* **1995**, *117*, 233.
54. Nehls, B. S.; Preis, E.; Fuldner, S.; Farrell, T.; Sherf, U. *Macromolecules* **2005**, *38*, 687.
55. Edmonds, M.; Abell, A. Modern Carbonyl Olefination. *WILEY-VCH Verlag GmbH & Co. KGaA, Weinheim* .**2004**.
56. Drury, A.; Maier, S.; R  ther, M.; Blau, W, J. *J. Mater. Chem.* **2003**, *13*, 485.
57. Pfeiffer, S.; H  rhold, H. H. *Synthetic Metals* **1999**, *101*, 109.
58. Pfeiffer, S.; H  rhold, H. H. *Macromol. Chem. Phys.* **1999**, *200*, 1870.
59. Parka, L. S.; Hana, Y. S.; Kima, S, D.; Kim, D. U. *Synthetic Metals* **2001**,*117*, 237.
60. Liao, J.; Wang, Q. *Macromolecules* **2004**, *37*, 7061.
61. Moratti, S. C.; Cervini, R.; Holmes, A. B.; Baigent, D. R.; Friend, R. H.; Greenham, N. C.; Gr  ner, J.; Hamer, P. J. *Synthetic Metals* **1995**, *71*, 2117.
62. Hohloch, M.; Segurab, J. L.; D  ttinge, S. E.; Hohnhob, D.; Steinhube, E.; Spreitzer, H.; Hanack, M. *Synthetic Metals* **1997**, *84*, 319.
63. Wessling, R. A. *J. Polym Sci, Polym. Symp.* **1985**, *72*, 55.
64. Tokito, S.; Momii, T.; Murata, H.; Tetsui, T.; Saito, S. *Polymer* **1990**, *31*, 1137.
65. Braun, D.; Heeger, A. J.; Kroemer, H. *J. Eletron. Mater.* **1991**, *20*, 945.

66. Wudl, F.; Hoger, S.; Zhang, C.; Pabkaz, K. *ACS Polym Prepr.* **1993**, *34*, 197.
67. Holzer, W.; Penzkofer, A.; Tillmann, H.; Hörhold, H. H. *Synthetic Metals* **2004**, *140*, 155.
68. Talaie, A.; Lee, Y. K.; Huh, G.; Kim, K. M.; Jeong, H. Y.; Choo, D. J.; Lee, J. Y.; Jang, J. *Materials Science and Engineering B.* **2001**, *85*, 199.
69. Weng, C. C.; Chou, C. H.; Wei, K. H.; Huang, J. Y. *Journal of Polymer Research* **2006**, *13*, 229.
70. Moratti, S. C.; Bradley, D. D. C.; Friend, R. H.; Greenham, N. C.; Holmes, A. B. *Mat. Res. Soc. Symp. Proc.* **1994**, 328, 371.
71. Xu, B.; Zhang, J.; Peng, Z. *Synthetic Metals* **2000**, *113*, 35.
72. Perepichka, D. F.; Perepichka, I. F.; Meng, H.; Wudl, F. *Light-Emitting Polymers. In Organic Light-Emitting Diodes.* CRC Press: Boca Raton, FL, **2006**.
73. Sierra, C. A.; Lahti, P. M. *Chem. Mater.* **2004**, *16*, 55.
74. Yang, Z.; Karasz, F. E.; Geise, H. J. *Macromolecules* **1993**, *26*, 6570.
75. Peng, K. Y.; Chen, S. A.; Fann, W. S. *J. Am. Chem. Soc.* **2001**, *123*, 11388.
76. Yang, Z.; Sokolik, I.; Earasz, F. E. *Macromolecules* **1993**, *26*, 1188.
77. Wanga, H.; Sun, Q.; Li, Y.; Liu, D.; Wang, X.; Li, X. *Reactive and Functional Polymers* **2002**, *52*, 61.
78. Akcelrud, L. *Prog. Polym. Sci.* **2003**, *28*, 875.
79. Ali, B.; Jabar, S.; Salih, W.; Tamimi, R. K. A.; Attar, H. A.; Monkman, A. P. *Optical Materials* **2009**, *32*, 350.
80. Cacialli, F.; Feast, W. J.; Friend, R. H.; Jong, M.; Lövenich, P.W.; Salaneck, W. R. *Polymer* **2002**, *43*, 3555.
81. Pinto, M. R.; Hu, B.; Karasz, F. E.; Akcelurud, L. *Polymer* **2000**, *41*, 2603.
82. Pang, Y.; Li, J. *Macromolecules* **1998**, *31*, 6730.

83. Wilson, J. N.; Windscheif, P. M.; Evans, U.; Myrick, M. L.; Bunz, U. H. F. *Macromolecules* **2002**, *35*, 8681.
84. Chu, Q.; Pang, Y.; Ding, L.; Frank E. Karasz. *Macromolecules* **2003**, *36*, 3848.
85. Egbe, D. A. M.; Bader, C.; Klemm, E.; Ding, L.; Karasz, F. E. Grummt, U. W.; Birckner, E. *Macromolecules* **2003**, *36*, 9303.
86. Tekin, E.; Egbe, D. A. M.; Kranenburg, J. M.; Ulbricht, C.; Rathgeber, S.; Birckner, E.; Rehmann, N.; Meerholz, K.; Schubert, U. *Chem. Mater.* **2008**, *20*, 2727.
87. Egbe, D. A. M.; Tekin, E.; Birckner, E.; Pivrikas, A.; Sariciftci, N. S.; Schubert, U. S. *Macromolecules* **2007**, *40*, 7786.
88. Schenning, A. P. H. J.; Tsipis, A. C.; Meskers, C. J.; Beljonne, D.; Meijer, E. W.; Brédas, J. L. *Chem. Mater.* **2002**, *14*, 1362.
89. Chénais, S.; Forget, S. *Recent Advances in Solid State Organic Lasers*, Universite Paris 13 /C.N.R.S. France.
90. McGehee, M, D.; Heeger, A. J. *Adv. Mater.* **2000**, *12*, 1655.
91. Moses, D. *Appl. Phys. Lett.* **1992**, *60*, 3215.
92. Rothberg, L. J.; Papadimitrakopoulos, M. Y. F.; Gavin, M, E.; Kwock, E. W.; Miller, T, W. *Synthetic Metals* **1996**, *80*, 41.
93. Graupner, W,; Leising, G.; Lanzani, G.; Nisoli, M.; Silvestri, S. D.; Scherf, U. *Phys. Rev. Lett.* **1996**, *76*, 847.
94. Tessler, N.; Denton, G. J.; Friend, R. H. *Nature* **1996**, *382*, 695.
95. Hide, F.; Garcia, M. A. D.; Schwartz, B.; Andersson, M.; Pei, Q.; Heeger, A. J. *Science* **1996**, *273*, 1833.
96. Holzer, W.; Penzkofer, A.; Schmitt, T.; Hartmann, A.; Bader, C.; Tillmann, H.; Raabe, D.; Stockmann, R.; Hörhold, H. H. *Optical and Quantum Electronics* **2001**, *33*, 121.

97. Karastatris, P.; Mikroyannidis, J. A.; Spiliopoulos, I. K.; Fakis, M.; Persephonis, J. *Polym. Sci.: Part A: Polym. Chem.* **2004**, *42*, 2214.
98. Mahfouda, A.; Sarangana, A.; Nelson, T. R.; Blubaugh, E. A. *Journal of Luminescence* **2006**, *118*, 123.
99. Samuel, D. W.; Turnbull, G. A. *Polymer laser: recent Advances, Materials today*, September **2004**, ISSN: 1369 7021, Elsevier Ltd **2004**
100. Kranzelbinder, G.; Leising, G. *Rep. Prog. Phys.* **2000**, *63*, 729.
101. Braun, D, *Semiconducting Polymer LEDs, Materials today* June. **2002**, ISSN:1369 7021, Elsevier Science Ltd
102. Braun, D.; Heeger, A. J. *Thin Solid Films* **1992**, *216* , 96.
103. Chen, Z, K.; Wang, L. H.; Kang, E. T.; Huang, W. H. *Phys. Chem. Chem. Phys.* **1999**, *1*, 3789.
104. Pinzón, H. A. M.; Pardo, D, R, P.; Alvarado, J. P. C.; Reyes, J. C. S.; Vera, R.; Sierra, B. A. P. *Universitas Scientiarum* **2010**, *15*, 68
105. Sarker, A. M.; Ding, L.; Lahti, P. L.; Karasz, F. K. *Macromolecules* **2002**, *35*, 223.
106. Chuang, C. Y.; Shih, P. ; Chien, C. H.; Wu, F. I.; Shu, C. F. *Macromolecules* **2007**, *40*, 247.
107. Gold. J. F. *Short Life Times of Light Emitting Polymers*, University of Cambridge, Cavendish Laboratory, Cambridge.

Orange-Red Light Emitting MEH-PPV with Narrow MWD: Synthesis, Characterization and Photophysical studies

2.1 Introduction and Motivation
2.2 Results and Discussion
2.3 Conclusions
2.4 Experimental Section
2.5 References

Abstract

This chapter describes the synthesis, purification, photophysical and amplified spontaneous emission (ASE) characteristics of Poly[2-methoxy-5-(2'-ethylhexyloxy)-1,4-phenylenevinylene] (MEH-PPV). Gleich polymerization route was used for the synthesis of MEH-PPV. The material obtained was purified by using sequential extraction method. The synthesized MEH-PPV showed narrow molecular weight distribution (MWD) and enhanced fluorescent quantum yield in most of the organic solvents such as dichlorobenzene, 1,2-dichlorobenzene, toluene, xylene, chloroform and THF. The studies show that the luminescence efficiency is comparable to that of Rhodamine 6G. The variation in the features of amplified spontaneous emission with increasing polymer concentration is also described. At very low polymer concentration, narrow emissions were observed for the 0-0 and 0-1 vibronic bands. The ASE characteristics show that MEH-PPV is a potential candidate for laser medium.

2.1 Introduction and Motivation

Poly(*p*-phenylenevinylene) (PPV) and its derivatives form an important class of conjugated emissive polymers that have attracted enormous attention in polymers based optoelectronic devices, owing to their efficient luminescence, charge transport properties and ease of processing in solution phase.¹⁻³ Poly[2-methoxy-5-(2'-ethylhexyloxy)-1,4-phenylenevinylene] (MEH-PPV) is one of the extensively studied electroluminescent PPV derivative.⁴ The exact mechanism of polymerization of relevant monomers to yield PPV and its derivatives is not completely understood and a number of processes have been suggested.⁵ The idea behind the structural design of MEH-PPV is the use of asymmetric substitution of methyloxyl and branched ethylhexyloxyl side chains to improve the solubility in

common organic solvents and minimize intermolecular aggregation. Nevertheless, there does still exist a significant tendency towards molecular aggregation. Molecular aggregation in PPV backbone gives rise to morphological defects that will affect its optical properties.⁶ The light emitting efficiency has been improved by proper selection of good solvent and low polymer concentration that helps to reduce degree of aggregation in solution.⁷ For the first time in 1992, the laser action of MEH-PPV in the liquid state was achieved in yellow/red wavelength region.⁸

There are many approaches generally used for the synthesis of MEH-PPV they are, the Gilch route⁹, the Wessling route¹⁰ and Horner condensation polymerization.¹¹ From the beginning, most applied synthetic approaches for the preparation of MEH-PPV are dehydrohalogenation of xylylene dihalides or thermal elimination of sulfonium salt precursor polymers. But these methods are not feasible because partial gelation by cross linking or incomplete elimination leads to undesirable side chain reactions which are difficult to control.¹² Gilch type MEH-PPVs are now commercially available from Sigma-Aldrich and American Dye Source, Inc. W. Holzer et al reported that gel permeation chromatogram of the Gilch-type MEH-PPV shows strong broadening in its MWD and also have large polydispersity value.¹³ Based on their studies, they pointed out that Gilch type MEH-PPVs have few dominant defects such as 1,6-polymerization, HX elimination, phenylene-ethylene-phenylene moieties and finally the polymer possesses high molecular weight. Due to structural defects optical properties of MEH-PPV was diminished. Till date, there are so many studies carried out for the improvement of photoluminescence quantum yield enhancement of MEH-PPV.^{14,15}

This chapter reports the synthesis, purification, thermal studies, fluorescent quantum yield studies and preliminary Laser studies of fully conjugated emissive polymer. Here Poly[2-methoxy-5-(2'-ethylhexyloxy)-1,4 phenylenevinylene] (MEH-PPV) was taken as a model material. The molecular weight plays crucial role on the structural and optical properties of the emissive polymers. PPVs with low molecular

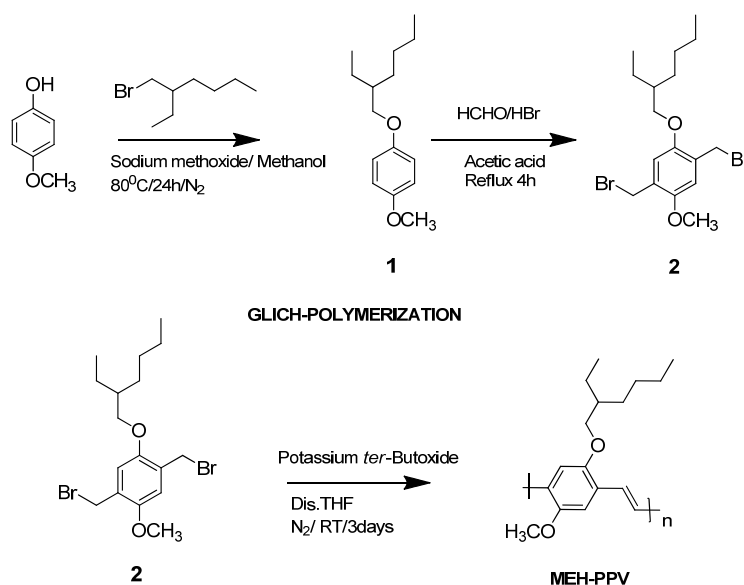
weight is optimally suited for the fabrication of all optical device applications because of the ease of thin film preparation, enhanced solubility compared to high molecular weight one and good combination of high nonlinearity.^{3,15} However, MEH-PPV with low molecular weight (below 60000 g/mol) and narrow molecular weight distribution is not commercially available. In general, commercially available synthetic polymers have a broad distribution of molecular weight. In this study conventional Glich polymerization method used for the synthesis of MEH-PPV. The obtained red polymer was purified by sequential extraction method. Sequential extraction is a technique to fractionate polymer mixtures to fractions that have narrower molecular weight distribution.

2.2 Results and Discussion

2.2.1 Monomer and Polymer Synthesis

The monomer, 1,4-bis(bromomethyl)-2-(2'-ethylhexyloxy)-5-methoxybenzene (**2**) and the polymer MEH-PPV were synthesized by using an adapting a reported procedure with some modifications.¹⁶ The synthesis of MEH-PPV is shown in Scheme 2.1. Details of preparation methods are explained in experimental section. 4-Methoxyphenol reacted with 2-ethylhexylbromide in the presence of sodium methoxide to produce 2-[(2'-ethylhexyloxy)-5-methoxybenzene] (**1**). It was further reacted with HBr/acetic acid in the presence of paraformaldehyde to yield bisbromomethylated monomer (**2**). The monomer was polymerized by Glich polymerization reaction using potassium *tert*-butoxide as a catalyst in dry tetrahydrofuran (THF) for 3 days at ambient temperature under nitrogen atmosphere. A large quantity of dry THF was used to prevent the formation of gel in the polymerization system. The polymer was purified by pouring the red polymer solution into methanol, filtering and subsequently washing the residue repeatedly with methanol. The purification procedure was repeated at least twice by dissolving and re-precipitating the polymer into methanol. The polymer was filtered through a thimble and was

purified by sequential extraction with methanol, hexane and THF. Methanol washing separated excess reagents from the polymer mixture. The low molecular weight fractions were dissolved in hexane and collected separately. High molecular weight fractions were extracted with THF. The THF soluble fraction was used for further analysis. After extraction, the dissolved polymer was re-precipitated in methanol. The precipitate was collected by filtration and then dried in vacuum. Using a simple procedure such as sequential extraction, we could separate polymer fraction with narrow molecular weight distribution. As mentioned earlier, the THF fraction was used for further investigations. The color of the MEH-PPV changed from dark red-orange to fluorescent red-orange after purification. The yield obtained was 35%. The obtained red polymer exhibited excellent solubility in common organic solvents such as toluene, THF, chloroform, 1,2-dichlorobenzene, xylene etc. The polymer formed transparent pin-hole free films



Scheme 2.1 Synthesis of MEH-PPV

The gel permeation chromatogram (GPC) of the polymer is shown as Figure 2.1. The polymer was analyzed using toluene as eluent. The number average molecular

weight (M_n) and weight average molecular weight (M_w) are 33831g/mol and 46777g/mol respectively. Low molecular weight can enhance the solubility of the polymer. The polydispersity index (PDI) of the polymer was found to be 1.38. The low polydispersity index of the MEH-PPV suggests that the molecular weight distribution of the polymer was almost uniform.

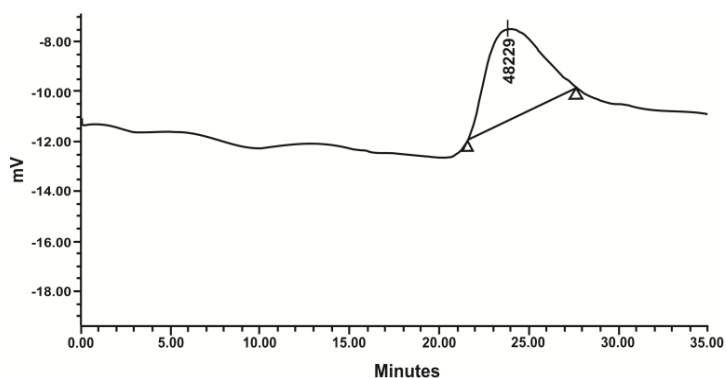
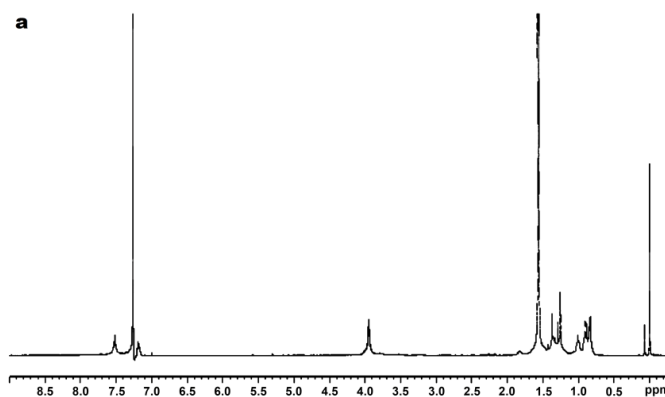


Figure 2.1 Gel permeation chromatogram (GPC) of MEH-PPV (Waters-2414 column with toluene as eluent, at a flow rate of 0.5mL/min at 25⁰C)

The structure of the polymer was confirmed by spectroscopic techniques. ¹H NMR and FTIR are shown in Figure 2.2 (a & b). In ¹H NMR spectra, the two aromatic peaks at 7.5ppm and 7.2ppm correspond to the aromatic protons and vinylic (-CH=CH-) protons, respectively. The peaks for all other protons including methylenoxy protons and aliphatic protons appeared below 4ppm. FTIR spectrum consists of 964cm⁻¹ band that is assigned to the *trans*-substituted olefinic C-H bending.¹⁶



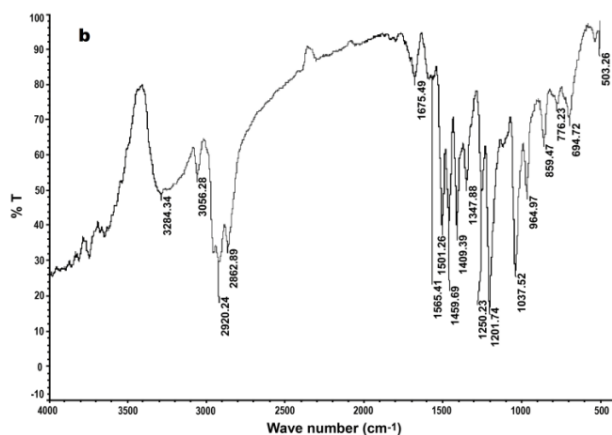


Figure 2.2 (a) ^1H NMR spectrum (b) FTIR spectrum of MEH-PPV

2.2.2 Thermal Analysis

The thermal stability of MEH-PPV was analyzed by thermo gravimetric analysis (TGA) under nitrogen atmosphere at a heating rate of $10^0\text{C}/\text{min}$ (Figure 2.3).

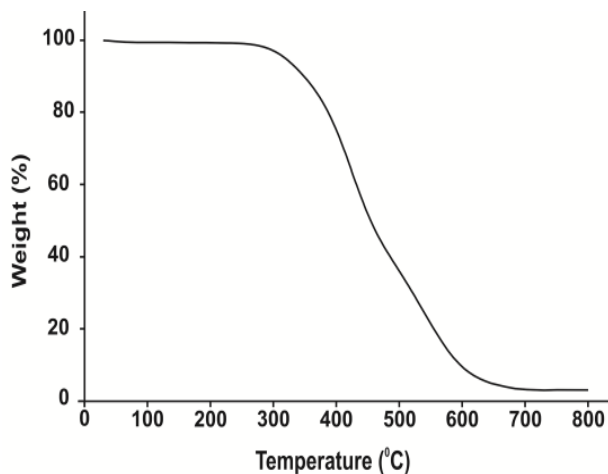


Figure 2.3. TGA plot for MEH-PPV under nitrogen atmosphere at a heating rate of $10^0\text{C}/\text{min}$

From the graph, it is clear that the TGA thermogram shows a double stage degradation process under nitrogen atmosphere. The first stage of the degradation is observed around 345^0C and continues till around 470^0C , with maximum degradation at 424^0C . The second stage of the degradation is observed between

450⁰C and 680⁰C with a maximum rate of mass loss around 583⁰C. The decomposition of MEH side groups and PPV backbone occurs at these temperatures, as reported in the previous literature.¹⁷ The thermal transitions such as glass transition temperature (T_g), melting temperature (T_m), and crystallization temperature (T_c) of the polymer was investigated by differential scanning calorimetry (DSC) (Figure 2.4). MEH-PPV was found to be amorphous, without showing any melting or crystallization peaks during heating/cooling cycles. A well defined T_g is observed at 58⁰C.

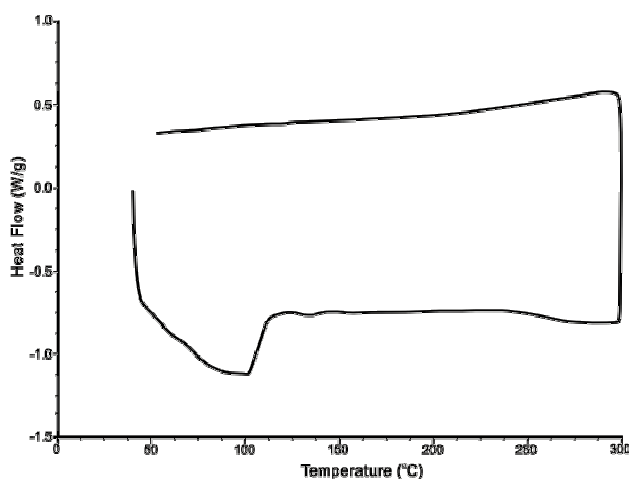


Figure 2.4 Differential scanning calorimetry (DSC) thermogram plot of MEH-PPV in nitrogen atmosphere at a heating rate of 10⁰C/min

2.2.3 X-ray diffraction data (XRD)

Powder X-ray diffraction (XRD) (Rigaku X-ray diffractometer, Cu-K α radiation (1.542 \AA) was used to investigate the molecular organization of the MEH-PPV (Figure.2.5). A featureless XRD profile is seen in this figure and no crystalline peaks are present in the spectrum confirming the amorphous nature of MEH-PPV.

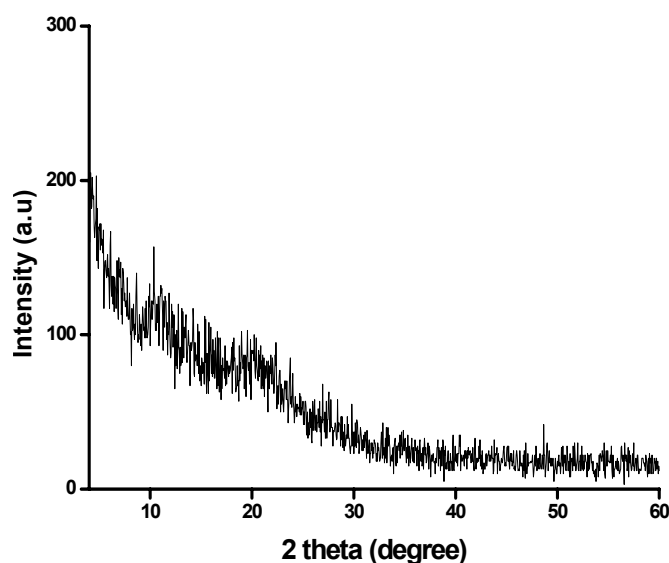


Figure 2.5 XRD plot of MEH-PPV

2.2.4. Photophysical studies

2.2.4.1 Absorption and fluorescence studies

Absorption and fluorescence spectrum of MEH-PPV in THF solution is shown in Figure. 2.5. Absorption peak is found to be at 495nm and the emission peak at 550nm with a shoulder around 590nm. Usually the overlap region of absorption and emission spectrum corresponds to the self quenching in the material. Here in the case of MEH-PPV it is clear from the Figure 2.6 that the self quenching will be low since the overlapping of the spectrum is less¹⁸. Photoluminescence spectrum shows that MEH-PPV emits light in orange-red region. The optical band gap of MEH-PPV was obtained from the onset of UV-Vis absorption spectrum and was estimated as 2.10eV. The calculated optical band gap is in agreement with previous reports.¹⁸

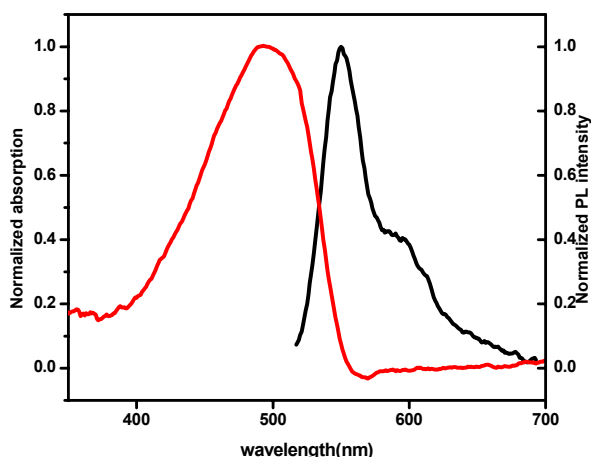


Figure 2.6 Absorption and PL spectrum of MEH-PPV in tetrahydrofuran

2.2.4.2 Fluorescence Quantum Yield Studies of MEH-PPV in Different Organic Solvents

The fluorescence quantum yield (Φ_F) of a compound is defined as the fraction of molecules that emit a photon after direct excitation by the source. This quantity is not the same as the total number of emitted photons which escape a bulk sample divided by the total number of absorbed photons, although in many instances the two quantities are nearly equal.¹⁹ The most dependable method of determining quantum yield is the comparative method proposed by Williams et al.²⁰ It is a time consuming process but provides much higher accuracy by calculating the slope of the line generated by plotting the magnitude of the integrated fluorescence intensity against the solution absorbance. However more accurate method to determine quantum yield is to prepare solutions with optical densities in the range of 0.01 to 0.1. Therefore fluorescence quantum yield (Φ_F) calculated by the equation,

$$\Phi_X = \Phi_{ST} \frac{(\text{Grad}_X) (\eta^2_X)}{(\text{Grad}_{ST}) (\eta^2_{ST})}$$

Where the subscripts ST and X denote standard and test samples respectively, 'Grad' is the gradient from the plot of integrated fluorescence intensity

vs absorbance, and n is the refractive index of the solvent. The fluorescence quantum yield of MEH-PPV was determined by using Rhodamine 6G as the standard. The quantum yield of Rhodamine 6G obtained from literature is 0.95.²¹

We have studied the fluorescence quantum yields of MEH-PPV in different solvents. The solvents selected for the present study are 1,2-dichlorobenzene, chlorobenzene, toluene, xylene, chloroform and THF.

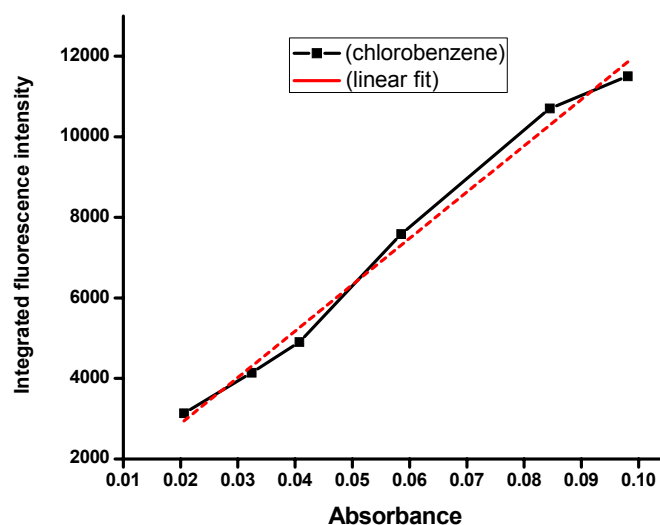


Figure 2.7 Integrated fluorescence intensity vs absorbance of chlorobenzene

The graph of the absorbance of chlorobenzene vs. integrated fluorescence intensity (the area of fluorescence) and the resulting linear fits are shown in Figure 2.7. The gradient obtained from the graph is 115003.41. The fluorescence quantum yield of MEH-PPV in chlorobenzene was found to be 0.90. We have also calculated quantum yield for different solvents like 1,2-dichlorobenzene, toluene, xylene, chloroform and THF and are tabulated in Table 2.1. The fluorescence quantum yield of MEH-PPV was calculated for different solvents having same concentration. The reported fluorescent quantum yield of MEH-PPV was below 0.4.¹³ From these results, it is clear that narrow molecular weight distribution of MEH-PPV shows enhanced quantum yield in all selected solvents and the quantum yield. 1,2-dichlorobenzene and chlorobenzene are in fact comparable to that of Rhodamine

6G. Therefore we can conclude that narrow MWD and low molecular weight improves the florescent quantum yield of MEH-PPV.

Solvent	Refractive index	Quantum yield (Φ_F)
1,2 Dichlorobenzene	1.55	0.93
Chlorobenzene	1.52	0.90
Toluene	1.49	0.68
Xylene	1.49	0.51
Chloroform	1.44	0.86
THF	1.40	0.62

Table 2.1 Quantum yield of MEH-PPV in different solvents

***2.2.4.3 Amplified spontaneous emission (ASE)**

Amplified spontaneous emission is a significant technique used in laser spectroscopy. Emissive polymers with combined optoelectronic and mechanical properties have been applied as active media in LASER systems. Since the first observation of lasing action in conjugated polymer solution several years ago (Moses 1992), lasing studies of luminescent organic polymers caught the attention of researchers and remains even today an active field of research.²² Amplified spontaneous emission or super-luminescence is produced by spontaneous emission that has been optically amplified by the process of stimulated emission in a gain medium. Gain medium is also known as active laser medium. The amplified spontaneous emission is identified by spectral narrowing, temporal shortening, threshold behaviour of the light emission and directionality in the output of the beam.²² Mahfoud et al studied the role of aggregation in amplified spontaneous emission effect of MEH-PPV in solution and film.²³ They found that the photophysics of ASE depends on the solvents and concentration in both aromatic and non-aromatic solvents.

* Amplified spontaneous emission rests presented herein was investigated in collaboration with International School of Photonics (ISP), CUSAT.

We have studied amplified spontaneous emission with solutions pumped with 532nm Q-switched Nd: YAG laser pulses (10ns, 10Hz repetition rate).²⁴ The experiment setup is shown in Figure 2.8. The pump power was varied using a variable neutral density filter. When the sample was excited using a beam in the form of stripe, it forms a cylindrically shaped active gain medium. The fluorescence emitted by the chromospheres is strongly amplified by the active medium and emits a highly directional output beam. We have also studied the concentration dependence on the evolution of amplified spontaneous emission from MEH-PPV in tetrahydrofuran (THF).

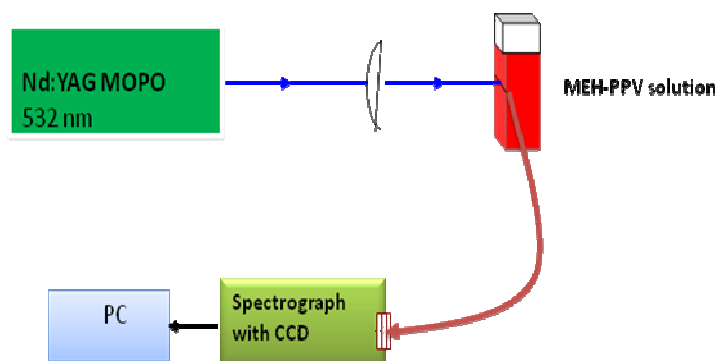


Figure 2.8 Experiment setup for recording amplified spontaneous emission (ASE) spectra

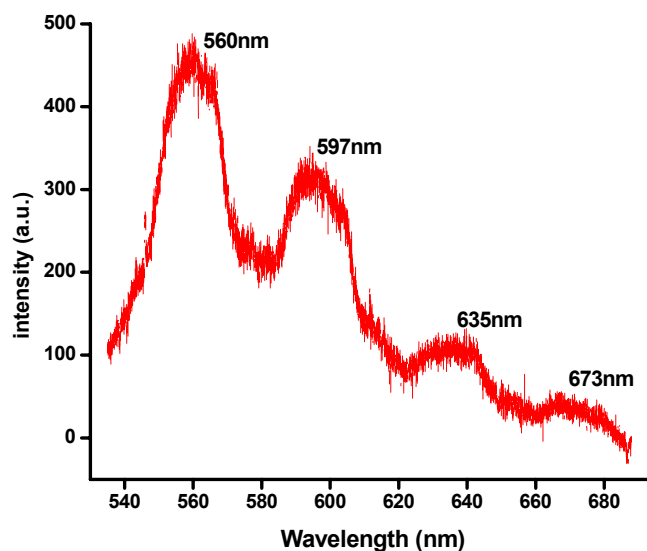


Figure 2.9. Vibronic bands at lower concentration of MEH-PPV in THF

At very low concentration such as 0.18mg/mL, the spectrum shows four vibronic bands shown as in Figure 2.9. The four bands are present at around 560nm, 597nm, 635nm and 673nm, of which the band at 560nm is prominent.²⁵ From the analysis of the band positions, these four bands can be realized as the vibronic bands (0-0), (0-1), (0-2) and (0-3) respectively.²⁶ The differences of evolution of ASE vibronic bands can be explained by comparing various concentrations of solutions and are depicted in Figure 2.10.

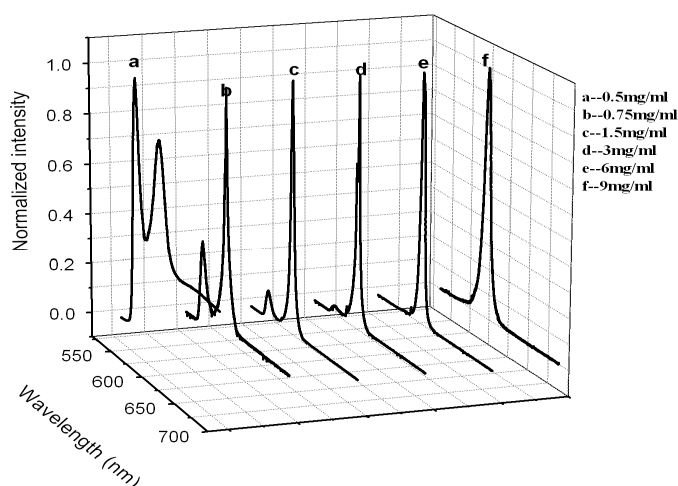


Figure 2.10 Evolution of ASE for various concentrations of MEH-PPV

From the graph, it is clear that on decreasing the concentration the (0-0) and (0-1) bands are well developed as separate narrow peaks. In the previous investigations of the polymer properties, researchers have reported ASE emission was present only around the 0-1 vibronic transition.²⁷ Now we have observed that, ASE takes place in both the first (0-0) and second (0-1) vibronic transition from the polymer chains. At very low concentrations (0-0) first vibronic transition from the polymer chain is active. The (0-0) band is a characteristic of interchain exciton. As the concentration was increased, the distance between the polymer chains decreased. As a result the aggregation between conjugation segments increases. The (0-1) band is related to the excitons in the aggregated state. The spectrum indicates that at very low concentration (0.5mg/mL) two well defined vibronic transitions at (0-0) and (0-1) are observed. The shorter wavelength

emission dominates over the longer wavelength emission. But with increasing concentration, a decrease in the ASE emission bandwidth and a red shift of the ASE peak was detected. At higher concentration i.e. 9mg/mL (0-1) vibronic band, was completely suppressed and longer wavelength band emerged as a narrow band of high intensity. Therefore one can notice that the evolution of ASE will depend on the concentration of the solution. At higher concentrations there was a reduction in ASE bandwidth indicating that aggregation between the single polymer chains is increased. So the capability of the solution to generate ASE is also diminished. It was observed that single polymer chains are responsible for the generation of ASE emission in the solution. Fakis et al reported that the photoluminescence efficiency and ASE were reduced by the presence of aggregation in solution.²⁸ Samples showed dual wavelength lasing up to an optimum concentration above which the shorter wavelength emission (0-0) is suppressed. This is due to the effect of concentration quenching more on short wavelength in comparison with that of the higher wavelength emission. Therefore we can conclude that the photophysics of ASE depend on the concentration of solution and single polymer chains are suitable for generating ASE in MEH-PPV.

2.3. Conclusions

MEH-PPV was synthesized through Glich method, purified and characterized. Purified sample showed narrow polydispersity index, low molecular weight and excellent thermal stability. The amorphous nature of MEH-PPV was revealed by XRD and DSC analysis. Fluorescent quantum yield studies showed that due to narrow MWD, MEH-PPV has enhanced quantum efficiency comparable to that of Rhodamine 6G. Amplified spontaneous emission studies showed that at low concentrations, MEH-PPV solution gave two well defined narrow peaks corresponding to (0-0) and (0-1) transitions. Based on these results, it is concluded that ASE emission characteristics are strongly dependent on the concentration of MEH-PPV solution. The overall studies showed that the newly obtained MEH-PPV is a good candidate for laser active media.

2.4 Experimental Section

2.4.1 General Techniques

All reactions were performed in oven-dried glassware under a nitrogen atmosphere with magnetic stirring unless otherwise noted. Reagents and solvents were purchased from commercial suppliers and were used without further purification. Solvents used for experiments were distilled and dried according to procedures given in standard manuals. All reactions were followed by TLC to completion. TLC analysis was performed by illumination with a UV lamp (254 nm) or staining with iodine. All column chromatographic separations were performed with 60-120 mesh silica gel purchased from SD Fine-chem.as the stationary phase. ¹H NMR spectra were recorded on a Bruker Avance III 400 MHz instrument in CDCl₃, and chemical shifts were measured relative to residual solvent peak (δ 7.26). The following abbreviations were used to describe coupling: s = singlet, d = doublet, t = triplet, q = quartet, m = multiplet. FTIR spectra were recorded using KBr pellet technique on a Thermo Nicolet, Avatar 370spectrometer. Melting points were recorded on a Fisher-Johns melting point apparatus. Elemental analyses were performed on a Elementar Vario EL III analyzer. The absorption and fluorescence spectra were recorded using UV-Visible spectrophotometer (JASCO V-570) and Fluoromax-3 fluorimeter respectively. The Powder X-ray diffraction (XRD) patterns were obtained using a (Rigaku X-ray diffractometer with Cu K α radiation (1.542Å). The molecular weight of the synthesized polymers was determined by GPC, (Waters 2414) using a column packed with polystyrene gel beads. The polymer was analyzed using toluene as eluent, at a flow rate of 0.5mL/min at 25⁰C. The molecular weight was calibrated using polystyrene standards. Glass transition temperature was determined from differential scanning calorimeter (DSC), (Q-100, TA Instruments) under nitrogen at heating rate of 10⁰C/min. Thermal stability was determined from thermo gravimetric analyzer (TGA), (Q-50, TA Instruments) under nitrogen at a heating rate of 10⁰C/min.

2.4.2 Experimental procedure for Amplified Spontaneous Emission (ASE)

The amplified spontaneous emission (ASE) was studied in MEH-PPV dissolved in THF. The ASE studies of the solution were conducted by taking the sample solution in a quartz cuvette of 1cm x 1cm x 3cm dimensions. The emission spectra were recorded by exciting the sample with 532nm radiation at which the sample has good absorption. The pump beam was obtained from a Q-switched frequency doubled Nd-YAG laser which gives pulses of 10ns duration at 532nm with a repetition rate of 10Hz. A cylindrical lens was used to focus the pump beam in the shape of a stripe on the sample. The pump beam was absorbed by the front layer of the sample and it created a stripe like excited gain medium. A vertical slit was incorporated in the path of the beam between the cylindrical lens and the sample so as to vary the stripe length of the laser beam falling on the sample. In our studies the slit was selected such that the pump beam has a width of 4mm and 8mm. The emission from the sample was collected from the edge of the front surface of the cuvette using an optical fibre in a direction normal to the pump beam. The emission spectra were recorded with Acton monochromator attached with a CCD camera. The emitted beam from the edge of the cuvette was so strong and highly directional that we could collect it even at a distance of 2.5cm from the cuvette without focusing.

2.4.3 Materials

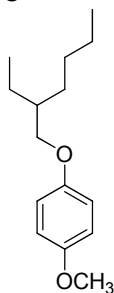
All reagents were commercially available and used as received unless otherwise stated. Tetrahydrofuran (THF) was freshly distilled over sodium before it was used. 4-Methoxyphenol and 2-ethylhexyl bromide were purchased from Aldrich. Other chemicals and solvents were purchased locally.

2.4.4 Synthesis of monomer and polymer

2.4.4.1 Synthesis of 1-Methoxy-4-(2-ethylhexyloxy) benzene (1)

A mixture of 4-methoxyphenol (0.04mol) and sodium methoxide (0.07mol) in methanol was refluxed for 1h. After cooling to room temperature, 2-

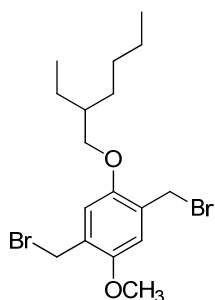
ethylhexyl bromide (8mL, 0.04mol) was added drop-wise and further refluxed for 24h until the brownish solution turned light yellow. Methanol was removed under reduced pressure. Residue obtained was dissolved in dichloromethane, washed several times with NaOH followed by brine solution and dried over MgSO₄. After removing the solvent clear liquid product was obtained (yield=54%).



¹H NMR (400 MHz, CDCl₃) δ (ppm): 6.86 ppm (s, 4H), 3.83 ppm (m, 5H, -OCH₂ and -OCH₃), 2.61-0.94 ppm (m, 15H).

2.4.4.2 Synthesis of 1,4-bis(bromomethyl)-2-(2'-ethylhexyloxy)-5-methoxy benzene (2)

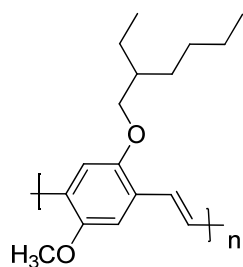
A sample (0.01mol) of 2-[(2'-ethylhexyloxy)-5-methoxy benzene] was dissolved in 30mL glacial acetic acid and paraformaldehyde (0.06mol) was added. The resulting solution was cooled down to 0°C and 7mL (30-33%) HBr in glacial acetic acid was added drop-wise to the above solution with continuous stirring. After the addition the reaction mixture was heated to 75°C and stirred for an additional 4h. The reaction mixture was then cooled, concentrated and stored in a refrigerator overnight. A pale white precipitate was obtained which was dissolved in a minimum amount of dichloromethane and washed with NaHCO₃ solution. The organic layer was separated and dried over MgSO₄. Solvent was removed and the residue was further dissolved in acetone and re-precipitated in methanol. The yield obtained was 94%.



¹H NMR (400 MHz, CDCl₃) δ (ppm): 6.87 ppm (s, 2H), 4.54 ppm (s, 4H), 3.89 ppm (5H), 1.64-0.92ppm (m, 15H).

2.4.4.3 Synthesis of Poly[2-methoxy-5-(2'-ethyl-hexyloxy)-1,4-phenylenevinylene] {MEH-PPV}

1g of the monomer was first dissolved in 50mL of THF. Four equivalents of potassium *tert*-butoxide was dissolved in 100mL of THF and added slowly to the stirred monomer solution under nitrogen atmosphere. After completing the addition of the base, the reaction was allowed to proceed by stirring at room temperature for further 3days. A large quantity of THF was used to prevent the formation of gel in the polymerization system. At the end of reaction, the solution was poured into methanol under constant stirring and the product was collected by filtration. After that sequential extraction was performed with methanol, hexane and THF. The polymer was recovered from the THF fraction by rotary evaporation and dried in a vacuum oven at 40°C. Yield= 0.3g (35%).



¹H NMR (400 MHz, CDCl₃) δ (ppm): 7.2-7.5 ppm (m, 4H), 4 -3.94 ppm (m, 5H), 1.64-0.92ppm (m, 15H).

IR (KBr) ν: 3056, 2920, 2662, 1675, 1565, 1501, 1459, 1347, 1250, 1201, 1037, 964, 859, 778, 694, 503.

Anal.Calcd. For C₁₇H₂₄O₂: C: 78.42, H: 9.29;
Found: C: 77.38, H: 9.09.

2.5 References

1. Ahlskog, S.; Reghu, M.; Noguchi, T.; Ohnishi, T. *Synthetic Metals* **1997**, *89*, 11.
2. Heller, C. M.; Campbell, I. H.; Laurich, B. K.; Smith, D. L.; Bradley, D. D. C.; Burn, P. L.; Ferraris, J. P.; Müllen, K. *Physical Review B* **1996**, *54*, 5516.
3. AlSalhi, M. S.; Alam, J.; Dass, L. A.; Raja, M. *Int. J. Mol. Sci.* **2011**, *12*, 2036.

4. Marchioni, F.; Chiechi, R.; Patil, S.; Wudl, F.; Chen Y.; Shinar, J. *Appl. Phys. Lett.* **2006**, *89*, 061101.
5. Neef, C. J.; Ferraris, J. P. *Macromolecules* **2000**, *33*, 2311.
6. Chou, H.L.; Lin, K. F.; Fan, Y.L.; Wang, D. C. *Journal of Polymer Science: Part B: Polymer Physics* **2005**, *43*, 1705.
7. Hua, C. C.; Kuo, C. Y.; Chen, S. A. *Appl. Phys. Lett.* **2008**, *93*, 123303.
8. Masilamani, V.; Ibnaouf, K. H.; Alsalhi, M. S.; Yassin, O. A. *Laser Physics* **2007**, *17*, 1367.
9. Amrutha S, R.; Jayakannan M. *J. Phys. Chem. B.* **2006**, *110*, 4083.
10. Grimsdale, A. C.; Chan, K. L.; Martin, R. E.; Jokisz, P. G.; Holmes, A. B. *Chem. Rev.* **2009**, *109*, 897.
11. Pfeiffer, S.; Hörhold, H. H. *Synthetic Metals* **1999**, *101*, 109.
12. Pfeiffer, S.; Hörhold, H. H. *Macromol. Chem. Phys.* **1999**, *200*, 1870.
13. Holzer, W.; Penzkofer, A.; Tillmann, H.; Hörhold, H. H. *Synthetic Metals* **2004**, *140*, 155.
14. Talaie, A.; Lee, Y. K.; Huh, G.; Kim, K. M.; Jeong, H. Y.; D.J. Choo, D. J.; Lee, J. Y.; Jang, J. *Materials Science and Engineering B85* . **2001**, *85*, 199.
15. Chao, C. S.; Whang, W. T.; Chuang, K. R. *Journal of Polymer Research* **2000**, *7*, 175.
16. Wudl, F.; Barbara, S.; Srdanov, G. *U.S. Pat. No.5189136*, **1993**.
17. Wang, H.; Tao, X.; Newton, E. *Polym Int.* **2004**, *53*, 20.
18. Misra, F.; Kumar, P.; Srivastava, R.; Dhawan, S.K.; Kamalasan, M. N.; Chandra, S. *Indian Journal of Pure & Applied Physics* **2005**. *43*, 921.
19. Demasa, J. N.; Crosby, G. A. *The Journal of Physical Chemistry* **1971**, *75*, 991.
20. Williams, A. T. R.; Winfield, S. A.; Miller, J. N. *Analyst.* **1983**, *108*, 1067.
21. Allen, M. W. *Measurement of Fluorescence Quantum Yields*. Technical note 52019, Thermo Fisher Scientific, Madison, WI, USA

22. Holzer, W.; Penzkofer, A.; Schmitt, T.; Hartmann, A.; Bader, C.; Tillmann, H.; Raabe, D.; Stockmann, R.; Hörhold, H. H. *Optical and Quantum Electronics* **2001**, *33*, 121.
23. Mahfouda, A.; Sarangana, A.; Nelson, T. R.; Blubaugh, E. A. *Journal of Luminescence* **2006**, *118*, 123.
24. Sreelekha, G. *Ph D Thesis*. CUSAT. **2012**
25. Sreelekha, G.; Vidya, G.; Geetha, K.; Joseph, R.; Prathapan, S.; Radhakrishnan, P.; Vallabhan, C. P. G.; Nampoory, V. P. N. *International Journal of Photonics* **2011**, *3*, 31.
26. Cossiello, R. F.; Akcelrud, L.; Atvars, T.D. *Z. J. Braz., Chem. Science.* **2005**, *16*, 74.
27. Nguyen, T. Q.; Martini, I. B.; Liu, J.; Schwartz, B, J. *J. Phys.Chem. B.* **2000**, *104*, 237.
28. Fakis, M.; Tsigaridas, G.; Polyzos, I.; Giannetas, V.; Persephonis, P. *Physical Review B* **2003**, *68*, 035203.

Substituent Effects on Light-Emitting Segmented Block PPV Copolymers: Synthesis, Characterization and Photophysical Studies

3.1	Introduction and Motivation
3.2	Results and Discussion
3.3	Conclusions
3.4	Experimental Section
3.5	References

Abstract

Two segmented block PPV copolymers of 2,5 dialkoxy substituted distyrylbenzene block containing bulky side groups with different steric characteristics, have been synthesized through Horner-Emmons condensation reaction. Copolymers of substituted distyrylbenzene block acting as the chromophoric group and hexamethylene spacer units alternating along the polymer backbone. The newly synthesized polymers are, long aliphatic chain (octyloxy) substituted poly[1,6-hexanedioxy-(1,4-phenylene)-1,2-ethenylene-(2,5-dioctyloxy-1,4-phenylene)-1,2-ethenylene-(1,4-phenylene)] (**P1**) and bulky ring substituted poly[1,6-hexanedioxy-(1,4-phenylene)-1,2ethenylene-(2,5-dicyclohexylmethyloxy-1,4-phenylene)-1,2-ethenylene-(1,4-phenylene)] (**P2**). The structures of the copolymers were determined by ^1H NMR, ^{13}C NMR, FTIR and elemental analysis. The copolymers exhibited excellent film forming ability from various organic solvents such as chloroform, dichloromethane, tetrahydrofuran, and toluene. Thermal properties were investigated using DSC and TGA under nitrogen atmosphere. The HOMO and LUMO energy levels of the copolymers were estimated by cyclic voltammetry. Band gap from absorption edge of the UV-Vis spectra and cyclic voltammetry analysis concluded that copolymer **P2** has lower band gap compared to **P1**. Both copolymers show excellent fluorescence quantum yield in dichloromethane. Photoluminescence studies show that copolymer **P1** gives blue emission and **P2** gives bluish-green emission. Furthermore, a single metal-semiconductor junction device was fabricated. The current-voltage (*I-V*) measurements also suggest the suitability of these copolymers in polymer based LEDs.

3.1 Introduction and Motivation

In 1990, Cambridge group discovered that conjugated polymers can be used as active emissive layers in polymer based optoelectronic devices triggering extensive work on this class of polymers.¹ Poly(1,4-phenylenevinylene)s has proved to be a major class of the luminescent polymer and have been extensively investigated since the discovery of electroluminescence (EL) phenomenon in

conjugated polymers.^{2,3} Un-substituted PPV is insoluble in most organic solvents, therefore the processability of PPVs is very difficult. Various new PPV derivatives and its copolymers have been synthesized to enhance the solubility, film forming property and EL efficiency over the past few years.⁴⁻⁸ Furthermore for technologically important applications photoactive conjugated phenylenevinylene segments were attached as side chains to polystyrene, ϵ -caprolactone and polyacrylamide backbones.^{7,8} Substitutions have altered the electronic and physical properties of the PPV via electromeric and steric effects. The major requirements in polymer light emitting diodes include good processability, high photoluminescence, improved charge transporting properties and long operating life times.^{9,10} High thermal stability and good mechanical properties of light emitting polymers are also important to overcome device degradation and increased life time during device operation.¹⁰ As a result, development of efficient and useful PPV derivatives and its copolymers for different optical application still present a great challenge.

Blue light emitting PPVs are the subject of great research interest; because blue light emission is the key to fabricating full color electroluminescent displays. However, it is difficult to get blue light emission in fully conjugated PPVs due to relatively low band gap. Consequently, there are several methods to decrease effective conjugation length suitable for the generation of blue light emitting PPVs. For the first time, Burn et al prepared a new type of segmented PPV derivative, which was derived from homopolymer precursor having large band gap which emits blue light.¹¹ Segmented block copolymers (SBCs) interrupting the conjugated backbone of the polymer by introducing non-conjugated spacer (flexible block) can provide a blue shift in the emission spectrum consequent to increase in band gap energy.^{12,13} Electromeric effects of substituents group can also alter absorption and emission characteristics of the polymer^{14,15} Judicious introduction of non-conjugated spacer and bulky substituents should change the photophysical properties of the copolymer according to the required application. Distyrylbenzene (DSB) units are the major chromophoric group present in the PPV related SBC type polymers, in which

substitution leads to alter the emission spectra without any decrease in the high DSB fluorescence quantum yield.¹⁶

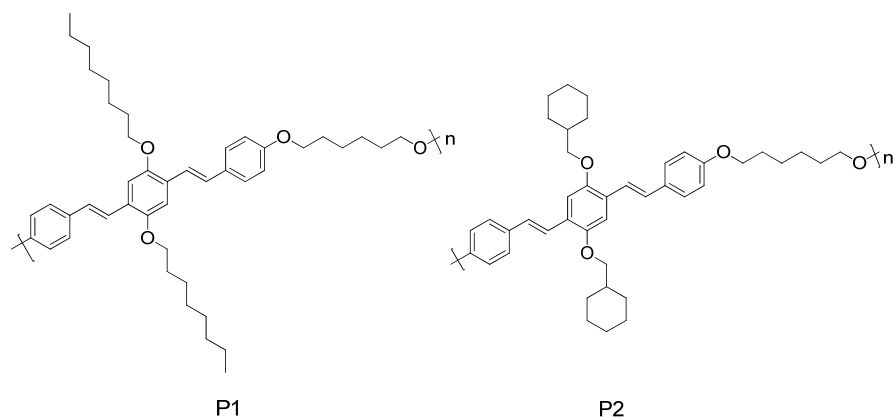


Figure 3.1. Molecular structure of segmented block copolymers **P1** and **P2**

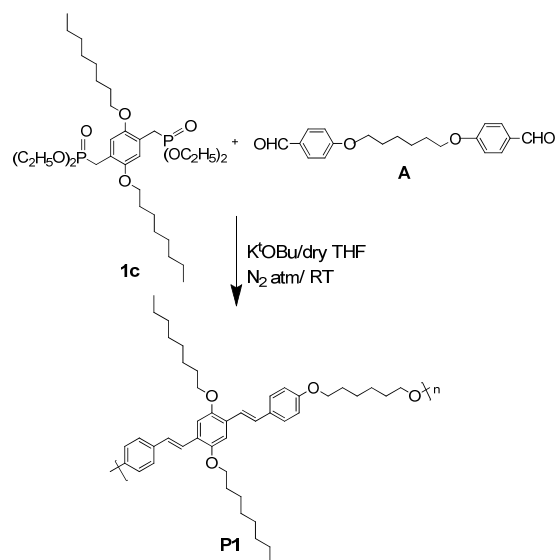
This chapter reports the substituent effects on segmented PPV block copolymers, along with their synthesis, structural, electrochemical, thermal and optical properties. The Voltage vs. Current data was collected to confirm the Schottky diode action. Different types of bulky substituent groups used for current study in order to explore its effects on polymer backbone. Long octyloxy substituent group attached to copolymer **P1** and a bulky (cyclohexylmethoxy) ring substituent group was attached to second copolymer **P2**. In both the polymers, identical spacer (1,6-hexanedioxy) group was introduced. The molecular structure of copolymers **P1** and **P2** are displayed in Figure 3.1. To the best of our knowledge, very few examples of segmented block copolymer bearing bulky ring substituent are known in literature. The copolymers were synthesized by using Horner-Emmons condensation polymerization that could be accomplished under mild conditions at room temperature. Horner-Emmons polycondensation¹⁷ offers a number of important advantages for synthesizing segmented block copolymers with all *trans*-double bonds providing high degree of geometric control from easily accessed dialdehyde and bisphosphonate monomers. This chapter describes a detailed investigations on the optoelectronic, electrochemical and morphological properties by considering the effect of bulky substituent groups attached in their DSB units.

Synthesis of monomer **2c** also followed similar reaction strategies adopted for monomer **1c**. Hydroquinone was reacted with KOH and bromomethylcyclohexane in dimethyl sulphoxide (DMSO) to achieve (dicyclohexylmethoxy) benzene (**2a**) in a Williamson ether formation reaction in satisfactory yields of about 55%. Dibromomethylation of **2a** was carried out in glacial acetic acid using paraformaldehyde and HBr as the bromomethylating agent to form 1,4-bis (bromomethyl)-2,5-bis(cyclohexylmethoxy) benzene (**2b**). Bisphosphonate ester derivative, 2,5-di-*n*-cyclohexylmethoxy-1,4-xylene-diethylphosphonate ester (**2c**) was obtained in high yield (90%) by the reaction of the dibromomethylated derivative with triethylphosphite at 90°C. Long aliphatic chains are the standard flexible unit present in the segmented block copolymers that has previously used for the preparation of various SBCs.^{20,21} Dialdehyde monomer **A** was prepared by condensation of 4-hydroxybenzaldehyde with 1,6-dibromohexane using Williamsons etherification reaction. The structure of the monomers was confirmed by using ¹H NMR spectra.

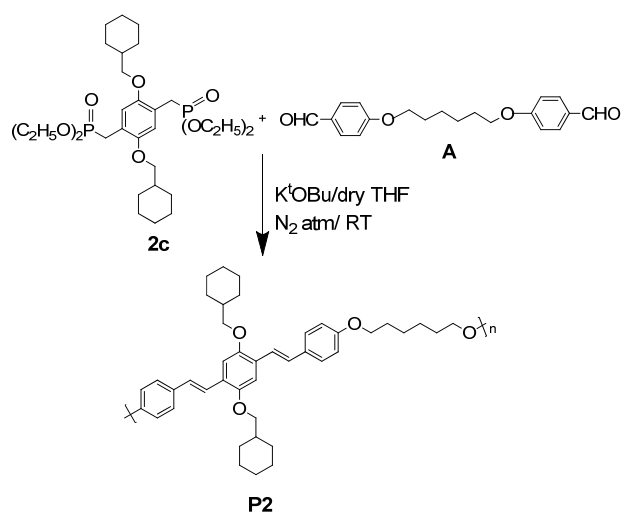
3.2.2 Synthesis of Copolymers

The copolymers were synthesized by Horner-Emmons condensation protocol, which is known to produce *trans*-alkenes. Preparation of copolymers is depicted in Scheme 3.2 and Scheme 3.3 respectively. Specifically, the dialdehyde monomer 1,6-bis(4-formylphenoxy)hexane (**A**) reacted with bisphosphonate ester derivatives such as 2,5-di-*n*-octyloxy-1,4-xylenediethylphosphonate ester (**1c**) and 2,5-di-*n*-cyclohexylmethoxy-1,4-xylenediethylphosphonate ester (**2c**) to afford the copolymers **P1** and **P2**. Polymerization was performed in freshly distilled dry tetrahydrofuran (THF) by adding solid potassium *tert*-butoxide as base to the monomer mixture. The reaction was carried out in 24h under nitrogen atmosphere. The resultant yellow-green copolymer was soluble in THF solvent and hence overall conversion of functional groups was completed more effectively. The work-up procedure consisted of precipitation into methanol followed by sequential extraction with methanol, hexane and finally THF to remove the oligomers and other impurities. THF fraction was collected and again the copolymer was re-

precipitated into methanol. Copolymer **P1** was obtained as yellow solid, while **P2** was obtained as orange solid. Both the copolymers were formed in high yield (89-97%) and were completely soluble in common organic solvents like THF, chloroform, dichloromethane, toluene etc.



Scheme 3.2 Synthesis of copolymer **P1** via Horner-Emmons Condensation Polymerization.



Scheme 3.3 Synthesis of copolymer **P2** via Horner-Emmons Condensation Polymerization.

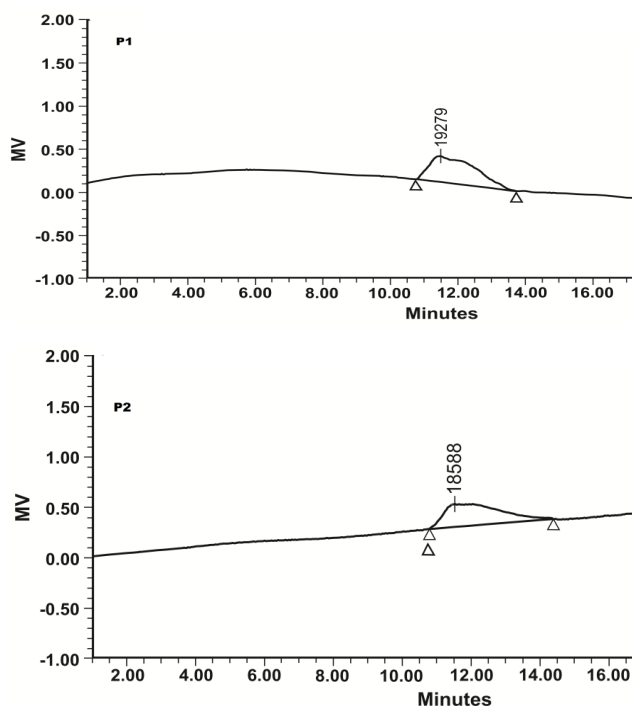


Figure 3.2 Gel permeation chromatograms of **P1** and **P2** (Waters alliance 2690 column with THF as eluent, at a flow rate of 0.5 mL/min at 25⁰C)

The weight average molecular weight (M_w), number average molecular weight (M_n) and polydispersity index of the copolymers were determined by Gel permeation chromatography (GPC) using tetrahydrofuran (THF) as eluent. Figure 3.2 shows the GPC traces of **P1** and **P2**. The weight average molecular weight of **P1** was found to be 14340g/mol⁻¹ and number average molecular weight was observed to be 10453g/mol⁻¹ corresponds to 16 repeating units. The weight average molecular weight of (M_w) of **P2** was 12499g/mol⁻¹ and number average molecular weight (M_n) was 8162g/mol⁻¹ corresponds to 13 repeating units. The low molecular weight of **P2** compared to **P1** is probably due to its early precipitation during polymerization that is induced by the more rigid backbone of **P2**. The polydispersity index (PDI) of **P1** and **P2** are 1.4 and 1.5 respectively and that is exceptional in the case of polycondensation polymerization reactions. The decrease in polydispersity index of these copolymers is

expected to be the consequence of sequential extraction with different solvents such as methanol, hexane and THF. The copolymers can be spin coated onto glass substrate giving highly transparent, pin-holes free and uniform thin films.

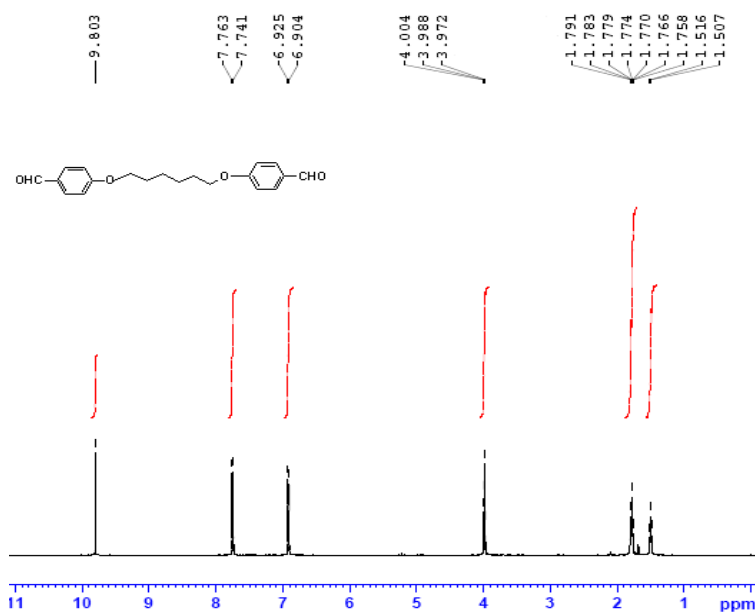
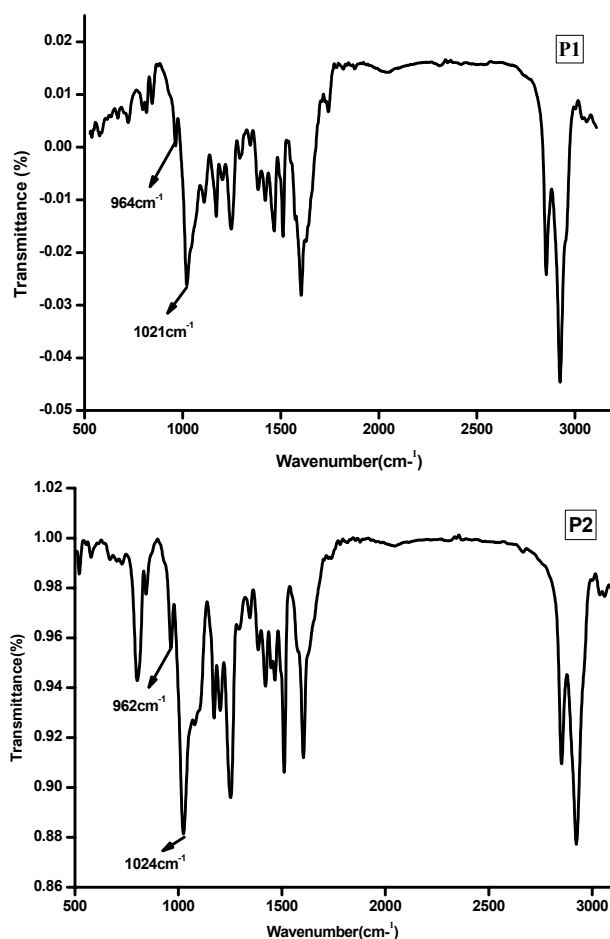


Figure 3.3 ^1H NMR spectrum of dialdehyde monomer (A)

^1H NMR, ^{13}C NMR and FT-IR spectroscopy and elemental analysis were used for the structural characterization of the copolymers. The copolymers **P1** and **P2** synthesized using Horner-Emmons reaction consist of vinylene double bonds having *all-trans* (*E*) configuration, which is clearly shown by FT-IR spectroscopy.¹⁷ FT-IR spectra of copolymers **P1** and **P2** are shown in Figure 3.4. Out-of-plane bending mode of C-H bonds in the *trans*-vinylene groups of copolymer **P1** appears at 964cm^{-1} the same for **P2** appears at 962cm^{-1} . Furthermore characteristic absorption peaks of aldehyde group are completely absent showing complete polymerization. Strong peak at 1021cm^{-1} for **P1** and 1024cm^{-1} for **P2** were interpreted as C–O–C stretching vibrations of aryl-alkyl ether nature of the compounds.

Figure.3.4 FTIR spectra of copolymers **P1** and **P2**

The ^1H NMR spectra of copolymers **P1** and **P2** are shown in Figure 3.5. ^1H NMR spectrum (Figure 3.3) of 1,6-bis(4-formylphenoxy)hexane (**A**) shows a characteristic peak at δ 9.80 assigned to the aldehydic protons. This aldehydic proton peak disappeared after the polymerization. Vinylic and aromatic protons appeared in the δ 6.81-7.39 region. Resonances belonging to *trans*-vinylene protons ($J = 16$ Hz) were found at δ 7.14-7.02 region. Additional signals due to aromatic protons were present at about δ 7.39-6.81 region for both of the copolymers. In the case of **P1**, signal observed in the δ 3.90 region is attributable the methylene protons attached to oxygen. Other aliphatic protons appeared in the δ 0.80 to 2.81 regions. In the case of **P2**, two signals are observed in the δ 3.76 to 4.72 regions. These are attributable to two types of methylene protons attached to

3.2.3 Thermal Analysis of Segmented Block Copolymers

Differential scanning calorimetry (DSC) and thermo gravimetric analysis (TGA) are the most favoured technique used for the quick evaluation of thermal properties of the polymers.

Polymer	Mw (g.mol ⁻¹)	PDI	T _g (°C)	T _m (°C)	T _c (°C)	T _d (°C)
P1	14340	1.4	50	130	85	442
P2	12499	1.5	82	122	-	451

Table 3.1 Physical and thermal properties of **P1** and **P2**

The thermal and physical properties of copolymers are shown in Table 3.1. TGA thermograms of **P1** and **P2** are shown in Figure 3.6. TGA analysis indicates that copolymer **P1** and **P2** are stable up to 326°C and 356°C respectively. The maximum degradation temperature (T_d) of **P1** and **P2** were found to be 442°C and 451°C respectively. Thus, the better rigidity shown by **P2** is as a result of larger steric hindrance produced by cyclohexylmethoxy substituent compared to octyloxy substituent present in **P1**. Weight loss of copolymers at different temperature ranges are displayed in Table. 3.2. Major weight losses of copolymers are seen at 500°C, where as **P2** shows 66% weight loss and **P1** shows 82% weight loss. Therefore copolymer **P2** shows higher thermal stability than **P1**.

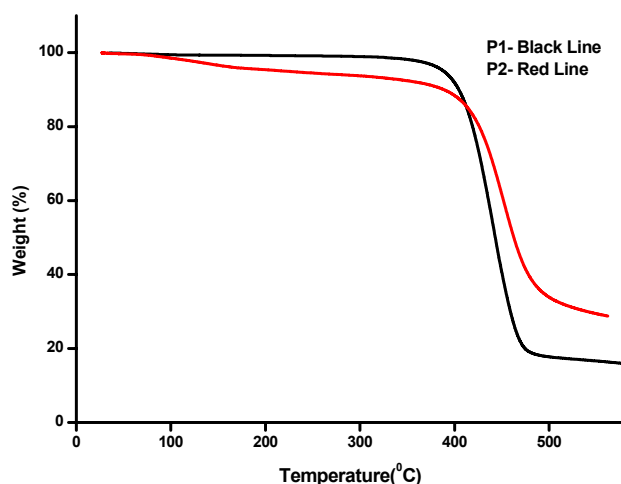


Figure 3.6 TGA thermograms of **P1** and **P2**

Code of copolymer	Weight loss (%) for temperature ranges		
	200 ⁰ C	400 ⁰ C	500 ⁰ C
P1	.7%	8.13%	82.24%
P2	4.61%	11.6%	66.12%

Table 3.2 Weight loss (%) of copolymers at different temperatures (From TGA results)

Glass transition temperature (T_g), melting temperature (T_m), crystallization temperature (T_c) of the copolymers were determined by DSC in nitrogen atmosphere at a heating rate of 10°C/min. Figure 3.7 shows the DSC thermograms of **P1** and **P2**. T_g of **P1** and **P2** are found to be 50⁰C and 82⁰C respectively. T_g of **P2** is considerably higher than that of **P1** because of the influence of rigid bulky cyclohexylmethoxy groups present in the distyrylbenzene block. In the case of **P1**, T_g diminishes systematically as the length of the soft block (hexamethylene spacer) increases. This is because, the octyloxy substituent groups in the 2,5 positions of the distyrylbenzene block is sufficiently long and flexible to plasticize the methylene spacer block.²² Hence octyloxy groups act as a plasticizer as its shape is analogous to the soft methylene spacer block. Higher T_g value of **P2** indicates the suitability of this copolymer in optoelectronic devices with higher stability and life-time. **P1** gives a broad melting temperature (T_m) at 130⁰C and a broad crystallization temperature (T_c) at 85⁰C. These broad melting temperature and crystallization temperature are also account for the presence of crystalline regions in copolymer **P1**. Copolymer **P2** shows a sharp T_m at 122⁰C but no crystallization temperature was observed during the cycle. Due to the presence of melting temperature and crystallization temperature confirms that the copolymer **P1** was expected to be more crystalline compared to **P2**. Observance of both T_g and T_m shows semicrystalline nature of these copolymers.

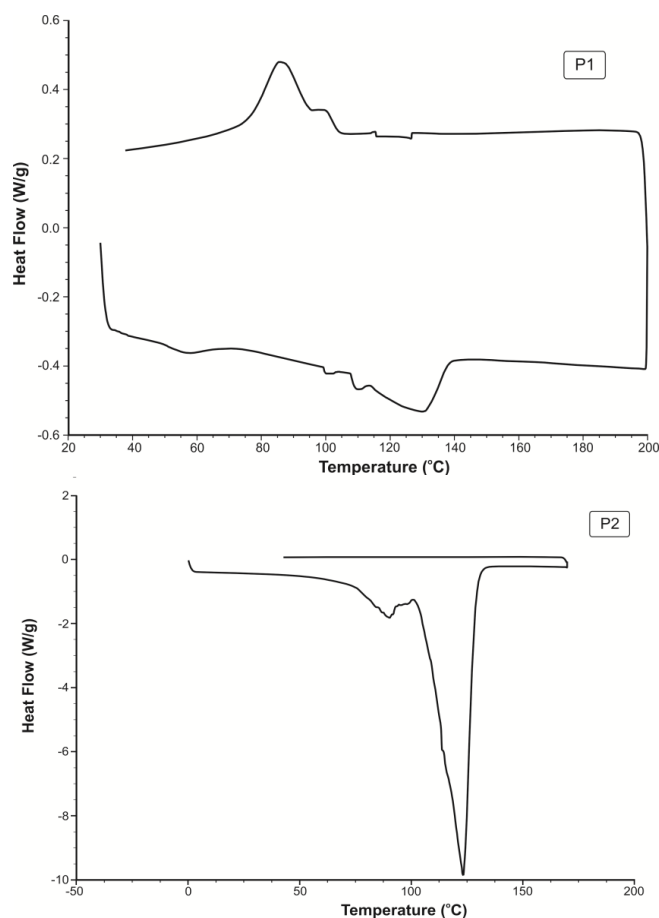


Figure.3.7 DSC thermograms of **P1** and **P2**

3.2.4 X-ray diffraction (XRD) studies

Powder X-ray diffraction (XRD) [Rigaku X-ray diffractometer, Cu-K α radiation (1.542Å)] was used to investigate the molecular organization of the copolymers. Powder XRD pattern for **P1** and **P2** is shown in Figure 3.8. **P1** and **P2** show a first peak with d-spacings values and its corresponding 2θ values are $d_1=7.44\text{Å}^0$ ($2\theta=11.9^0$) and $d_1=7.78\text{Å}^0$ ($2\theta=11.25^0$) respectively. This sharp peak is due to interchain scattering of two main chain backbones separated by bulky substituents which also confirms the side chain related semicrystalline nature of these copolymers.²³ The second amorphous-halo peak of **P1** and **P2** at $d_2=3.74\text{Å}^0$ ($2\theta=24^0$) and $d_2=4.27\text{Å}^0$ ($2\theta=23^0$) respectively arise from the side-to-side distance

between the bulky side groups.²⁴ Copolymer **P2** shows a slightly larger d-spacing than **P1** because of less coplanar backbone structure of **P2** in its powder form.

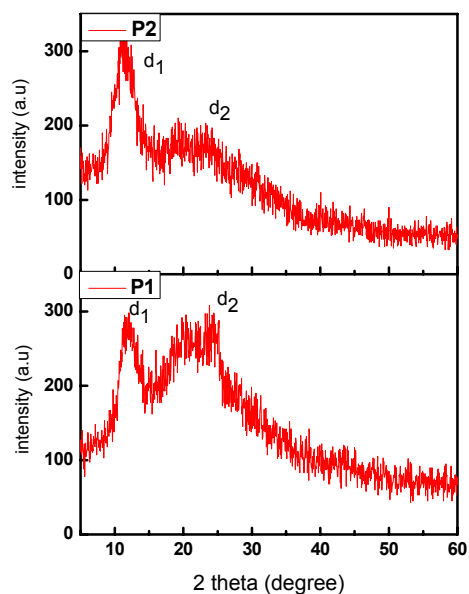


Figure 3.8 Powder XRD patterns of **P1** and **P2**

3.2.5 Scanning electron microscopy (SEM)

The morphology of the polymers was determined in a powder form by scanning electron microscopy (Hitachi FESEM SU6600). SEM images for **P1** and **P2** are included in Figure 3.9. From this figure, significant difference in the morphology of the copolymers is discernible. Long octyloxy chain substituted **P1** has flake like morphology and bulky rigid ring substituted **P2** seems to possess inter-connected small rod like morphology. From SEM images, **P1** appears to be more crystalline in nature than **P2**, in agreement with DSC data.

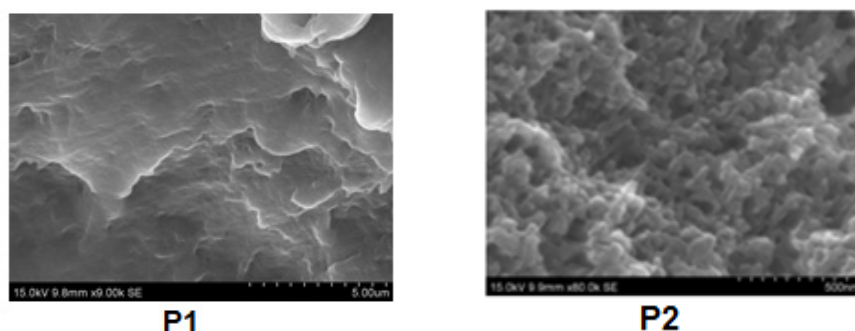


Figure 3.9 SEM micrographs of **P1** and **P2** in powder form

3.2.6 Photophysical studies

The UV-Vis spectra and photoluminescence spectra corresponding to **P1** and **P2** in dichloromethane are shown in Figure 3.10.

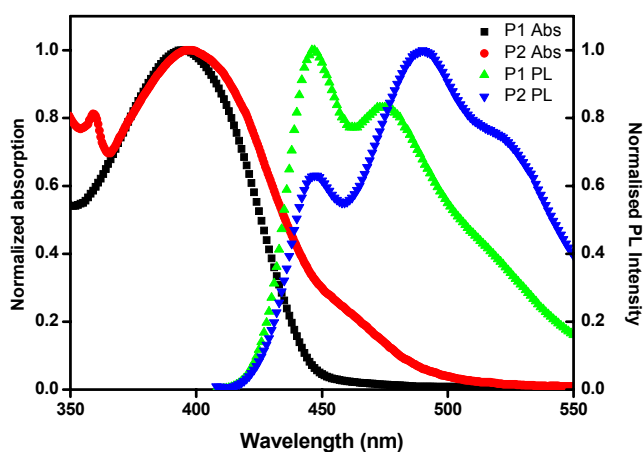


Figure 3.10 Normalized UV-Vis spectra and photoluminescence spectra of **P1** and **P2** in dichloromethane (10^{-2} mg/mL) at room temperature (excitation wavelength used for **P1** is 394nm and **P2** is 397nm)

UV-Vis absorption and photoluminescence spectral data for **P1** and **P2** in dichloromethane solution and thin film forms are displayed in Table 3.3.

Copolymer	UV-Vis (nm)		PL (nm)		E_g^{OP} (eV)	Fluorescence quantum yield (Φ_F)
	Solution	Film	Solution	Film		
P1	394	411	446,475	492	2.75	0.113
P2	397	412	446,489,521	527	2.46	0.138

Table 3.3 Photophysical data of **P1** and **P2**

In solution state, **P1** and **P2** show an absorption peak at about 393nm and 397nm, respectively. This absorption was assigned to the π - π^* transition of the conjugated backbone. The shape of the absorption spectrum of both copolymers are almost the same but a slight red shift (~3nm) can be observed in the absorption tail of **P2** which may be due to the presence of strain induced molecular structural packing of this copolymer.²⁵ Figure 3.11 shows that the light emissions of **P1** and **P2** under UV irradiation at 365nm. Photoluminescence spectrum of **P1** in dichloromethane at room temperature, a major emission band at 446nm and a shoulder at 475nm can be seen. **P2** shows a major emission band at 489nm and two shoulder bands at 446nm and 521nm. The emission maximum of copolymer **P2** is red shifted by 43nm with respect to that of with **P1**. First two emission peaks present in **P1** and **P2** originate from the individual distyrylbenzene units and the third peak present in **P2** is a result of aggregation of chromophore groups in the backbone. The optical band gaps of **P1** and **P2** was calculated from the onset of the absorption spectra in dichloromethane solution, values are found to be 2.75eV and 2.46eV respectively. A significant variation can be observed in the band-gaps of **P1** and **P2**. The lower band-gap of **P2** is due to the introduction of steric strain induced effect of cyclohexylmethoxy groups present in the backbone. Hence, the band-gap could be effectively tuned by changing the bulky groups present in the SBC backbone which also enhanced the solubility of the polymers. The UV-Vis spectra and photoluminescence spectra of **P1** and **P2** in thin film forms are depicted in Figure 3.12. **P1** and **P2** show absorption maximum at 411nm and 412nm, respectively. The emission maxima of **P1** and **P2** can be seen at 492nm and 527nm, respectively. Emission spectrum of **P2** in film state is shifted towards the red region (bathochromic shift) compared to **P1** same as in solution state. The photoluminescence spectra of the copolymers in film state red-shifted much more compared to their solution counterparts. A possible explanation for this bathochromic shift is based on close packing of polymeric molecules in their condensed state. This close packing leads to interchain interactions within the polymeric molecules resulting in the lowering of transition

energy.²⁶ **P1** emits very intense blue light whereas **P2** emits intense bluish-green light by suitable engineering of their band-gaps.

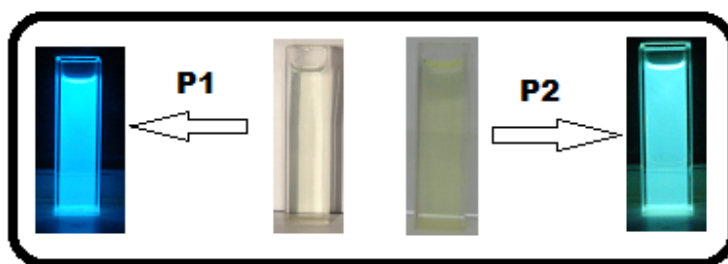


Figure 3.11 Light emissions of **P1** and **P2** under UV irradiation at 365nm

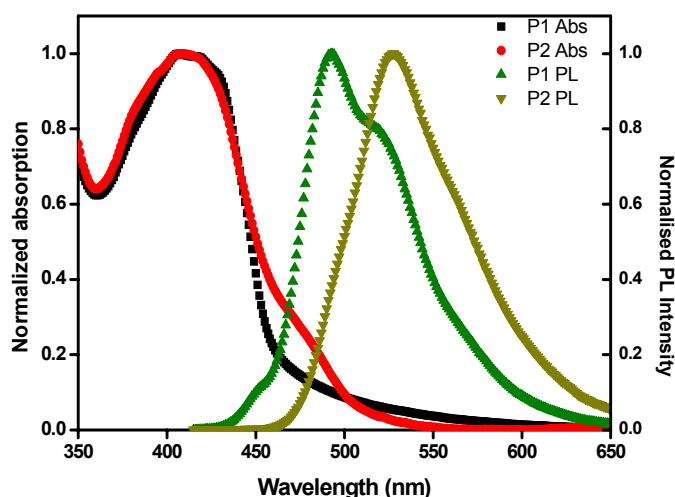


Figure 3.12 Normalized UV-Vis spectra and photoluminescence spectra of **P1** and **P2** thin films (excitation wavelength used for **P1** is 411 nm and **P2** is 412 nm)

3.2.6.1 Fluorescence quantum yield of copolymers

Fluorescence quantum yield (Φ_F) is an intrinsic property of a fluorophore and is important for the characterization of novel fluorescent molecules. It is the ratio of number of photons emitted to the number of photons absorbed by the sample. The quantum yield can also be described as the relative rates of radiative and non-radiative relaxation pathways, which deactivate the excited state. The most reliable method used for the determination of fluorescence quantum yield is the comparative method of Williams et al. It is easier to determine the relative

quantum yield of a fluorophore by comparison to a reference fluorophore with known quantum yield.²⁷ Solutions of the standard and the test samples with identical absorbance at the same excitation wavelength can be supposed to be absorbing the same number of photons. In-order to minimize re-absorption effects the absorbance should never exceed 0.1 at and above the excitation wavelength. Hence, a simple ratio of fluorescence intensities of the two solutions recorded under same conditions will yield the ratio of the quantum yield values.²⁸ Fluorescence quantum yield (Φ_F) calculated by using following equation:

$$\Phi_X = \Phi_{ST} \frac{(\text{Grad}_X) (\eta^2_X)}{(\text{Grad}_{ST}) (\eta^2_{ST})}$$

Where the subscripts ST and X denote standard and test samples respectively, 'Grad' is the gradient from the plot of integrated fluorescence intensity vs. absorbance and η is the refractive index of the solvent. The comparative quantum yield of the block copolymers **P1** and **P2** were determined by using coumarin-481 dye as the standard. Reported fluorescence quantum yield (Φ_F) of coumarin-481 in ethanol was 0.08.²⁹ The excitation wavelength was 398nm. The fluorescence quantum yield (Φ_F) of **P1** and **P2** was found to be 0.11 and 0.14 respectively in dichloromethane solution. Both of the copolymers **P1** and **P2** show excellent quantum yield in dichloromethane, when they are compared to coumarin-481 dye. Copolymer **P2** shows improved fluorescence quantum yield (Φ_F) than **P1**, due to the presence of rigid ring substituent present in its distyrylbenzene (DSB) units. The fluorescence quantum yield (Φ_F) of **P1** and **P2** indicates that both of the block copolymers are very attractive for optoelectronic applications.

3.2.7 Electrochemical studies

HOMO-LUMO levels of the polymers were analyzed using a BAS CV50W voltammetric analyzer. Polymers were dissolved in dichloromethane containing 0.1M tetra-*n*-butylammonium hexafluorophosphate as supporting electrolyte. A platinum disc electrode was used as working electrode and a

platinum wire was used as counter electrode and the potentials were referred to Ag/AgCl (calibrated against the FC/FC⁺ redox system) was 4.8eV below vacuum levels. Ferrocene was used as external standard. Figure 3.13 shows the cyclic voltammogram of ferrocene/ferrocenium (FOC) system. E_{foc} is the arithmetic average of the reduction and oxidation potential of FOC versus Ag/AgCl. According to our test, cyclic voltammogram of ferrocene/ferrocenium shows two peaks at 0.36V and 0.55V hence E_{foc} is equal to 0.46 V which can be used in equation to calculate the E_{HOMO} and E_{LUMO}. The estimations were done with the empirical relations,³⁰

$$E_{\text{HOMO}} = (\text{IP}) \text{ eV} = -e (E_{\text{ox, on}} - E_{\text{foc}}) - 4.8$$

$$E_{\text{LUMO}} = (\text{EA}) \text{ eV} = -e (E_{\text{re, on}} - E_{\text{foc}}) - 4.8.$$

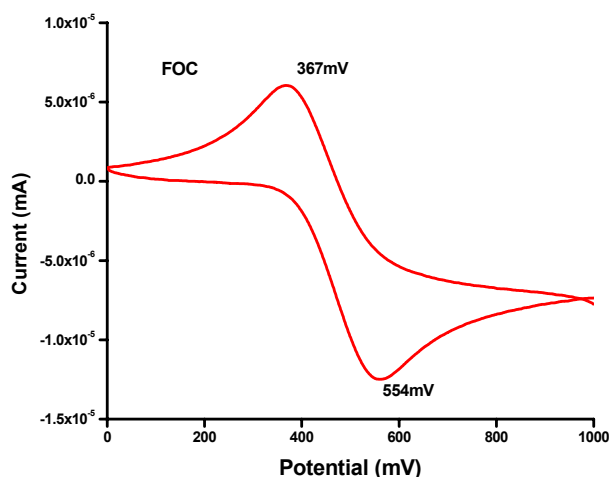


Figure 3.13 Cyclic voltammogram of ferrocene/ferrocenium (FOC)

The *p-doping* and *n-doping* processes occur under the anodic and cathodic scans. Figure 3.14 shows the current-voltage curve for **P1** and **P2** from the cyclic voltammetry measurements. The shape of cyclic voltammogram of **P1** and **P2** are found to be similar.

Copolymer	E _{ox, on} (V)	E _{re, on} (V)	HOMO (eV)	LUMO (eV)	E _g ^{EC} (eV)
P1	0.920	-1.827	-5.260	-2.513	2.74
P2	0.675	-1.751	-5.016	-2.588	2.42

Table 3.4 Electrochemical data of **P1** and **P2**

Electrochemical data of **P1** and **P2** are displayed in Table 3.4. On the base of the measured oxidation potentials, HOMO (IP) levels of **P1** and **P2** have been estimated to be $\sim 5.260\text{eV}$ and $\sim 5.016\text{eV}$. Similarly from measured redox potentials, the LUMO (EA) levels of **P1** and **P2** have been calculated to be $\sim 2.513\text{eV}$ and $\sim 2.588\text{eV}$ respectively. The electrochemical band gap (E_g^{EC}) was calculated from the equation,

$$E_g^{\text{EC}} = e (E_{\text{ox, on}} - E_{\text{re, on}})$$

The electrochemical band gap of **P1** and **P2** was found to be 2.74eV and 2.42eV respectively. The band gap obtained from CV was very close to the optical band gap derived from UV-Vis spectra (as shown in Table 3.3).

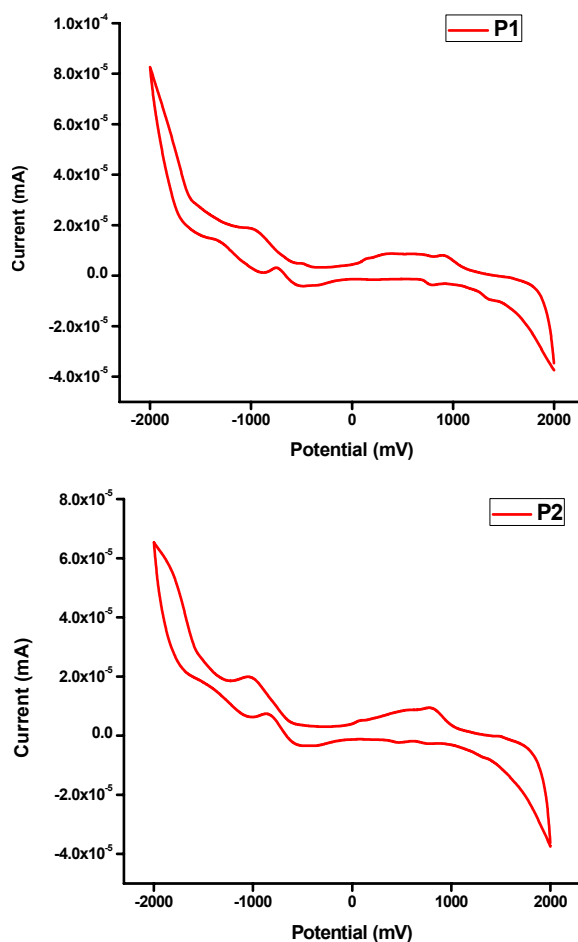


Figure 3.14 Cyclic voltammograms of **P1** and **P2** prepared in dichloromethane containing 0.1M tetra-n-butyl ammonium hexafluoro-phosphate as supporting electrolyte

***3.2.8 Measurement of I-V characteristics**

The thin films **P1** and **P2** made from dichloromethane were spin cast (SPS Spin wafer 150, 2000 rpm, 30s) from solutions on top of Indium Tin Oxide (ITO) coated glass plates which is the anode. Aluminium contacts (top-electrode as cathode) were made on top of the spin coated copolymer layers by thermal evaporation to form a Schottky (metal-semiconductor) junction.³¹ The current-voltage characteristics were analyzed using Keithley 2400 source meter (2-point probe method) for the two diode configurations to confirm the formation of metal-semiconductor junction. The current-voltage (I-V) characteristics of the devices with the configuration of ITO/copolymer/Al are shown in Figure 3.15. Forward bias current was obtained, when the ITO electrode was positively biased and the Al electrode was negatively biased. Therefore the current increased with increasing the forward bias voltage, which is mandatory for the fabrication of polymer light emitting diodes. Both of the copolymers exhibit very low onset voltage i.e. **P1** shows 2.71V and **P2** gives 1.65V. Figure 3.16 shows a three dimensional atomic force microscopy (AFM) image of the spin coated film of polymers **P1** and **P2** from dichloromethane solution. The thickness of the films thus obtained was measured using Dektak 6M stylus profilometer and films with thickness 50 nm (± 5 nm). AFM analysis show that polymers have smooth surface with the root mean square (RMS) value of **P1** gives 1.38nm and **P2** gives 5.541nm.

* The device fabrication and related characterizations are carried out in collaboration with Department of Physics, CUSAT

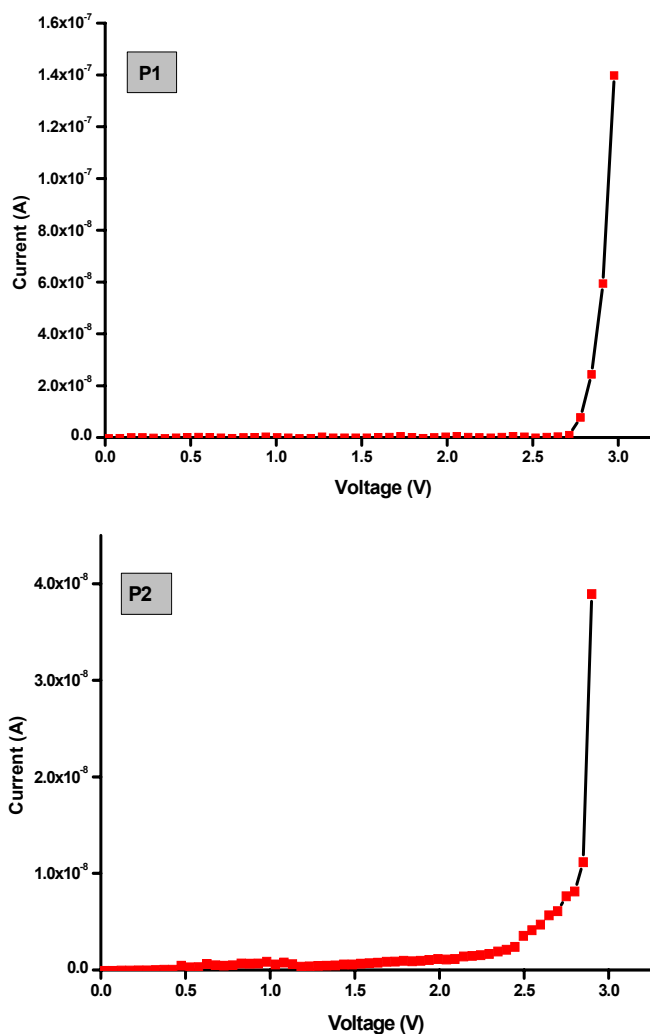


Figure 3.15 I-V characteristics of ITO /copolymer/Al devices of **P1** and **P2**

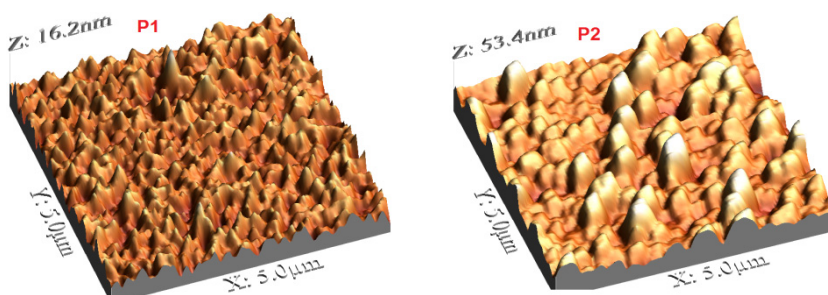


Figure 3.16 Three dimensional atomic force microscopy image of the spin coated film of **P1** and **P2**.

Figure 3.17 shows the energy diagram of ITO/Copolymer/Al device configuration of **P1** and **P2**. The barrier heights of the copolymers were found to be 0.56eV and 0.31eV at the interface of ITO (4.7eV)/HOMO state for holes and 1.69eV and 1.62eV at the interface of Al (4.2eV)/LUMO for electrons. The HOMO level of both polymers is very close to the work function of ITO which enables the effective supply of holes through ITO. An intermediate layer between the emissive polymer and ITO can also be avoided as a result of this. From the energy band diagram, one can assume that both copolymers easily injected holes from the ITO electrode than that of electron from the Al electrode. These results are well coincide with the turn-on voltage of the copolymers. Therefore we can conclude that the required energy levels and good film forming property of these copolymers are fulfilled for fabricating PLEDs.

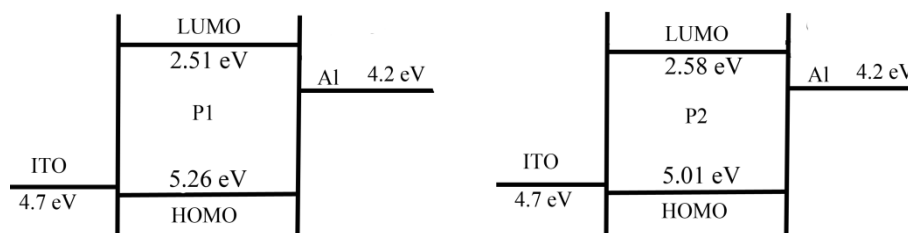


Figure 3.17 The energy diagram of ITO/Copolymer/Al devices of **P1** and **P2**

3.3 Conclusions

The focus and trust of this chapter is to address a substituent's effects on the synthesis and properties of new segmented block PPV copolymers. Using this approach, long octyloxy chain substituted segmented copolymer **P1** and rigid cyclohexylmethoxy ring substituted **P2** were synthesized by Horner-Emmons condensation polymerization. ^1H NMR, ^{13}C NMR and FTIR spectra of the polymers are consistent with their expected molecular structures. The resulting copolymers are soluble in common organic solvents and easily spin-cast onto indium–tin oxide (ITO) substrate without any defects. The Horner-Emmons methodology yielded copolymers with relatively good molecular weights and narrow molecular weight distribution. Differential scanning calorimetric

measurements show that placement of bulky ring groups in **P2** on its DSB chromophoric fragment alter the glass transition temperature at 82°C but that placement of long octyloxy groups present in **P1** lowers the glass transition substantially at 50°C. The decrease in T_g of **P1** is attributable to copolymer self-plasticization by the octyloxy groups. Due to structural rigidity, **P2** shows enhanced thermal stability than **P1**. Comparative fluorescent quantum yield studies show that both copolymers give excellent fluorescent quantum yield in dichloromethane solution. An effective tuning of band-gap could be achieved by changing the substituted bulky groups present in the copolymer backbone thereby altering the blue emission in **P1** to bluish-green emission in **P2**. The I-V measurements and their corresponding energy band diagrams also confirm the suitability of these copolymers in optoelectronic applications such as PLEDs.

3.4 Experimental Section

3.4.1 General Techniques

All reactions were performed in oven-dried glassware under a nitrogen atmosphere with magnetic stirring unless otherwise noted. Reagents and solvents were purchased from commercial suppliers and were used without further purification. Solvents used for experiments were distilled and dried according to procedures given in standard manuals. All reactions were followed by TLC to completion. TLC analysis was performed by illumination with a UV lamp (254 nm) or staining with Iodine. All Column chromatography was performed with 60-120 mesh silica gel purchased from SD fine - chem. limited, as the stationary phase. ^1H NMR spectra were recorded on a Bruker Avance III 400 MHz instrument in CDCl_3 , and chemical shifts were measured relative to residual solvent peak (δ 7.26). The following abbreviations were used to describe coupling: s = singlet, d = doublet, t = triplet, q = quartet, m = multiplet. ^{13}C NMR spectra were recorded on Bruker Avance III instruments at 100 MHz with chemical shifts relative to residual solvent peak (δ 77.0). FTIR spectra were recorded using KBr pellet technique on a Thermo Nicolet, Avatar 370 spectrometer. Melting points of

the compounds were recorded on a Fisher-Johns melting point apparatus. The elemental analysis was carried out by Elementar Vario EL III analyzer. The absorption and fluorescence spectra were recorded using UV-Visible spectrophotometer (JASCO V-570) and Fluoromax-3 fluorimeter was used to record the fluorescence spectra of the samples, respectively. The electrochemical cyclic voltammetry (CV) was conducted on a BAS CV50W voltammetry analyzer. Polymers were dissolved in dichloromethane containing 0.1M tetra-n- butyl ammonium hexafluoro-phosphate as supporting electrolyte, at a scanning rate of 10mV/s at room temperature under the protection of argon. The Powder X-ray diffraction (XRD) patterns were obtained using a (Rigaku X-ray diffractometer with Cu K α radiation (1.542Å). The molecular weight of the synthesized polymers was determined by GPC, (Waters alliance 2690) using a column packed with polystyrene gel beads. The polymer was analyzed using tetrahydrofuran (THF) as eluent, at a flow rate of 0.5 mL/min at 25⁰C. The molecular weight was calibrated using polystyrene standards. Glass transition temperature was determined from differential scanning calorimeter (DSC), (Q-100, TA Instruments) under nitrogen at heating rate of 10⁰C/min. Thermal stability was determined from thermo gravimetric analyzer (TGA), (Q-50, TA Instruments) under nitrogen at a heating rate of 10⁰C/min. Homogeneous and good quality thin films in nanometer thickness scales were obtained by spin coating (SPS Spin wafer 150) the solution at different spin speeds in different durations on ultrasonically cleaned glass substrates. The thickness of the films measured by Dektak 6M stylus profiler. The morphology of the polymers was determined by Scanning Electron Microscopy (SEM) (Hitachi FESEM SU6600). Atomic force microscopy image of copolymer film was analyzed by Park systems XEI 100 AFM. The current-voltage characteristics were analyzed using Keithley 2400 source meter (2-point probe method).

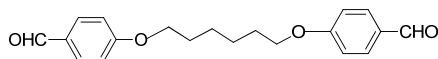
3.4.2 Materials

All reactions were carried out in oven-dried glassware using reagents and chemicals as commercially supplied from Aldrich and Merck unless otherwise noted. Tetrahydrofuran (THF) was distilled from calcium hydride and then from sodium/benzophenone ketyl. Dimethyl sulfoxide (DMSO) and dimethylformamide (DMF) were distilled prior to use. Hydroquinone, bromomethylcyclohexane, triethyl phosphite, 4-hydroxybenzaldehyde, 1,6-dibromohexane, and potassium *tert*-butoxide were purchased from Aldrich Chemicals. HBr in glacial acetic acid, paraformaldehyde and all other reagents/solvents were purchased locally and purified by following the standard procedures. All reactions were followed by TLC to completion.

3.4.3 Synthesis of monomers

3.4.3.1 Synthesis of dialdehyde monomer: 1,6-bis (4-formylphenoxy)hexane (A)

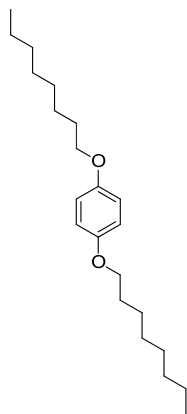
This compound was synthesized according to the reported procedure with slight modifications.³² A solution of 4-hydroxybenzaldehyde (4g, 0.3mol) and 1,6-dibromohexane(3g, 0.1mol) in 50mL distilled DMF was stirred and heated to reflux. A total of 3g potassium carbonate was added in small portions; the solution was stirred and refluxed for 24h. The resulting mixture was poured into 1L distilled water and the precipitate was collected after standing for 4h, dried in air at ambient temperature and purified by recrystallizing from methanol. The yield of dialdehyde was 75% with mp 78-80°C.



¹H NMR (400 MHz, CDCl₃) δ (ppm): 9.80 (s, 2H), 7.74-7.76 (d, 4H), 6.90-6.92 (d, 4H), 3.97-4.00 (t, 4H), 1.75-1.79 (m, 6H), 1.50-1.51(d, 2H).

3.4.3.2 Synthesis of 1,4-dioctyloxybenzene (1a)

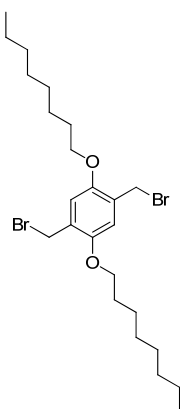
To 100mL freshly distilled dimethyl sulfoxide (DMSO), powdered potassium hydroxide (10g, 0.17mol) was added with violently stirring for half an hour under nitrogen atmosphere. Hydroquinone (3 g, 0.02mol) then *n*-octyl bromide (10mL, 0.5mol) was added drop wise to the reaction mixture. The reaction proceeded for 24h at 80⁰C temperature and then the mixture was poured into large amount of distilled water. Light-yellow solid was obtained as the crude product after filtration. Silky white solid was afforded after the crude product was re-crystallized from ethanol and finally dried under vacuum. Yield: 89%, mp: 56⁰C.



¹H NMR (400MHz, CDCl₃, δ): 6.76 (s, 4H), 3.75–3.8 (t, 4H), 1.40–1.72 (m, 24H), 0.92–1.00 (t, 6H).

3.4.3.3 Synthesis of 1,4-bis(bromomethyl)-2,5-bis(octyloxy)benzene (1b)

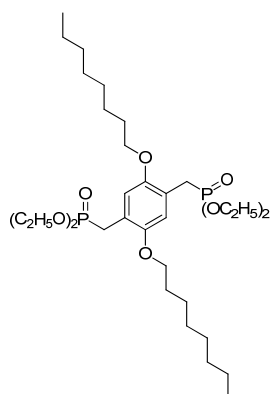
A mixture of compound **1a** (2.9g, 0.01mol) and paraformaldehyde (1.5g, 0.05mol) in 70mL of glacial acetic acid were taken in a 250mL two-neck flask. HBr in glacial acetic acid (5mL, 30-33wt %) was added drop wise to the above solution at 0⁰C and stirred for 0.5h under N₂ atmosphere. It was gradually heated to 80⁰C and stirred for an additional 4h. The light brown colored reaction mixture was cooled and filtered, and the solid was washed with water until the filtrate was neutral. The solid was dissolved in 100mL of dichloromethane and washed with NaHCO₃ solution and saturated brine solution. The organic layer was separated and dried over anhydrous Na₂SO₄, and the solvent was evaporated to obtain the product as a white crystalline solid, Yield 3.8g (71%).



$^1\text{H NMR}$ (400MHz, CDCl_3 , δ): 6.86 (s, 2H), 4.53 (s, 4H), 3.89 (t, 4H), 1.75-0.92 (m, 30H).

3.4.3.4 Synthesis of 2,5-di-*n*-octyloxy-1,4-xylene diethylphosphonate ester (**1c**)

A mixture of 1,4-bis(bromomethyl)-2,5-bis(octyloxy)benzene (**1b**) (3g, 5.75 mmol) and triethyl phosphite (5mL, 30mmol) was heated at 90°C for 2h under nitrogen atmosphere. Excess triethyl phosphite was separated by vacuum distillation. Product **1c** was obtained as colourless thick oil (90%). It was used without any further purification.

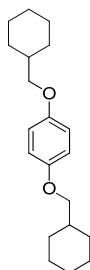


$^1\text{H NMR}$ (400 MHz, CDCl_3) δ (ppm): 6.92 (s, 2H), 4.02 (q, 8H), 3.92 (t, 4H), 3.28 (d, 4H) 1.77 (q, 4H), 1.29-1.24 (m, 32H), 0.89 (t, 6H).

3.4.3.5 Synthesis of 1,4-bis(cyclohexylmethoxy)benzene (**2a**).

Hydroquinone (3g, 0.02mol) and powdered potassium hydroxide (11.2g, 0.20mol) were taken in a 250mL flask containing 50mL distilled DMSO and the mixture was heated under nitrogen atmosphere for 30 minutes. Bromomethylcyclohexane (10mL, 0.056mol) was added and heated at 80°C for 36h under nitrogen atmosphere. It was cooled and poured into excess water and extracted into dichloromethane. The organic layer was washed with NaOH followed by brine solution and dried over anhydrous Na_2SO_4 , and the solvent was

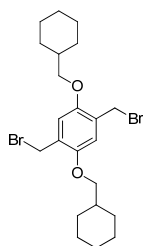
evaporated. The crude product was further purified by passing through a silica gel column using 5% CH₂Cl₂ in hexane as the eluent. Yield: 55%. mp: 120⁰C



¹H NMR (400 MHz, CDCl₃) δ (ppm): 6.80 (s, 4H), 3.68-3.70 (d, 4H), 0.98-2.17 (m, 22H).

3.4.3.6 Synthesis of 1,4-bis(bromomethyl)-2,5-bis(cyclohexylmethoxy)benzene (2b).

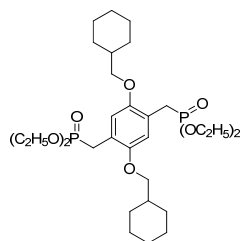
A mixture of compound **2a** (4.5g, 0.01mol) and paraformaldehyde (1.5g, 0.05mol) in 50mL glacial acetic acid was taken in a 250mL two-neck flask. HBr in glacial acetic acid (5mL, 30-33wt %) was added drop-wise to the above solution at 5°C and stirred for 30 minutes under nitrogen atmosphere. It was gradually heated to 80°C and stirred for additional 4h. The brown coloured reaction mixture was cooled and filtered, and the solid was washed with water until the filtrate was neutral. The solid was dissolved in 100mL dichloromethane and washed with NaHCO₃ solution and saturated brine solution. The organic layer was separated and dried over anhydrous Na₂SO₄, and the solvent was evaporated to obtain white crystalline solid. Yield: 70%. mp: 155°C.



¹H NMR (400 MHz, CDCl₃) δ (ppm): 6.78 (s, 2H), 4.53 (s, 4H), 3.76-3.78 (d, 4H), 1.62-1.84 (m, 14H), 0.98-1.29 (m, 8H).

3.4.3.7: Synthesis of 2,5-di-n-cyclohexylmethoxy-1,4-xylene-diethylphosphonate ester (2c):

A mixture of 1,4-bis (bromomethyl)-2,5-bis (cyclohexylmethoxy) benzene (**2b**) (4g, 0.01mol) and triethylphosphite (15mL, 0.09mol) was heated to 90°C for 2h under nitrogen atmosphere. Excess triethylphosphite was separated by vacuum distillation. The product **2c** was obtained as light yellow thick oil (90%). It was used without any further purification.

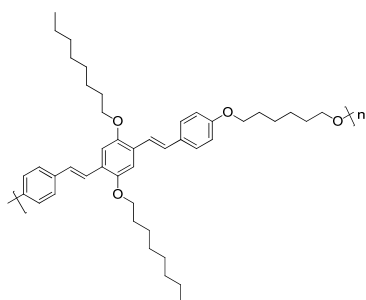


$^1\text{H NMR}$ (400 MHz, CDCl_3) δ (ppm): 6.80 (s, 2H), 3.90-4.05 (m, 8H), 3.58-3.63 (t, 4H), 3.11-3.16 (d, 4H), 1.62-1.78 (m, 22H), 1.24-1.26 (m, 14H).

3.4.4 Synthesis of Polymers Using Horner-Emmons Polycondensation Reaction

3.4.4.1 Synthesis of Poly[1,6-hexanedioxy-(1,4phenylene)-1,2-ethynylene-(2,5-dioctyloxy-1,4 phenylene)-1,2ethynylene-(1,4phenylene)] (PI)

A solution of 0.25g potassium *tert*-butoxide in anhydrous freshly distilled tetrahydrofuran (THF) was added to a stirred solution of (1g, 1.5mmol) of the 2,5-di-*n*-octyloxy-1,4-xylenediethylphosphonate ester monomer (**1c**) and (0.25g, 0.76mmol) dialdehyde monomer (**A**) in 10mL distilled THF at room temperature. The mixture was stirred for 24h under nitrogen atmosphere. A viscous yellow-green precipitate was formed. The reaction mixture was transferred to methanol while stirring. The polymer is obtained after drying and removing the solvent. On crude polymer mixture, sequential extraction was performed with methanol, hexane and THF. The copolymer was recovered from the THF fraction by using rotary evaporation. The resultant yellow solid was dried under vacuum over night. The yield was 97%.



$^1\text{H NMR}$ (400 MHz, CDCl_3) δ (ppm): 6.80-7.39 (m, 14H), 3.93-3.98 (m, 8H), 1.80-1.23 (m, 32H), 0.79-0.83 (m, 6H).

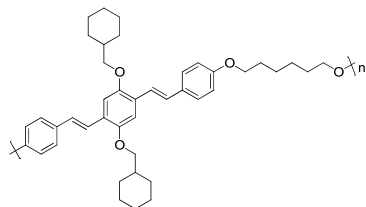
$^{13}\text{C-NMR}$ (100MHz, CDCl_3) δ (ppm): 158.69, 150.98, 130.77, 128.19, 127.68, 126.91, 121.40, 114.70, 110.5, 69.67, 67.92, 31.83, 29.56, 29.44, 29.32, 29.27, 26.31, 25.92, 22.69, 14.11.

IR (KBr) ν : 2924, 2854, 1604, 1512, 1467, 1421, 1385, 1248, 1203, 1172, 1021, 64, 845, 816, 797, 723, 670 cm^{-1} .

Anal. Calcd. For $\text{C}_{44}\text{H}_{60}\text{O}_4$: C 80.98, H 9.20; Found: C 80.44, H 8.37.

3.4.4.2 Synthesis of Poly [1,6-hexanedioxy-(1,4phenylene)-1,2ethenylene-(2,5-dicyclohexyl methoxy-1,4phenylene)-1,2ethenylene-(1,4phenylene)](P2)

A solution of 0.25g potassium *tert*-butoxide in anhydrous freshly distilled tetrahydrofuran (THF) was added to a stirred solution of 1.5g (2.4mmol) of 2,5-di-*n*-cyclohexylmethoxy-1,4-xylene-diethylphosphonate ester monomer (**2c**) and 0.6g (1.8mmol) of dialdehyde monomer (**A**) in a 10mL distilled THF at room temperature. The mixture was stirred for 24h under nitrogen atmosphere. A viscous orange colour precipitate was formed. The reaction mixture was transferred to methanol while stirring. The polymer is obtained after drying and removing the solvent. After that sequential extraction were performed with methanol, hexane and THF. The copolymer was recovered from the THF fraction by using rotary evaporation. The product was obtained as orange solid and the yield was 89%.



¹H NMR (400 MHz, CDCl₃) δ (ppm): 6.81-7.39 (m, 13H), 4.70-4.71(d, 4H), 3.92-3.95 (t, 4H), 1.06-2.20 (m, 32H).

¹³C-NMR (100MHz, CDCl₃) δ (ppm): 157.68, 150.20, 150.11, 134.82, 129.82, 129.17, 127.23, 126.65, 125.89, 124.40, 120.48, 113.75, 113.13, 109.93, 109.65, 74.15, 66.94, 37.18, 37.18, 37.06, 33.22, 29.33, 29.14, 29.02, 28.90, 28.25, 25.63, 24.97, 24.91.

IR (KBr) ν : 2923, 2852, 1604, 1511, 1466, 1421, 1386, 1293, 1202, 1172, 1024, 964, 844, 801, 723, 703, 670 cm⁻¹.

Anal.Calcd. For C₄₂H₅₂O₄: C 80.20, H 8.28; Found: C 80.18, H 7.29.

3.5 References

1. Burroughes, J. H.; Bradley, D. D. C.; Brown, A. R.; Marks, R. N.; Mackay, K.; Friend, R. H.; Burns, P.L.; Holmes, A. B. *Nature* **1990**, *347*, 539.
2. Friend, R. H.; Gymer, R.W.; Holmes, A. B.; Burroughes, J.H.; Marks, R. N.; Taliani, C.; Bradley, D. D. C.; Dos Santos, D. A.; Brédas, J. L.; Lögdlund, M.; Salaneck, W. R. *Nature* **1999**, *397*, 121.
3. Grimsdale, A. C.; Chan, K. L.; Martin, R. E.; Jokisz, P. G.; Holmes, A. B. *Chem. Rev.* **2009**, *109*, 897.
4. Song, S. Y.; Jang, M. S.; Shim, H. K.; Song, I. S.; Kim, W. H. *Synthetic Metals* **1999**, *102*, 1116.
5. Peng, Z.; Zhang, J.; Xu. B. *Macromolecules* **1999**, *32*, 5162.
6. Babudri, F.; Cardone, A.; Farinola, G. M.; Naso, F.; Cassano, T.; Chiavarone, L.; Tommasi, R. *Macromol. Chem. Phys.* **2003**, *204*, 1621.
7. Nur, Y.; Colak, D.G.; Cianga, I.; Yagci, Y.; Hacaloglu, J. *J Therm Anal Calorim.* **2009**, *98*, 527.
8. Zhang, R.; Zhang, G.; Shen, J. *Chem. Commun.* **2000**, 823.
9. Bernius, M.T.; Inbasekaran, M.; O' Brien, J.; Wu, W. *Adv. Mater.* **2000**, *12*, 1737.
10. Wang, H.; Tao X.; Newton, E. *Polym. Int.* **2004**, *53*, 20.
11. Burn, P. L.; HoImes, A. B.; Kraft, A.; Bradley, D. D. C.; Brown A. R.; Friend R. H. *J. Chem. Soc., Chem. Commun.* **1992**, 32.
12. Cacialli, F.; Feast, W. J.; Friend, R. H.; Jong, M.; Lövenich, P.W.; Salaneck, W. R. *Polymer* **2002**, *43*, 3555.
13. Hay, M.; Klavetter, F. L. *J. Am. Chem. Soc.* **1995**, *117*, 7112.
14. Sarker, A. M.; Gürel, E. E.; Zheng, M.; Lahti, P. M.; Frank E. Karasz. F. E. *Macromolecules* **2001**, *34*, 5897.

15. Cheng, M.; Xiao, Y.; Yu, W.L.; Chen, Z. K.; Lai, Y. H.; Huang, W. *Thin Solid Films* **2000**, *363*, 110.
16. Birekner, E.; Grummt, U. W.; Rost, H.; Hartmann, A.; Pfeiffer, S.; Tillmann, S.; Hörhold, H. H. *Journal of Fluorescence* **1998**, *8*, 73.
17. Edmonds, M.; Abell A.; Modern Carbonyl Olefination. *WILEY-VCH Verlag . GmbH & Co. KGaA, Weinheim*. **2004**, 1.
18. Yingping, Z.; Zhan'ao, T.; Lijun, H.; Yongfang, L. *Polym. Adv. Technol.* **2008**, *19*, 86.
19. van der Made, A. W.; van der Made, R. H. *J. Org. Chem.* **1993**, *58*, 1262-1263.
20. Yang, Z.; Sokolik, I.; Earasz , F. E. *Macromolecules* **1993**, *26*, 1188.
21. Cheng, M.; Xiao, Y.; Yu, W. L.; Chen, Z. K.; Lai, Y. H.; W. Huang, W. *Thin Solid Films* **2000**, *363*, 110.
22. Gürel, E. E.; Pasco, S.T.; Karasz, F. E. *Polymer* **2000**, *41*, 6969.
23. Yasuda, T.; Yamamoto, T. *Macromolecules* **2003**, *36*, 7513.
24. Yamamoto, T.; Fang, Q.; Morikita, T. *Macromolecules* **2003**, *36*, 4262.
25. Peng, K. Y.; Chen, S.A.; Fann, W. S. *J. Am. Chem. Soc.* **2001**, *123*, 11388.
26. Gan, L. H.; Kang, E. T.; Liau, C. Y. *Polymer* **2001**, *42*, 1329.
27. Allen, M. W. *Measurement of Fluorescence Quantum Yields*. Technical note 52019, Thermo Fisher Scientific, Madison, WI, USA
28. *A Guide to Recording Fluorescence Quantum Yields*, Jobin Yvon Ltd. 2 Dalston Gardens, Stanmore, Middlesex HA7 1BQ UK.
29. Nad, S.; Kumbhakar, M.; Pal, H. *J. Phys. Chem. A.* **2003**, *107*, 4808.
30. Lu, C.; Wang, H.; Wang, X.; Li, Y.; Oiu, T.; He, L.; Li, X. *Journal of Applied Polymer Science* **2010**, *117*, 517.
31. Sreekanth J. Varma. *PhD Thesis*, CUSAT, **2012**.
32. Kang, I. N.; Hwang, D. H.; Shim, H. K.; Zyung, T.; Kim, J. J. *Macromolecules* **1996**, *29*, 165.

Synthesis and Characterization of a New Intense Blue-Light Emitting Ring Substituted Segmented PPV Block Copolymer

- 4.1 Introduction and Motivation
- 4.2 Results and Discussion
- 4.3 Conclusions
- 4.4 Experimental Section
- 4.5 References

Abstract

A soluble intense blue light emitting bulky ring substituted segmented PPV block copolymer, poly[1,6-hexanedioxy-(2,6-dimethoxy-1,4-phenylene)-1,2-ethenylene-(2,5-dicyclohexylmethoxy-1,4-phenylene)-1,2ethenylene-(3,5-dimethoxy-1,4phenylene)] (P3) was synthesized using Horner-Emmons condensation polymerization. Rigid cyclohexylmethoxy group substituted distyrylbenzene unit was the chromophoric group present in the copolymer. This rigid block was linked to flexible hexamethylene chain spacer through an ether linkage. Methoxy groups were incorporated to alter photophysical and electrochemical properties, and to improve solubility and processability of the copolymer. The obtained copolymer was soluble in common organic solvents such as dichloromethane, chloroform, tetrahydrofuran, toluene etc. The structure of the copolymer was confirmed on the basis of FT-IR, NMR techniques and elemental analysis. GPC analysis showed that the copolymer synthesized by us has narrow polydispersity index. Thermo-gravimetric analysis shows it has excellent thermal stability with maximum degradation temperature obtained as 422^oC. The HOMO and LUMO levels of copolymer were estimated from the cyclic voltammograms. XRD and DSC studies give information about the semicrystalline nature of the new copolymer. The UV-Vis absorption and fluorescent emission spectra reveals that the copolymer is a promising blue emissive material for light-emitting device application. Copolymer shows excellent fluorescent quantum yield in dichloromethane solution. Morphology of the copolymer was examined by using scanning electron microscopy (SEM). Preliminary photoluminescence studies and Schottky diode action from Voltage vs. Current data are confirmed the suitability of the copolymer for fabricating PLEDs.

4.1 Introduction and Motivation

Electroluminescence devices¹ have been studied extensively during the past 20 years due to their commercial application as a full color flat panel displays. After the

introduction of Polymer LED in 1990, there are several light emitting polymers studied extensively such as poly(*p*-phenylenevinylene),² poly(alkylthiophene),³ poly(fluorene),⁴ poly(*p*-phenylene)⁵ and their copolymers. Polymer LEDs have many advantages for flat panel displays because of variety of color emission, good thin film property, color tunability from blue to red emission region, low turn-on voltage, fast response time and good mechanical properties.⁶ Recently, there have been several attempts to improve the performance of PLEDs. In order to attain high purity, high photoluminescence profiles, low operating voltage and current, there has been important to develop the proper construction of the microstructures of the light emitting polymers. High thermal stability and good mechanical properties of light emitting polymers are also important to overcome device degradation and increased life time during device operation. Therefore numerous emitting polymers have been synthesized and investigated for flat panel device applications, still invention of new light emitting materials with high performance and efficiency remains a big challenge in the field of PLEDs. Mainly three principle colors such as blue, green and red emitting polymers have been demonstrated in PLEDs, but only red and green PLEDs reach the requirements for commercial uses. So efficient blue light emitting polymers⁷ are yet to be developed and optimized for commercial purposes.

It has recently been shown that shortening the effective conjugation length by attaching non-conjugated segments into the PPV backbone can alter their absorption and emission wavelengths, facilitate good film properties and induce excellent EL efficiencies.⁸ Blue emission color is not possible in fully conjugated light emitting polymers. In 1993 Karasz et al prepared highly soluble PPV copolymer containing well-defined blocks of rigid conjugated oligo(phenylenevinylene) and flexible non-conjugated aliphatic spacer units.⁹ The introduction of non-conjugated segment helps to improve the homogeneity of the film and also leads to π -electron confinement in conjugated segment part.¹⁰ Segmented block copolymers (SBC) where the conjugated backbone of the polymer is interrupted by introducing non-conjugated spacer (flexible block) exhibit enhanced solubility, provide a blue shift

in the emission spectrum and increase the energy band gap.¹¹ The shifting of emission spectrum is related to the substituted alkyl or alkoxy side group present in the distyrylbenzene (DSB) unit.¹² Non-conjugated spacer essentially reduces the conjugation length and is expected to cause hypsochromic shift of the emission, without any decrease in the high fluorescence quantum yield of the DSB unit.¹³ Various segmented block EL polymers have been synthesized by using Heck reaction,¹⁴ Wittig polymerization,¹⁵ Horner-Emmons reaction¹⁶ etc. Fluorescence quantum efficiency of conjugated polymers is decreased by aggregation quenching of the excited state due to interchain interactions between the polymer chains. Polymer chain interactions can be inhibited by increasing the space between the conjugated chains with bulky side chain substituents. Poly(2-methoxy-5-cyclohexylmethoxy-*p*-phenylenevinylene) (MCHM-PPV) exhibits enhanced photoluminescence intensity than the structurally similar poly(2-methoxy-5-(2-ethylhexyloxy)-*p*-phenylenevinylene) (MEH-PPV) due to the reduction of main chain aggregation in MCHM-PPV induced by cyclohexylmethoxy groups.¹⁷ Based on this, we reasoned that further introduction of auxochromes on the PPV backbone can provide additional advantages in terms of absorption and emission wavelengths, solubility and redox behaviour of SBCs.

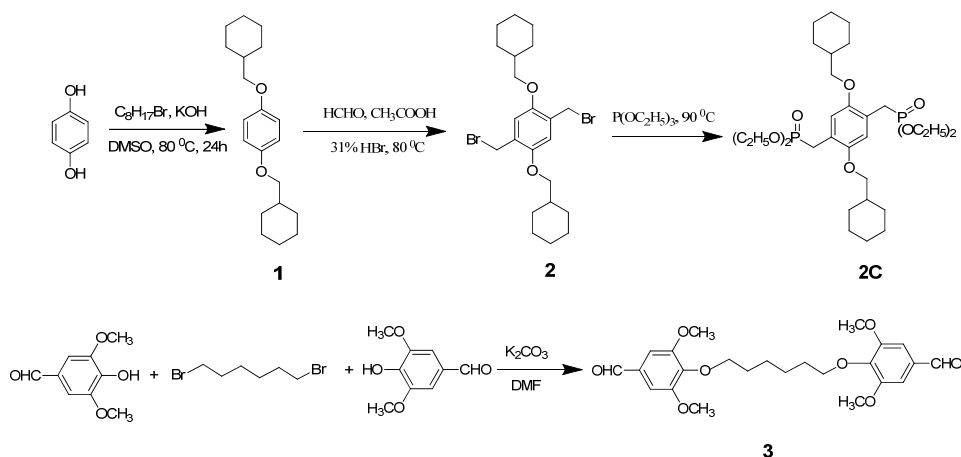
This chapter describes the synthesis, characterization, structural and photophysical studies of new bulky ring substituted segmented PPV block copolymer. A. Talaie et al reported that the device performance could be enhanced in fully conjugated polymers by increasing the chain length and the size of the ring situated within the polymer chemical structures.¹⁸ The copolymer poly[1,6-hexanedioxy-(2,6-dimethoxy-1,4-phenylene)-1,2-ethenylene-(2,5-dicyclohexylmethoxy-1,4-phenylene)-1,2-ethenylene-(3,5-dimethoxy-1,4-phenylene)] (**P3**) was synthesized by using Horner-Emmons condensation polymerization under mild conditions at room temperature. The structure and properties of the copolymer have been systematically examined in this work. The structure of the copolymer was confirmed by using FT-IR, NMR techniques and elemental analysis. The results show that bulky ring (cyclohexylmethoxy)

substituted SBC have enhanced solubility, narrow molecular weight distribution (MWD) and good thermal stability. The Voltage vs Current data confirms the Schottkey diode action of the copolymer.

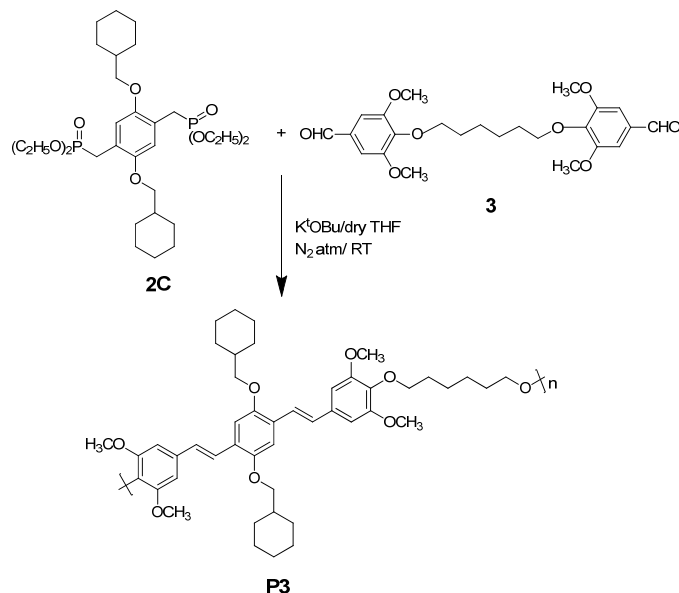
4.2 Results and Discussion

4.2.1 Monomer and Polymer Synthesis

The first step towards the required class of copolymer is the synthesis of appropriate monomers as depicted in Scheme 4.1. Synthesis of monomer, 2,5-di-n-cyclohexylmethoxy-1,4-xylene-diethylphosphonate ester (**2c**) has already been described in Chapter 3. Dialdehyde monomer, 1,6-Bis(4-formyl-2,6-dimethoxyphenoxy)hexane (**3**) was prepared by Williamson etherification type reaction on 4-hydroxy-3,5-dimethoxybenzaldehyde. Synthesis of copolymer is displayed in Scheme 4.2. Similar to general procedure of Horner-Emmons reaction, the condensation polymerization reaction was carried out between bisphosphonate ester monomer (**2c**) and 1,6-Bis(4-formyl-2,6-dimethoxyphenoxy)hexane (**3**) in anhydrous THF using potassium *tert*-butoxide as the base.^{19,20} The mixture was stirred for 24h under nitrogen atmosphere. The greenish yellow reaction mixture remained homogenous through the course of the reaction enabling high overall conversion of functional groups to completion more effectively. Work-up procedure consisted of precipitation of crude copolymer using methanol, collection of the precipitated polymer by gravity filtration, and transfer of the precipitate into an extraction thimble followed by sequential extraction with methanol, hexane and finally THF to remove the oligomers and other impurities. THF fraction was collected and again the copolymer was re-precipitated by using methanol. Copolymer obtained as pale yellow solid in 36% yield was completely soluble in common organic solvents like THF, chloroform, dichloromethane, toluene etc.



Scheme 4.1. Synthesis of bisphosphonate ester monomer (**2C**) and dialdehyde monomer (**3**)



Scheme 4.2. Synthesis route of copolymer (**P3**) via Horner-Emmons Condensation Polymerization.

We introduced a bulky ring substituent such as cyclohexylmethoxy groups into the 2,5 position of each distyrylbenzene (DSB) unit used for the synthesis. Resulting copolymer consists of well defined conjugation length as repeating units linked by long aliphatic flexible chain i.e. hexamethyleneglycol linkers attached through an ether bond. Methoxy groups are also attached into the backbone, in order to alter its absorption characteristics and to enhance solubility and

processability of the copolymer. The weight average molecular weight (M_w), number average molecular weight (M_n) and polydispersity index (PDI) of the copolymer was determined by GPC using tetrahydrofuran (THF) as eluent and calibrated with polystyrene as the standard. The M_w of the copolymer was found to be 12644g/mol^{-1} and M_n was 7966g/mol^{-1} corresponds to 11 repeating units (Figure 4.1). The polydispersity index of the copolymer was 1.6 and that is exceptional in the case of condensation polymerization reactions. The decrease of polydispersity index value of copolymer is due to the sequential extraction with different solvents such as methanol, hexane and THF. Thus, the introduction of ring substitution at the 2,5 positions of the distyrylbenzene units in segmented block copolymer resulted in better yield and improved solubility. The copolymer could be spin-cast from suitable solvents at ambient temperature to give transparent, bright greenish-yellow colored, homogeneous and pin-holes free thin films.

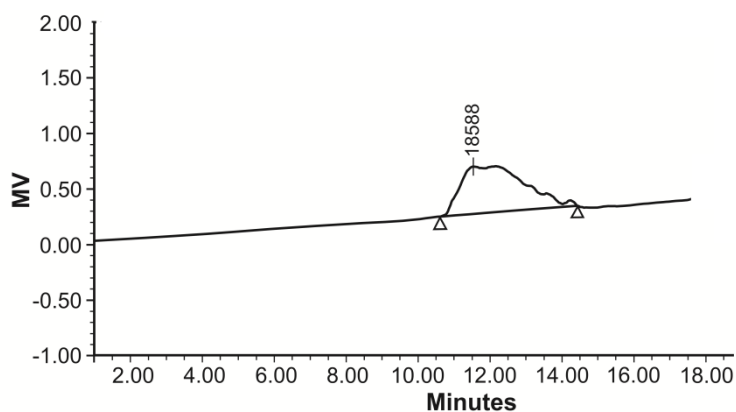
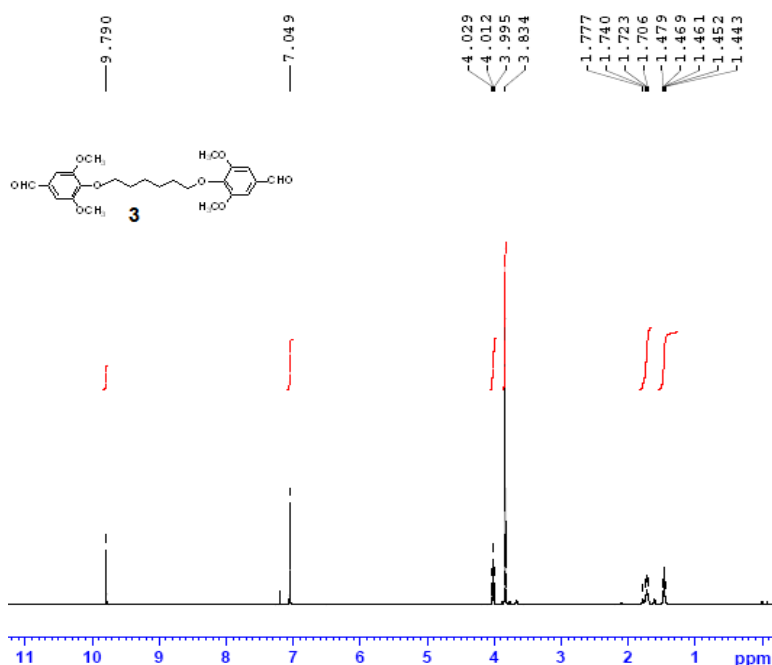


Figure 4.1 Gel permeation chromatogram of copolymer (Waters alliance 2690 column with THF as eluent, at a flow rate of 0.5 mL/min at 25°C)

Structural characterization of the copolymer was done by using ^1H NMR, ^{13}C NMR, FT-IR spectroscopic techniques and elemental analysis. ^1H NMR spectra of 2,5-di-n-cyclohexylmethoxy-1,4-xylene-diethylphosphonate ester (**2c**) and copolymer **P3** are presented for comparison in Figure.4.2. ^1H NMR signals of dialdehyde protons in monomer (**3**) are observed at δ 9.79. These dialdehyde proton signals completely disappeared in the ^1H NMR spectra of copolymer with concomitant appearance of vinylenic proton signals in the δ 7.0-7.8 region along

with aromatic proton signals. Signal appearing as a singlet at δ 6.5 may be attributed to aromatic protons. It is significant to notice that no signals attributable to vinylic protons appear below δ 6.5 confirming the absence of *cis*-vinylene double bond. Furthermore the doublet-like pattern observed at δ 7.4 exhibits coupling constant 16Hz confirming *trans* geometry. Thus it is safely concluded that dominant *trans*-configuration of vinylene double bond is present in the copolymer synthesized by us. Signals at δ 3.7-3.9 correspond to the methyleneoxy protons. Other aliphatic protons are observed in δ 2.19-1.28 region. ^{13}C NMR signals of copolymer are also in good agreement with the proposed structure (Figure 4.3). Figure 4.4 shows the FT-IR spectrum that also is indicative of complete polymerization. Out of plane bending mode of $-\text{CH}=\text{CH}-$ group in the copolymer is observed at 960cm^{-1} , which is the characteristic absorption peak position of *trans*-vinyl group. A very strong peak at 1027cm^{-1} suggests the presence of C–O–C stretching vibrations of aryl-alkyl ether linkage in this compound.



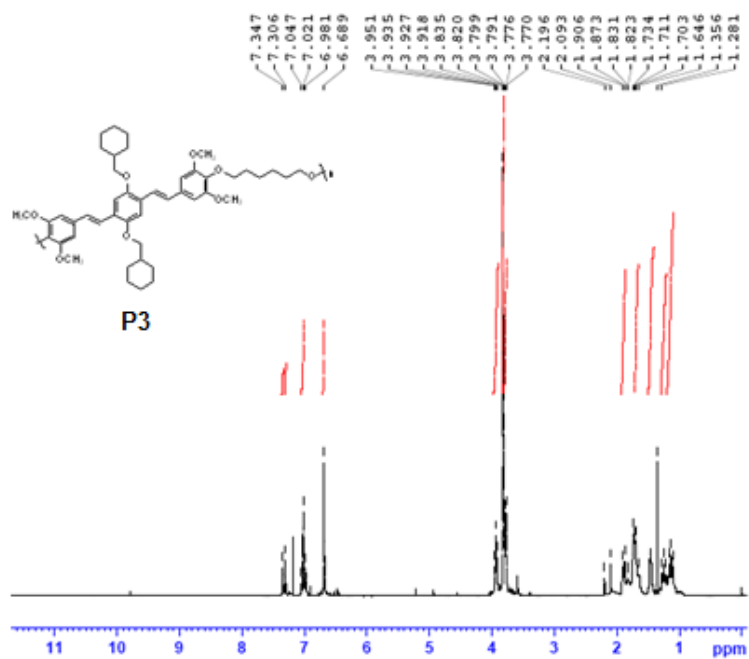


Figure. 4.2 ¹H NMR spectra of dialdehyde monomer (3) and copolymer (P3)

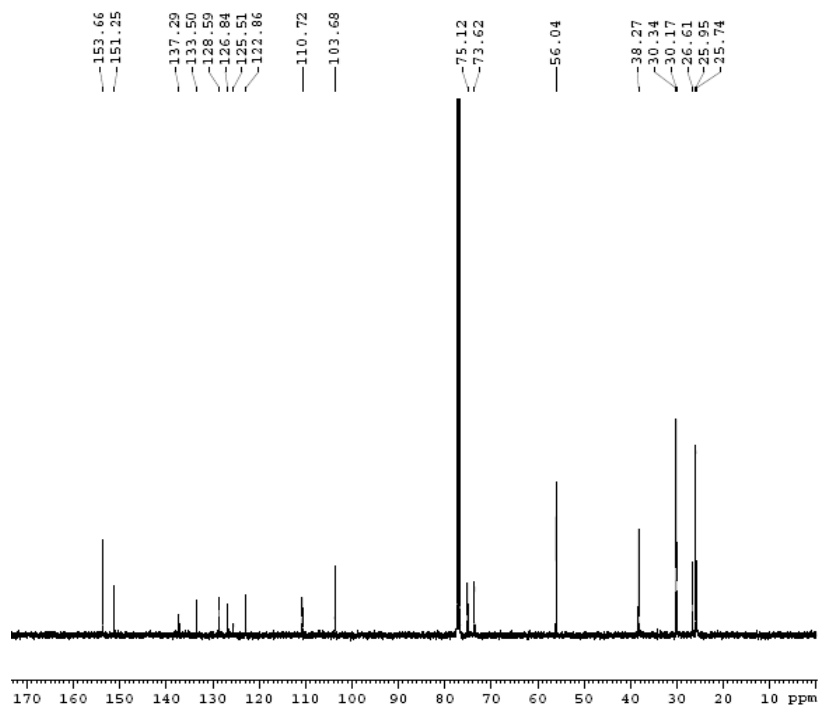


Figure 4.3 ¹³C NMR signals of copolymer (P3)

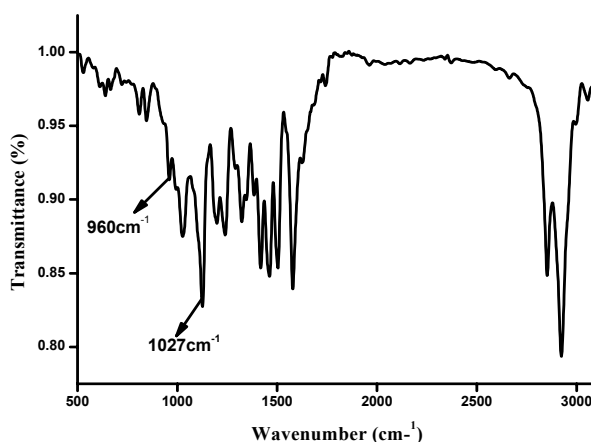


Figure 4.4 FTIR spectrum of copolymer (P3)

4.2.2 Thermal Analysis

Thermal properties of the copolymer **P3** under nitrogen atmosphere were evaluated by thermo gravimetric analysis (TGA, Figure 4.5) and differential scanning calorimetry (DSC, Figure 4.6). Excellent thermal stability was manifested in their TGA profile, with a maximum degradation temperature (T_d) at about 422^oC. The onset degradation temperature was found to be 342^oC. This enhanced thermal stability is due to the introduction of rigid ring substituent groups present in the distyrylbenzene blocks of the copolymer. As described in **chapter 3**, rigid ring substituted segmented copolymer **P2** shows enhanced thermal stability than **P1**.

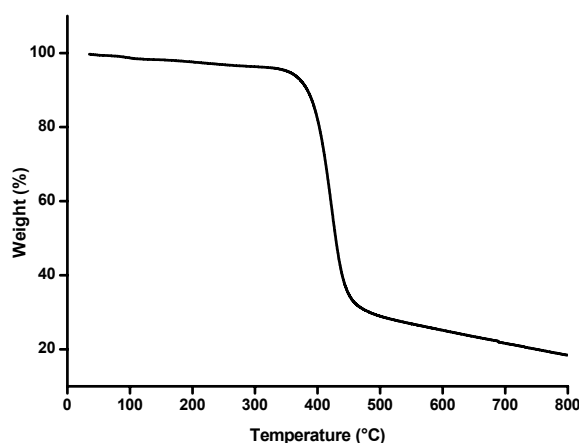


Figure 4.5 TGA plot of copolymer (P3) with a heating rate of 10^oC/min in the nitrogen.

The thermal properties were further investigated by differential scanning calorimetry (DSC) with heating and cooling rate at $10^{\circ}\text{C min}^{-1}$. Copolymer shows a glass transition temperature (T_g) at 53°C . DSC profile also shows a very broad melting peak between the temperature ranges from 112°C to 128°C . Both glass transition temperature and melting temperature (T_m) confirms the semicrystalline nature of the synthesized copolymer.²¹ No other peaks found in DSC thermogram of the copolymer.

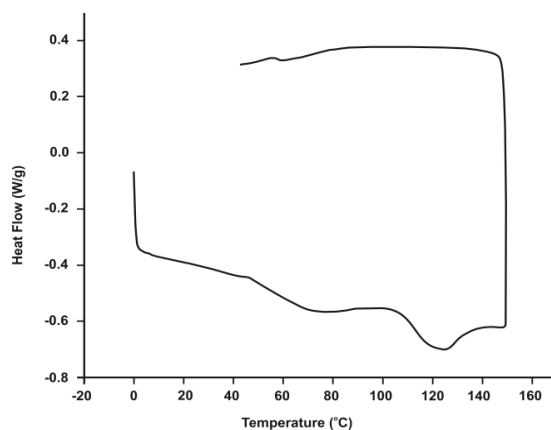


Figure 4.6 DSC plot of copolymer (P3) with heating and cooling rate at $10^{\circ}\text{C min}^{-1}$.

4.2.3 X-ray diffraction Analysis (XRD)

Powder X-ray diffraction (XRD) (Rigaku X-ray diffractometer, $\text{Cu-K}\alpha$ radiation (1.542\AA)) was used to investigate the molecular organization of the synthesized copolymer (P3) as shown in Figure.4.7.

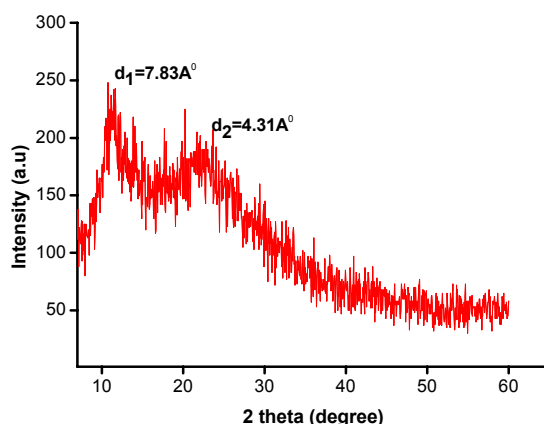


Figure 4.7 Powder XRD patterns of copolymer (P3)

The two major peaks are present in the powder XRD pattern. First peak $d_1=7.83\text{\AA}$ ($2\theta =11.2^\circ$) is somewhat sharp whereas the second peak $d_2 = 4.31\text{\AA}$ ($2\theta=21.6^\circ$) is broad. Interlayer spacing $d_1 =7.83\text{\AA}$ is attributed to the distance between copolymer main chains separated by bulky ring substituent groups present in the DSB units.²² The sharp peak can be ascribed to the presence of side chain crystallinity of the copolymer. The amorphous halo peak at interlayer spacing distance at $d_2 = 4.31\text{\AA}$ is typically arises from side to side distance between the rigid ring substituent groups.²³ Thus, it is clear that the new copolymer synthesized by us shows a semicrystalline nature in the solid state. Furthermore, XRD results support the DSC pattern discussed earlier.

4.2.4 Scanning electron microscopy (SEM)

Figure 4.8 shows the SEM image of copolymer in powder form. SEM pattern suggests that the copolymer shows a featureless morphology due to lack of structural coplanarity in their solid state.

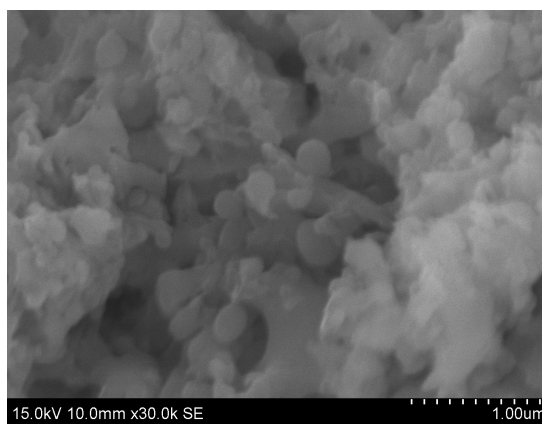


Figure 4.8 SEM micrograph of copolymer (P3)

4.2.5. Photophysical studies

The UV-Vis absorption and PL spectra of the copolymer in dichloromethane solution and in thin film are shown in Figure 4.9 and spectral details are displayed in Table 4.1. Copolymer is a pale yellow solid with absorption maxima in the UV range of the spectrum (398nm). The optical band

gap obtained from the onset of the absorption spectrum in solution was determined as 2.72eV. In the solid state as a thin film, the copolymer is having absorption at 401nm. Negligible 3nm red-shift in the solid state is indicative of insignificant aggregation between the polymer chains in its film state i.e. copolymer shows weak interchain π - π stacking in their ground state. The photoluminescence (PL) spectra in dichloromethane solution consist of a strong peak present at 451nm and a shoulder peak at 480nm. PL spectrum in the film state shows a strong peak at 481nm and shoulder peak at 460nm. Red shifted PL suggests the formation of intermolecular excited state dimers called excimers. PL spectrum of the copolymer in film state is 30nm red shifted compared with its solution state because of the dense packing of copolymer in its solid state than solution state that promotes excimer formation.²⁴ Figure 4.10 shows emission spectrum of copolymer ($\lambda_{\text{ex}}=365\text{nm}$). The fluorescence quantum yield (Φ_{F}) of the copolymer was determined by using comparative fluorescence quantum yield method of Williams et al. The detailed description of the measurement of fluorescence quantum yield has already been presented in **Chapter 3**. The solution measurements conducted versus coumarin-481 dye in ethanol as the standard gave a fluorescence quantum yield (Φ_{F}) of 0.08.²⁵ The fluorescence quantum yield (Φ_{F}) of copolymer (**P3**) in dichloromethane solution was obtained as 0.93. Therefore the synthesized copolymer shows enhanced fluorescence quantum yield in dichloromethane compared to coumarin-481 dye.

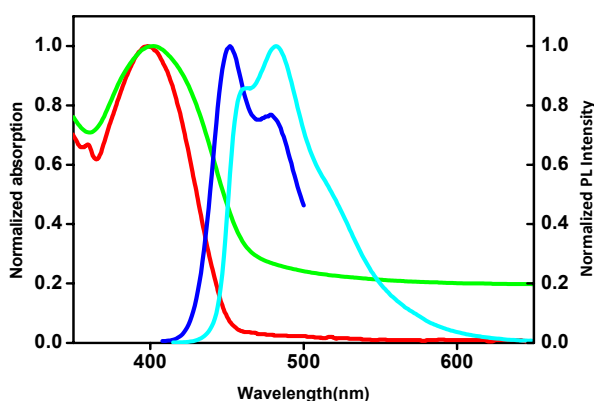


Figure 4.9 UV-Vis spectra and photoluminescence spectra of copolymer (**P3**) in solution and film state

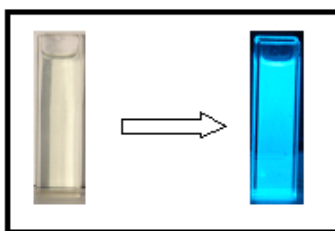


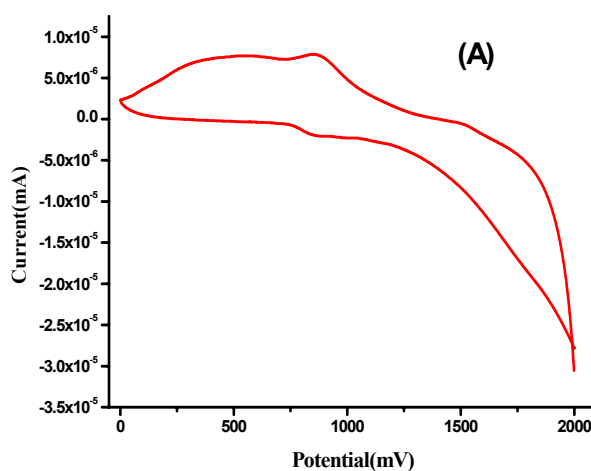
Figure 4.10 Light emission under UV irradiation with light at 365nm

UV-Vis (nm)		PL (nm)		E_g^{OP} (eV)	Fluorescence quantum yield (Φ_F)
Solution	Film	Solution	Film		
398	401	451, 480	460, 481	2.72	0.113

Table 4.1 Photophysical data of copolymer (P3)

4.2.6. Electrochemical studies

The redox potentials of copolymer were estimated by cyclic voltammetric measurement at room temperature in dichloromethane containing 0.1M tetra-*n*-butyl mmonium hexafluorophosphate as supporting electrolyte. A platinum disc electrode was used as working electrode and a platinum wire was used as counter electrode and the potentials referred to Ag/AgCl (calibrated against the FC/FC⁺ redox system) was 4.8eV below vacuum levels. A detailed description of the procedure is available in **Chapter 3**. Figure 4.11 shows the current-voltage curve for copolymer from the cyclic voltammetry measurements.



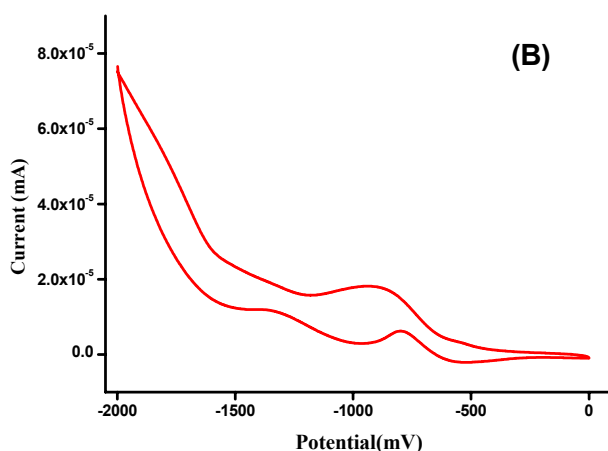


Figure 4.11 Cyclic voltammograms [*p*-doping (A) and *n*-doping (B)] of copolymer (P3).

From the onset oxidation potential and onset reduction potential of the copolymer, HOMO and LUMO energy levels as well as the electrochemical band gap were calculated according to the following equations:²⁶

$$E_{\text{HOMO}} = (\text{IP}) \text{ eV} = -e (E_{\text{ox, on}} - E_{\text{foc}}) - 4.8$$

$$E_{\text{LUMO}} = (\text{EA}) \text{ eV} = -e (E_{\text{re, on}} - E_{\text{foc}}) - 4.8.$$

$$E_{\text{g}}^{\text{EC}} = e (E_{\text{ox, on}} - E_{\text{re, on}})$$

Where $E_{\text{ox, on}}$ and $E_{\text{re, on}}$ are the measured onset potentials relative to Ag/Ag^+ . The *p*-doping and *n*-doping processes occur under the anodic and cathodic scans. Electrochemical data were displayed in Table 2. On the basis of measured oxidation and reduction potentials, corresponding HOMO and LUMO values are determined as -5.23eV and -2.52eV . The electrochemical band gap of the copolymer P3 was evaluated as 2.71eV . Band gap obtained from cyclic voltammetry was very close to the optical band gap derived from UV-Vis spectra ($E_{\text{g}}^{\text{OP}} = 2.72\text{eV}$ as indicated in Table 4.1).

$E_{\text{ox, on}}$ (V)	$E_{\text{re, on}}$ (V)	HOMO (eV)	LUMO (eV)	E_{g}^{EC} (eV)
0.88V	-1.79V	-5.23 eV	-2.52 eV	2.71eV

Table 4.2 Electrochemical data of copolymer (P3)

***4.2.7. Measurement of I-V characteristics**

The homogenous, transparent greenish-yellow coloured thin film of copolymer was made by spin casting (SPS Spin wafer 150, 2000 rpm, 30s) of solution of copolymer in dichloromethane on top of Indium Tin Oxide coated glass plates which act as anode. Aluminium contacts (top-electrode as cathode) were made on top of the spin coated copolymer layers by thermal evaporation to form a Schottky (metal- semiconductor) junction.²⁷ The current-voltage characteristics were analysed using Keithley 2400 source meter (2-point probe method) for the two diode configurations to confirm the formation of metal-semiconductor junction. Forward bias current was obtained, when the ITO electrode was positively biased and the Al electrode was negatively biased. Therefore the current increased with increasing the forward bias voltage, which is mandatory for the fabrication of polymer light emitting diodes. The diode behaviour of the device suggests that electrons and holes are injected from the ITO and Al electrodes. Figure 4.12 shows the Current vs. Voltage graph of copolymer in the forward and reverse bias respectively. From the graph, copolymer shows an onset voltage is 2.8V. Figure 4.13 shows a three dimensional atomic force microscopy (AFM) image of the spin coated film of copolymer from dichloromethane solution. The thickness of the film thus obtained was measured using Dektak 6M stylus profilometer and film with thickness 50nm (± 5 nm). AFM analysis show that copolymer have very smooth surface with the root mean square (RMS) value of 1.53nm.

Figure 4.14 shows the energy diagram of ITO/Copolymer(**P3**)/Al device configuration of the copolymer. The barrier heights of the copolymer was found to be 0.53eV at the interface of ITO (4.7eV)/HOMO state for holes and 1.68eV at the interface of Al (4.2eV)/LUMO for electrons. The HOMO level of polymer is very close to the work function of ITO which enables the effective supply of holes through ITO. An intermediate layer between the emissive polymer and ITO can also be avoided as a result of this. From the energy band diagram, one can assume

* The device fabrication and related characterizations are carried out in collaboration with Department of Physics, CUSAT

that copolymer easily injected holes from the ITO electrode. Therefore, the diode behaviour and good film forming property of this copolymer demonstrate its suitability of fabricating LEDs.

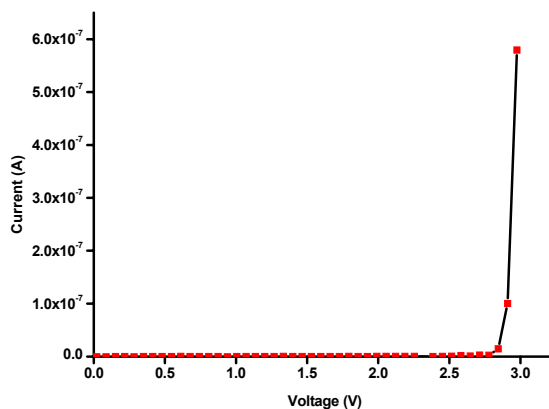


Figure 4.12 I–V characteristics: ITO/ copolymer (**P3**)/Al device

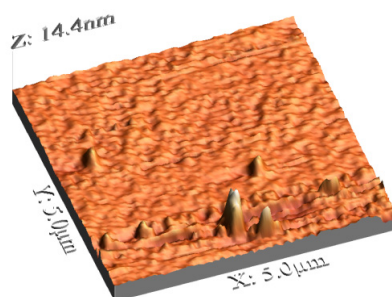


Figure 4.13 Three dimensional atomic Force Microscopy image of the spin coated film of copolymer **P3** from dichloromethane solution.

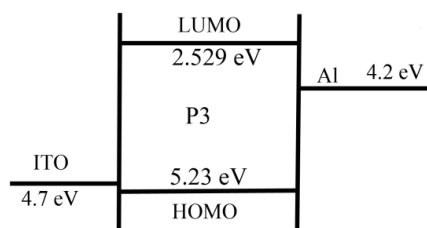


Figure 4.14 The hypothesized energy diagram of ITO/Copolymer (**P3**)/Al device

4.3 Conclusions

A new type of rigid cyclohexylmethoxy ring substituted segmented PPV block copolymer was synthesized using Horner-Emmons condensation

polymerization. The chemical structure of the SBC was assigned on the basis of ^1H NMR, ^{13}C NMR, FT-IR and elemental analysis data. Crude copolymer was purified by sequential extraction method. Purified copolymer exhibited high solubility in several polar and non-polar organic solvents. Gel permeation chromatography indicated narrow polydispersity index for the purified polymer sample used in this investigation. TGA studies show that the copolymer has good thermal stability. DSC thermogram shows both glass transition temperature (T_g) and broad melting temperature (T_m). Semicrystalline characteristic of the copolymer was confirmed by XRD and DSC analysis. AFM studies confirm the very low surface roughness of the spin coated film. In addition, the effect of structure on the optical properties was also investigated. Photoluminescence studies show that the copolymer gives intense blue light emission. Schottky diode characteristics from Voltage vs. Current data confirmed the suitability of the copolymer for fabricating PLEDs.

4.4 Experimental Section

4.4.1 Materials and Instruments

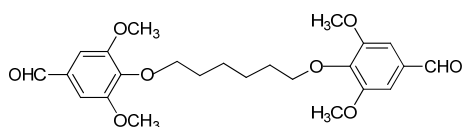
General description of spectroscopic and other characterization techniques used in this study is available in **Chapter 3** of this thesis. All reactions were carried out in oven-dried glassware using reagents and chemicals as commercially supplied from Aldrich and Merck unless otherwise noted. Tetrahydrofuran (THF) was distilled from calcium hydride and then from sodium/benzophenoneketyl. Dimethyl sulfoxide (DMSO) and dimethylformamide (DMF) were distilled prior to use. Hydroquinone, bromomethylcyclohexane, triethylphosphite, 4-hydroxy-3,5-dimethoxybenzaldehyde (syringaldehyde), 1,6-dibromohexane and potassium *tert*-butoxide were purchased from Aldrich Chemicals. HBr in glacial acetic acid, paraformaldehyde and all other reagents/solvents were purchased locally and purified by following the standard procedures.

4.4.2 Synthesis of Monomers

Synthesis of compounds **1**, **2** and **2c** has already been described in Chapter 3

4.4.2.1. 1,6-Bis(4-formyl-2,6-dimethoxyphenoxy)hexane (**3**)

A mixture of 4-hydroxy-3,5-dimethoxybenzaldehyde (4g, 0.02mol) and 1,6-dibromohexane (2.5g, 0.01mol) in 50mL distilled DMF was stirred and heated to reflux. A total of 3g (0.02mol) of potassium carbonate was added in portions and the mixture was stirred and refluxed for 24h. The resulting mixture was poured into 1L of distilled water and the precipitate was collected after standing for 4h, dried in air at ambient temperature and recrystallized from methanol to separate pure dialdehyde (yield=75%, mp 84⁰C).



¹H NMR (400 MHz, CDCl₃) δ (ppm): 9.79 (s, 2H), 7.04 (s, 4H), 3.99-4.02 (t, 4H), 3.83 (s, 12H), 1.44-1.77 (m, 8H).

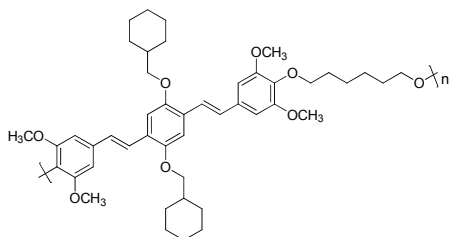
4.4.3 Synthesis of Polymer

4.4.3.1 Synthesis of Poly[1,6-hexanedioxy-(2,6-dimethoxy-1,4-phenylene)-1,2-ethynylene-(2,5-dicyclohexylmethoxy-1,4-phenylene)-1,2-ethynylene-(3,5-dimethoxy-1,4-phenylene)] (**P3**)

A suspension of potassium *tert*-butoxide (0.25g) in anhydrous freshly distilled tetrahydrofuran (THF) was added to a stirred solution of the 2,5-di-*n*-cyclohexylmethoxy-1,4-xylene diethylphosphonate ester monomer (**2c**), (1.5g, 2.4mmol) and of dialdehyde monomer (**3**) (0.8g, 1.7mmol) in 10mL of distilled THF at room temperature. The mixture was stirred 24h under nitrogen atmosphere. A viscous greenish-yellow precipitate was formed. The reaction mixture was poured into methanol, stirred vigorously for 1h, and the precipitated crude polymer was separated by gravity filtration. After drying, the crude polymer mixture was subjected to sequential extraction with methanol, hexane and THF. The polymer was recovered

from the THF fraction by rotary evaporation. The resultant pale yellow solid was dried under vacuum over night. The yield was 38% (0.628g).

¹H NMR (400 MHz, CDCl₃) δ (ppm): 7.34-7.30 (d, 2H), 6.98-7.04 (t, 4H), 6.68 (s, 4H), 3.95-3.82 (m, 16H), 3.79-3.77 (m, 5H), 2.19-1.28 (m, 26H).



¹³C-NMR (100MHz, CDCl₃) δ (ppm): 153.6, 151.2, 137.2, 133.5, 128.5, 126.8, 125.5, 122.8, 110.7, 103.6, 75.1, 73.6, 56, 38.2, 30.3, 30.1, 26.6, 25.9, 25.7.

IR (KBr) ν 2916, 2848, 1579, 1498, 1471, 1418, 1378, 1315, 1252, 1198, 1131, 1023, 952, 844, 804, 669, 633 cm⁻¹.

Anal.Calcd. For C₄₆H₆₀O₄: C 81.65, H 8.87; Found: C 81.38, H 8.29.

4.5 References

1. Liming, D.; Berthold, W.; Limin, D.; Lin, T.; Albert, W. H. M. *Adv. Mater.* **2001**, *13*, 915.
2. Segura, J. L. *Acta Polym.* **1998**, *49*, 319.
3. Igor, F. P.; Dmitrii, F. P.; Hong, M.; Wudl, F. *Adv. Mater.* **2005**, *17*, 2281.
4. Chen, B.; Wu, Y.; Wang, M.; Wang, S.; Sheng, S.; Zhu, W.; Sun, R.; Tian, H. *European Polymer Journal* **2004**, *40*, 1183.
5. Grimsdale, A. C.; Müllen, K. *Adv Polym Sci.* **2006**, *199*, 1.
6. Kraft, A.; Grimsdale, A. C.; Holmes, A. B. *Angew Chem. Int. Ed.* **1998**, *37*, 402.
7. Kim, D. Y.; Cho, H. N.; Kim, C. Y. *Prog. Polym. Sci.* **2000**, *25*, 1089.
8. Taehyoung, Z.; Do-Hoon, H.; In-Nam, K.; Hong-Ku, S.; Wol-Yon, H.; Jang-Joo, K. *Chem. Mater.* **1995**, *7*, 1499.

9. Yang, Z.; Sokolik, I.; Karasz, F. E. *Macromolecules* **1993**, *26*, 1188.
10. Erica, M, K.; Terry, L. Gustafsona.; Daike, K. W.; Runguang, G. S.; Arthur, J. E. *Synthetic Metals* **2001**, *116*, 189.
11. Sarker, A. M.; Gürel, E. E.; Zheng, M.; Lahti, P. M.; Karasz, F. E. *Macromolecules* **2001**, *34*, 5897.
12. Bush, T. E.; Scott, G. W. *J. Phys. Chem.* **1981**, *85*, 144.
13. Birckner, E.; Grummt, U. W.; Rost, H.; Hartmann, A.; Pfeiffer, S.; Tillmann, H.; Hörhold, H. H. *Journal of Fluorescence* **1998**, *8*, 73.
14. Pasco, S. T.; Lahti, P. M.; Karasz, F. E. *Macromolecules* **1999**, *32*, 6933.
15. Cheng, M.; Xiao, Y.; Yu, W. L.; Chen, Z.; K.; Lai, Y. H.; Huang, W. *Thin Solid Films* **2000**, *363*, 110.
16. Chu, Q.; Pang, Y.; Liming, D.; Karasz, F. E. *Macromolecules* **2003**, *36*, 3848.
17. Choo, D. .J.; Talaie, A.; Lee, Y. K.; Jang, J.; Parka, S. H.; Huh, G.; Yoo, K. H.; Lee, J. Y. *Thin Solid Films* **2000**, *363*, 37.
18. Talaie, A.; Lee, Y. K.; Huh, G.; Kim, K. M.; Jeong, H. Y.; Choo, D. J.; Lee, J. Y.; Jang, J. *Materials Science and Engineering B* . **2001**, *85*, 177.
19. Pfeiffer, S.; Hörhold, H. H. *Macromol. Chem. Phys.* **1999**, *200*, 1870.
20. Park, L. S.; Han, Y. S.; Kim, S. D.; Kim, D. U. *Synthetic Metals* **2001**, *117*, 237.
21. Wu, S. H.; Chen, J. H.; Shen, C. H.; Hsu, C. C.; Tsiang, R. C. C. *J. Polym. Sci.: Part A: Polym. Chem.* **2004**, *42*, 6061.
22. Yasuda, T.; Yamamoto, T. *Macromolecules* **2003**, *36*, 7513.
- 23 Yamamoto, T.; Arai, M.; Kokubo, H. *Macromolecules* **2003**, *36*, 7986.
24. Gan, L. H.; Kang, E. T.; Liao, C. Y. *Polymer* **2001**, *42*, 1329.
25. Nad, S.; Kumbhakar, M.; Pal, H. *J. Phys. Chem. A.* **2003**, *107*, 4808.
26. Ibrahim, M. A.; Konkin, A.; Roth, H. K.; Egbe, D. A. M.; Klemm, E.; Zhokhavets, U.; Gobsch, G.; Sensfuss, S. *Thin Solid Films* **2005**, *474*, 201.
27. Sreekanth. J. Varma. *Ph.D Thesis*, CUSAT, **2012**.

Chapter 5

Two Novel Intense Green Light Emitting Thienylene-Biphenylenevinylene Hybrid Polymers: Synthesis, Characterization and Photophysical Studies

Contents

- 5.1 Introduction and Motivation
- 5.2 Results and Discussion
- 5.3 Conclusions
- 5.4 Experimental Section
- 5.5 References

Abstract

Two novel hybrid polymers based on thienylene-biphenylenevinylene have been synthesized through Stille coupling polymerization method. The polymers exhibited complete solubility in common organic solvents such as dichloromethane, tetrahydrofuran, chloroform, toluene etc. Structure of the synthesized polymers was confirmed on the basis of ^1H NMR, ^{13}C NMR, FTIR and elemental analysis data. Gel permeation chromatograph (GPC) indicated that the polymer samples give narrow molecular weight distribution. Thermogravimetric analysis (TGA) demonstrated excellent thermal stability of the polymers. Due to the positional difference in bulky group substitution present in the biphenylene vinylene backbone, the structural and thermal properties of the two synthesized polymers show profound dissimilarities. Structural studies of the polymers were done by using XRD analysis. The polymers showed broad photoluminescence invisible region without any vibronic bands. Both of the polymers provide intense green emission with very high quantum yields. Cyclic voltammetry was used to estimate energy levels of the lowest unoccupied molecular orbit (LUMO), highest occupied molecular orbit (HOMO), and band gap (E_g^{EC}) of the polymers. Powder state morphology of the polymers was analyzed by using SEM and surface smoothness of the spin coated films was detected by AFM analysis. Based on cyclic voltammetry studies, Schottky diode has been constructed and these polymers show very low onset voltages. I - V measurements indicated that the two new polymers are promising candidates for fabricating polymer light emitting diodes.

5.1 Introduction and Motivation

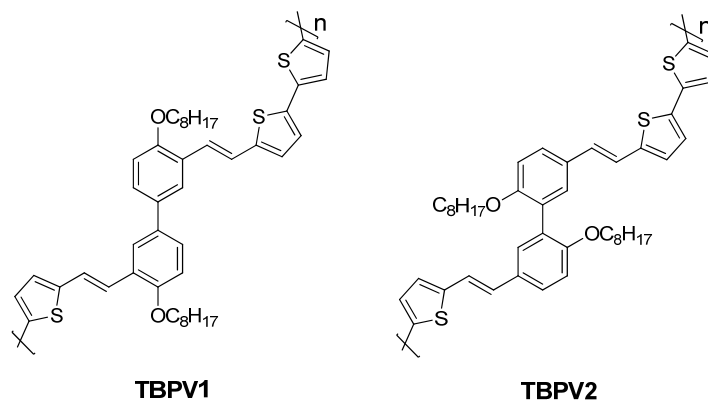
Conjugated light emitting polymers (LEPs) have attracted considerable attention due to their dynamic development in electro-optical applications. Optoelectronic devices like polymer light emitting diodes (PLED) have attracted

wide spread research attention owing to superior properties like easy processing, good mechanical properties, flexibility, lower operational power, color tunability, possibility of large area coatings etc.^{1,2,3} Internal efficiency of the optoelectronic devices is mainly dependent on electroluminescent and photoluminescent efficiency of emissive polymer such as emitted color, quantum efficiency, and balanced injection of electrons and holes.⁴ Device life time and luminescent stability are the primary constraints for commercialization of these optoelectronic devices. Many light emitting polymers have poor luminescent efficiency, life times and low color purity due to the presence of interchain interactions such as aggregation, excimer formation, and polaron pair formation.^{5,6} Therefore an effective way of synthesizing conjugated light emitting polymers with reduced π -stacking, high solubility, high thermal stability with high light-emitting efficiency is still a challenge for chemists.

Many organic luminescent polymers are composed of conjugated extended chains of alternating phenyl and vinyl units.⁷ The intrachain or interchain interactions (molecular aggregation) within these polymer chains would change their emitted color. One effective approach is to reduce these undesirable effects, by the introduction of structural asymmetry into the polymer backbone that limits its ability to pack effectively in the solid state. Among the approaches attempted to control the undesirable effects such as molecular aggregation, luminescence quenching etc in light emitting polymers, the confinement of conjugation length and increasing interlayer distances are widely reported in literatures.^{8,9} Confinement in conjugation length was achieved by introducing meta linkages in the main polymer chain backbone that can limit interchain interactions while allowing the polymer backbone to bend and twist more effectively than one with a para-linkage.¹⁰ Recently various research groups have reported the synthesis of poly(phenylenevinylene)s (PPV) containing bulky substituent groups such as

cyclohexyl,¹¹ adamantaneethylene,¹² cholestanyl,¹³ cyclohexylsilyl¹⁴ etc for controlling the molecular aggregation in the solid state. However some of the bulky group substituted PPVs containing adamantaneethylene and cholestanyl derivatives were not fully soluble in common organic solvents, which limited their processability in optical devices. Another approach is to design a polymer main chain that is structurally constrained to twist in a manner that hinders the effective molecular aggregation (π - π stacking) and also allow fine tuning of the emission wavelength, intensity and lifetime.¹⁵

A new type of blue light emitting-compounds based on biphenyl units was prepared by Hohnholz et al.¹⁵ The presence of biphenyl moiety in these compounds distorts the molecular backbone while amorphous nature was enhanced by steric hindrance. Such structural constraints induced blue shift of the emission spectrum due to large energy band gap (HOMO-LUMO).¹⁶ Poly(4,4'-biphenylenevinylene) systems are intermediate between the poly(phenylenevinylene)s and poly(*p*-phenylene)s (PPP)s. Hence it may logically be assumed that poly(4,4'-biphenylenevinylene) would exhibit electro-optical properties intermediate between those of PPV and PPP. Biphenylene polymers with solubilising alkoxy substituent groups were reported by Karaz et al.¹⁷ The band gap of thienylenevinylene was narrower than PPVs so that its absorption spectrum extended to longer wavelength and also the charge carrier mobility could be high. Thienylenevinylene shows very poor film forming property in comparison to PPVs.¹⁸ Thienylene units attached biphenylenevinylene backbone open the possibility to create different aryl-aryl connection and side chain attachment. Recently, synthesis of hybrid PPV/PPE polymers was independently reported by Egbe et al.¹⁹ and Chu et al.²⁰. These hybrid polymers showed high fluorescent quantum efficiency (in solution and in film state) and good electroluminescent properties. Fine tuning of emission wavelength is easier with hybrid polymers.

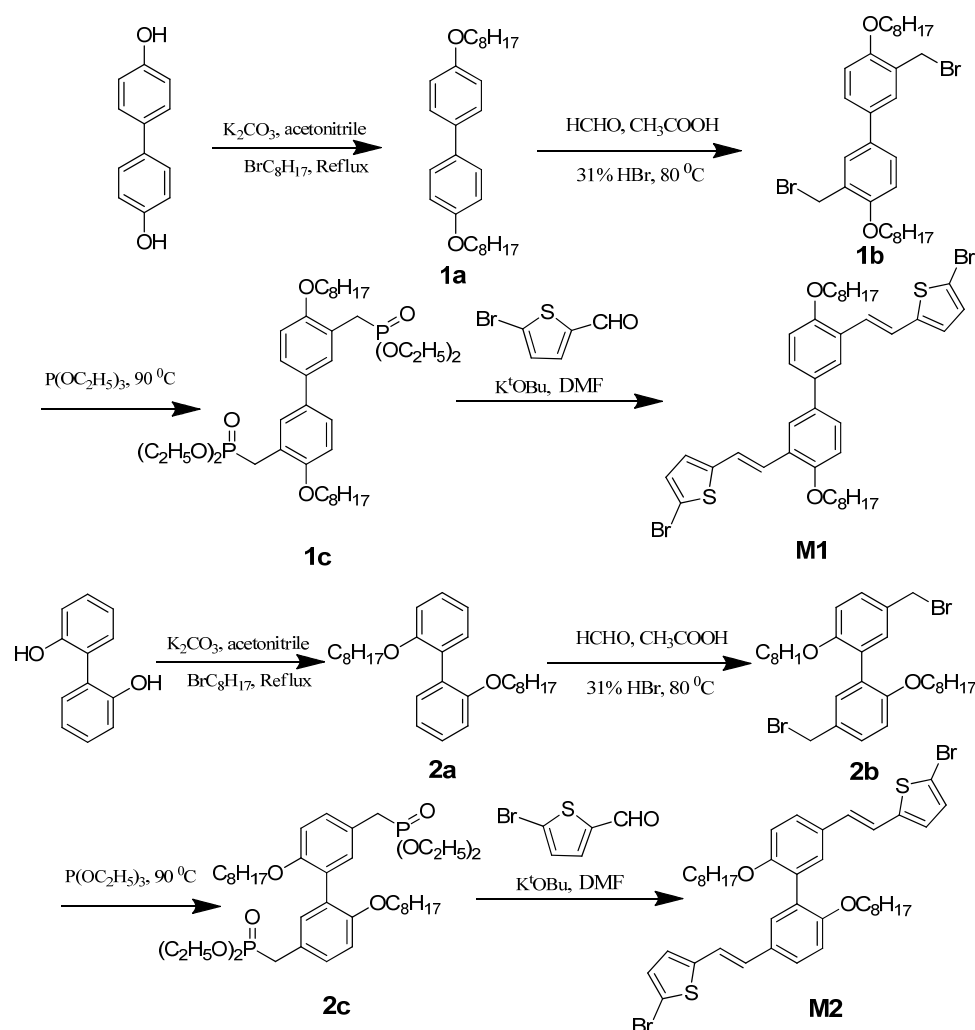
Figure 5.1 Molecular structure of polymers **TBPV1** and **TBPV2**

This chapter describes the synthesis and characterization of a novel class of intense green light emitting thienylene- biphenylenevinylene hybrid polymers with high thermal stability and excellent solubility. Their spectral, electrochemical, structural properties and morphology have been studied. The Voltage vs. Current data was collected to confirm the schottkey diode action of the new polymers. To the best of our knowledge, so far polymers having biphenylenevinylene-thienylene units fused together have not been reported in literature. For the synthesis of these polymers, a new type of monomers was designed and they consisted of biphenylenevinylene group linked to two thienylene units through a *trans*-vinylene double bond. Figure 5.1 shows the molecular structure of **TBPV1** and **TBPV2** Introduction of solubilising side chains enhanced processability. Introduction of solubilising side chains enhanced processability. Palladium-catalyzed Stille coupling reaction was the method of our choice for polymerization of the monomer units. This reaction has several advantages including mild reaction conditions and high yields. The Stille reaction encompasses Pd(0)-mediated cross-coupling of organohalides, triflates, and acyl chlorides with organostannanes.²¹ Highly electron rich thiophene containing polymers are easily synthesized using Stille coupling.²² The incorporation of thienylene units in the biphenylenevinylene backbone resulted in a modified energy band-gap with strong green PL emission and excellent film forming properties.

5.2 Results and Discussion

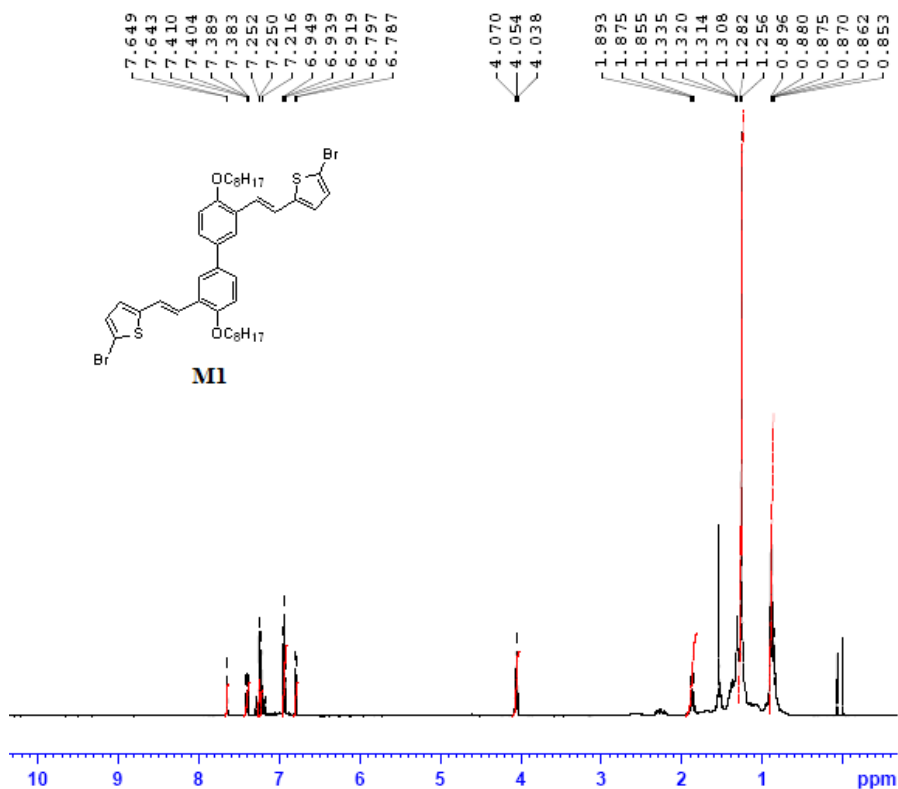
5.2.1 Monomer Synthesis

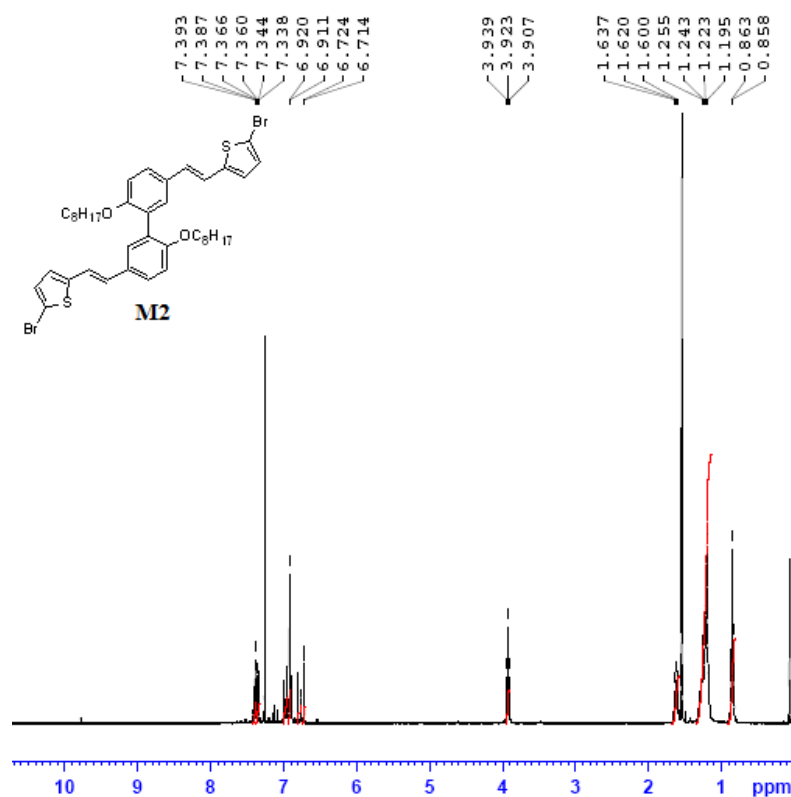
The synthesis of two new monomers is shown in Scheme 5.1. Compounds **1a**, **1b**, **1c**, **2a**, **2b** and **2c** were synthesized as per the modified procedure available in literature.¹⁷ 4,4'-Dioctyloxy-1,1'-biphenyl (**1a**) was prepared by *O*-alkylation of commercially available 4,4'-dihydroxy-1,1'-biphenyl using two equivalents of 1-bromooctane in acetone under reflux. Under these conditions **1a** was generated as pure white needles in very high yield. Double bromomethylation²³ of **1a** resulted in the formation of bis(bromomethylene) compound 3,3'-bis(bromomethyl)-4,4'-di(octyloxy)-1,1'-biphenyl (**1b**). Subsequent Michaelis–Arbuzov reaction²⁴ of triethylphosphite with bis(bromomethylene) compound yielded 3,3'-bis(diethylphosphonate)-4,4'-(dioctyloxy)-1,1'-biphenyl (**1c**) as a colourless thick oil. The monomer **M1** was synthesized by applying well known Wittig-Horner reaction.²⁵ The monomer 5,5'-(1*E*,1'*E*)-2,2'-(4,4'-bis(octyloxy)biphenyl-3,3'-diyl)bis(ethene-2,1-diyl)bis(2-bromothiophene) (**M1**) was prepared by the reaction between 3,3'-bis(diethylphosphonate)-4,4'-(dioctyloxy)-1,1'-biphenyl (**1c**) and 5-bromothiophene-2-carboxaldehyde in the presence of potassium *tert*-butoxide as the base. The yellow coloured waxy liquid formed was then isolated by using column chromatography which afforded bright yellow crystals in 35% yield. Second monomer 5,5'-(1*E*,1'*E*)-2,2'-(6,6'-bis(octyloxy)biphenyl-3,3'-diyl)bis(ethene-2,1-diyl)bis(2-bromothiophene)(**M2**) was also synthesized in a similar manner, starting with 2,2'-dihydroxy-1,1'-biphenyl. After Wittig-Horner reaction, monomer **M2** was obtained as light brown crystals in 22% yield. The monomers were completely soluble in common organic solvents such as tetrahydrofuran (THF), dichloromethane, hexane, chloroform, toluene etc due to the presence of long chain octyloxy substituents.

Scheme 5.1. Synthesis of monomers **M1** and **M2** via Wittig-Horner reaction

Monomers **M1** and **M2** showed remarkable differences in their melting points: 65°C for **M1** and 85°C for **M2**. The average conformational structure in the ground state 4,4'-linked monomer **M1** is expected to be more planar than **M2**, which has steric strain inducing substitution at the 2,2'-positions. Therefore, the 1,1'-bond (meta-meta bond) coupled stilbene units tends to be twisted easily, whereas the linkage in meta position doesn't interfere with the electronic properties of the biphenyl unit.²⁶ Depending on the positions of the octyloxy substituents present in the biphenyl moiety a distortion can be achieved. Two thiophene rings are linked with a conjugated biphenyl moiety through *trans*-

vinylene bond by the Wittig–Horner reaction. Consequently the monomer maintains planarity and the conjugated polymer system grows effectively, so that the band gap of the polymer could be reduced.²⁷ Monomers **M1** and **M2** were characterized by using ¹H NMR, ¹³C NMR, FT-IR spectroscopic techniques. Figure 5.2 displays the ¹H NMR spectrum of monomers **M1** and **M2**. The disappearance of aldehyde proton peaks around 10ppm in ¹HNMR spectra implied successful reaction via Wittig–Horner reaction. Based on our previous experience with the stereochemical outcome of Wittig-Horner reactions and coupling constant information, *trans* geometry is assigned to the newly generated carbon-carbon double bonds.

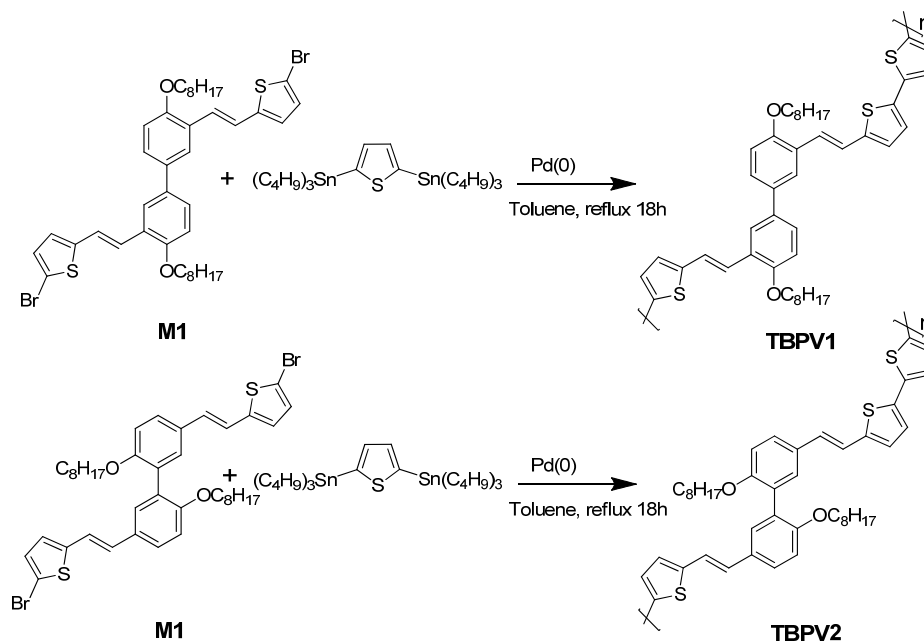


Figure 5.2 ^1H NMR spectrum of monomers **M1** and **M2**

5.2.2 Polymer Synthesis

The polymers were synthesized by Stille coupling reaction illustrated in Scheme 5.2. The Stille reaction carried out by using catalytic amount of $\text{Pd}(\text{PPh}_3)_4$ added to a mixture of 2,5-bis(tributylstannyl)thiophene and **M1** with freshly distilled toluene as solvent. The mixture was refluxed for 18h and the mixture was poured into methanol and filtered to remove the precipitated metallic palladium. The crude polymers were purified by sequential extraction with methanol, hexane, and THF to remove the oligomers and other impurities. THF fraction was collected and again the polymer was reprecipitated by using methanol. Polymer **TBPV1** was obtained as reddish brown solid in 87% yield. Similarly, polymer **TBPV2** was obtained as a dark brown solid in 77% yield. Polymers **TBPV1** and **TBPV2** possess good solubility in common polar and non-

polar organic solvents such as dichloromethane, toluene, THF, chloroform etc. The polymers were fully characterized on the basis of ^1H NMR, ^{13}C NMR, FT-IR spectroscopies and elemental analysis data. ^1H NMR spectrum of the polymers (Figure 5.3) is in good agreement with its molecular structure. Aromatic and vinylic protons appear in the δ 7.61–6.85 region. Methylenoxy protons appear at 3.98ppm to 4.01ppm for both polymers. ^{13}C NMR and FT-IR spectroscopic data were also in agreement with the proposed polymer structures. Due to the complexity of the aromatic/vinylic region, it was not possible to isolate the signal due to vinylic protons. Out-of-plane $-\text{CH}=\text{CH}-$ bending frequencies of polymer **TBPV1** appears at 954cm^{-1} and **TBPV2** appears at 952cm^{-1} , which is the characteristic absorption peak of *trans*-vinylene groups.²⁵ Therefore it is suggested that the generated double bonds are mainly in *trans*-configurations. We assume that the *trans* geometry of alkene linkages present in the monomers is maintained in the polymers generated by Stille coupling.



Scheme 5.2 Synthesis of **TBPV1** and **TBPV2** via Stille coupling polymerization.

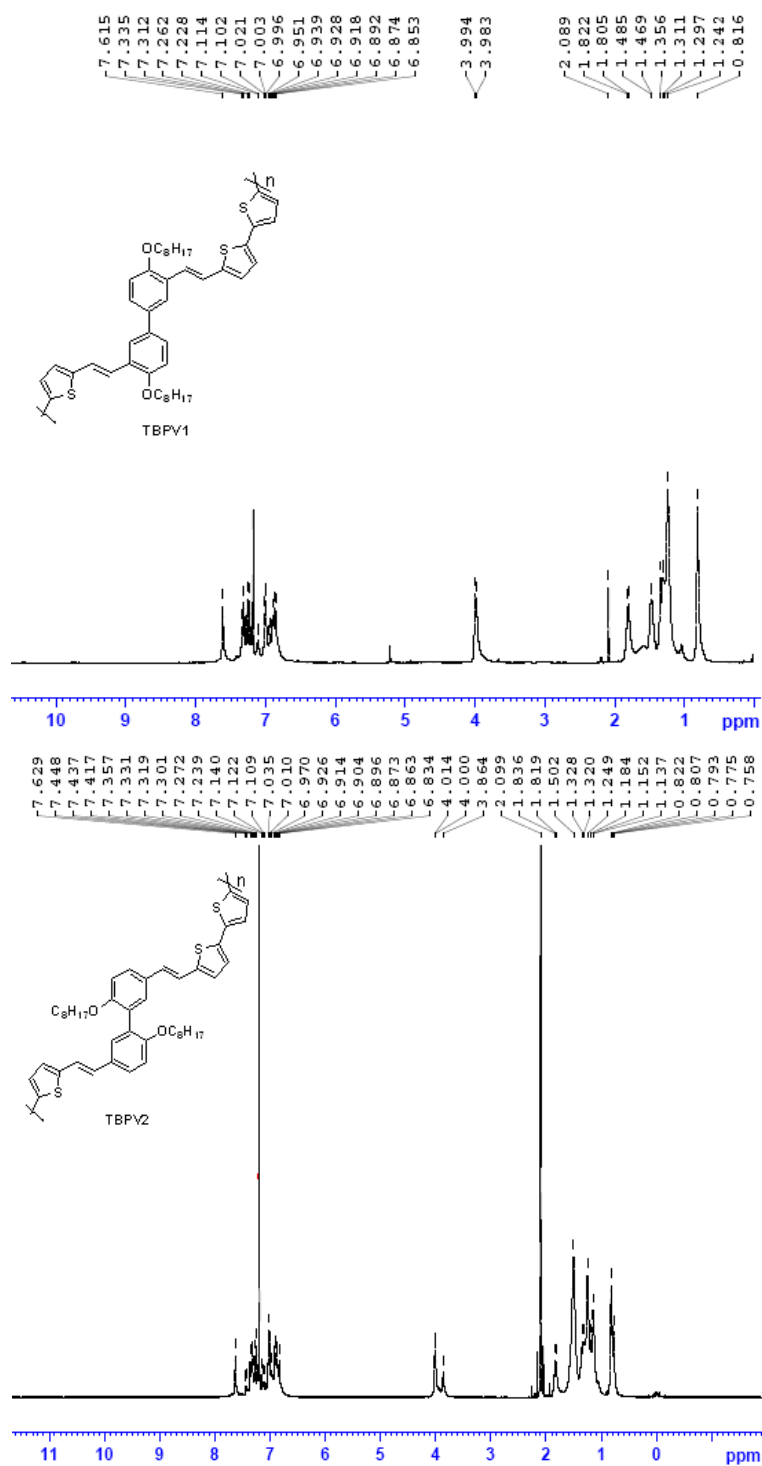


Figure 5.3 ¹H NMR spectrum of polymers **TBPV1** and **TBPV2**

The weight average molecular weight (MW) and the polydispersity index (PDI) were measured by gel-permeation chromatograph (GPC) against polystyrene standards using toluene as mobile phase. Gel permeation chromatograms of the polymers are shown in Figure 5.4. This showed a moderate MW of 4928 g/mol^{-1} with PDI of 1.66 for **TBPV1** and MW of 4549 g/mol^{-1} with PDI of 1.82 for **TBPV2**. Such relatively low molecular weights are typical of Stille coupling polymerization. The decrease of polydispersity index value of currently synthesized polymers is due to sequential extraction with different solvents such as methanol, hexane and THF. The polymers **TBPV1** and **TBPV2** could be spin coated at ambient temperature to give bright yellowish-orange coloured transparent, homogeneous and pin-holes free thin films.

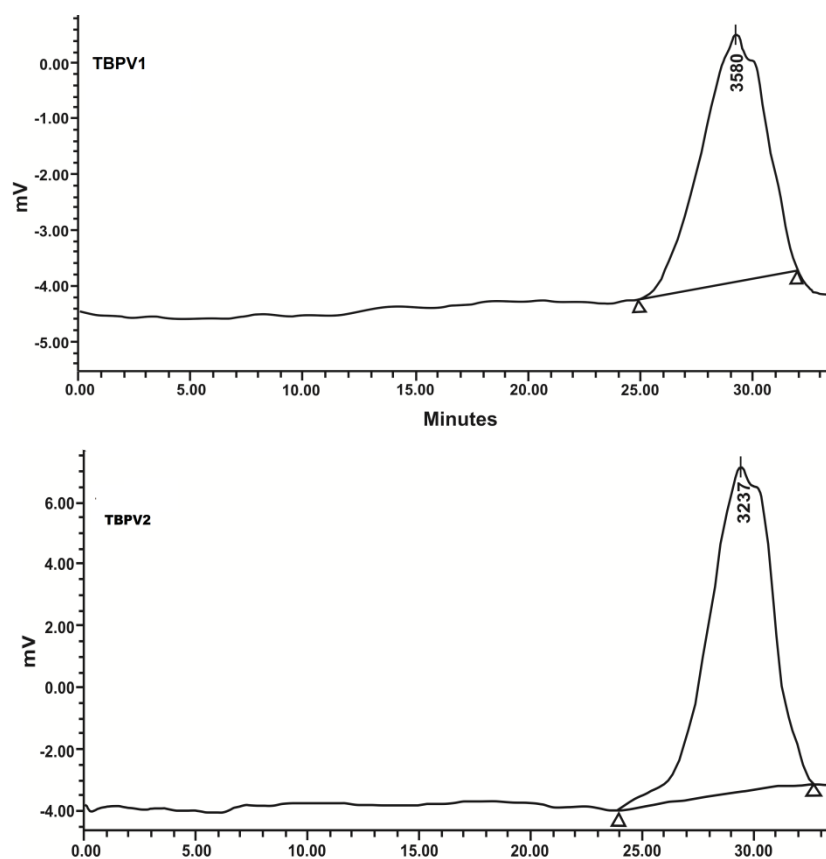


Figure 5.4 Gel permeation chromatograms of **TBPV1** and **TBPV2** (Waters 2414 column with toluene as eluent, at a flow rate of 0.5 mL/min at 25°C)

5.2.3 Thermal Properties

Thermal properties of the polymers were investigated by thermogravimetric analysis (TGA) (Figure 5.5) and differential scanning calorimetry (DSC) (Figure 5.6). The thermal and physical properties of copolymers are shown in Table 5.1. From TGA results, the maximum degradation temperature (T_d) is at 443°C for **TBPV1** and 452°C for **TBPV2**. Thienylene units present in the conjugated biphenylenevinylene backbone helps to enhance the thermal stability of **TBPV1** and **TBPV2**. This high thermal stability indicates that the polymers are adequate for applications in optoelectronic devices. The onset degradation for **TBPV1** and **TBPV2** are at 324°C and 361°C respectively. Polymer **TBPV2** shows enhanced thermal stability compared to **TBPV1** due to the steric strain induced by the bulky substitution at the 2,2'-positions of biphenyl backbone which reduces its coplanarity.

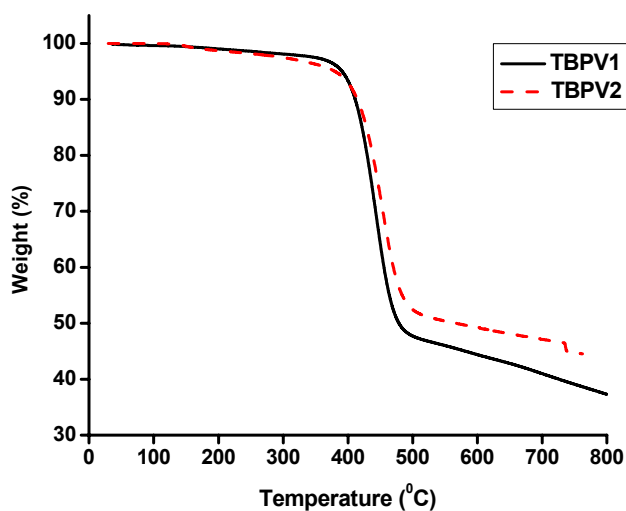


Figure 5.5 Thermal gravimetric curve (TGA) of **TBPV1** (solid line) and **TBPV2** (dashed line) at a heating rate of 10°C/min in nitrogen.

Polymer	Yield (%)	M_w (g/mol ⁻¹)	PDI	T_g (°C)	T_m (°C)	T_d (°C)
TBPV1	87%	4928	1.66	54	102	443
TBPV2	77%	4549	1.82	55	110	452

Table 5.1 Physical and thermal properties of polymers **TBPV1** and **TBPV2**

Differential scanning calorimetry (DSC) (Figure 5.6) of the polymers **TBPV1** and **TBPV2** show Glass transition temperature (T_g) at 54°C and 55°C respectively. Both polymers show moderate and comparatively similar T_g values, due to the influence of long octyloxy substituent chain present in the rigid biphenyl polymer backbone.²⁸ DSC profile of **TBPV1** shows a melting temperature at 102°C but **TBPV2** do not have a well defined melting peak, it shows a weak melting temperature at 110°C. Therefore **TBPV1** and **TBPV2** have both glass transition temperature and melting temperature (T_m) suggesting their semicrystalline nature.²⁹ From the DSC results **TBPV1** shows more crystalline characteristics than **TBPV2** because it is expected to be more planar. **TBPV2** shows less crystalline characteristics due to strain induced by 2,2' linkge.

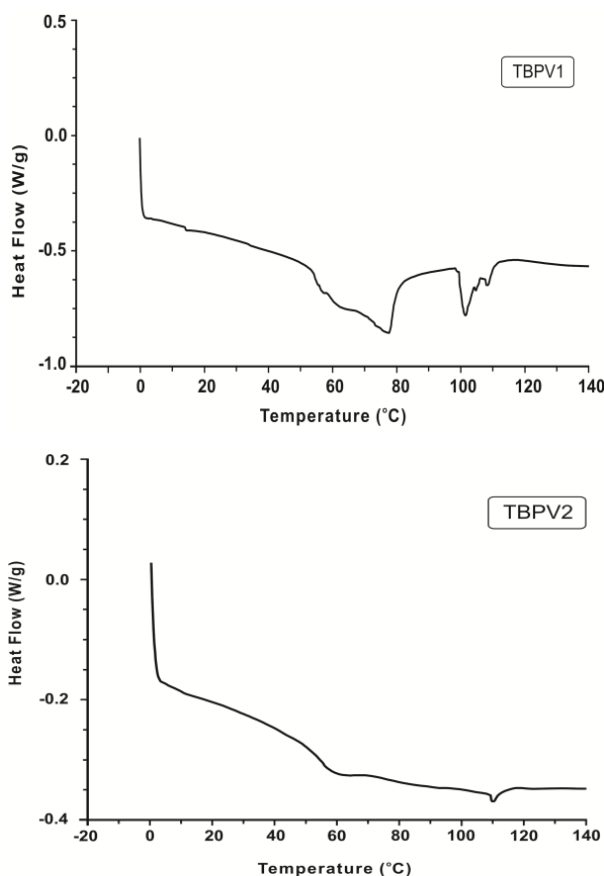


Figure 5.6 Differential scanning calorimetry (DSC) thermogram **TBPV1** and **TBPV2** in nitrogen atmosphere at a heating rate of 10 °C/min

5.2.4 X-ray diffraction analysis (XRD)

Powder X-ray diffraction (XRD) (Rigaku X-ray diffractometer, Cu-K α radiation (1.542Å)) was used to investigate the crystalline nature and molecular organization of the polymers. The XRD pattern is shown in Figure 5.7. **TBPV1** shows two main peaks, with d-values 7.64Å, 4.02Å. **TBPV2** also shows similar peaks with d values 7.53Å, 4.17Å. The d_1 values of **TBPV1** and **TBPV2** are observed corresponds to the number of carbons in the octyloxy side chain and the distance between the π - conjugated main chains separated by the octyloxy group.³⁰ Due to the presence of octyloxy side chains present in the biphenylene backbone, both polymers show side chain crystallinity. It was previously reported that the octyloxy substituted PPV layers show side chain induced semicrystalline nature.³¹ The diffraction peaks at 2θ values of **TBPV1** at 22.6° ($d_2= 4.02\text{Å}$) for and **TBPV2** at 21° ($d_2= 4.17\text{Å}$) corresponds to the interlayer distance between the π - π stacks of the polymer.³² If it is observed that slightly larger π - π distance which denote that the coplanarity of these two polymers is lesser in their solid state.³³

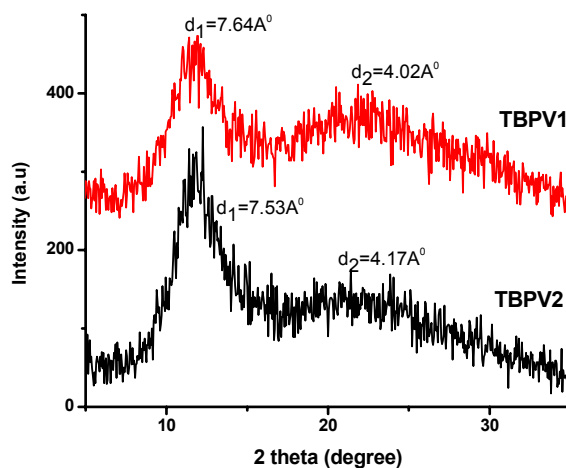


Figure 5.7 Powder XRD patterns of **TBPV1** and **TBPV2**.

5.2.5 Scanning electron microscopy (SEM)

The morphology of the polymers in powder form was studied by using scanning electron microscopy (Hitachi FESEM SU6600). Figure 5.8 shows the

SEM images of **TBPV1** and **TBPV2** respectively. From these figures, both of the polymers appeared to be circular plate like morphology. Therefore these morphologically similar polymers particularly differentiated by their dissimilar positions such as 4,4' or 2,2' linked substitution of long octyloxy side chain in the rigid biphenylenevinylene backbone.

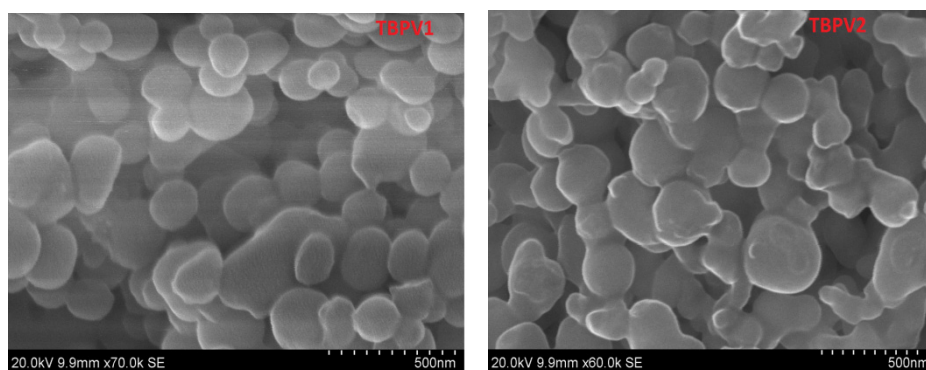


Figure 5.8 SEM micrographs of **TBPV1** and **TBPV2** in powder form

5.2.6 Photophysical studies

5.2.6.1 Absorption and photoluminescence (PL) studies of monomers

Two new monomers 5,5'-(1E,1'E)-2,2'-(4,4'-bis(octyloxy)biphenyl-3,3'-diyl)bis(ethene-2,1-diyl)bis(2-bromothiophene) (**M1**) and 5,5'-(1E,1'E)-2,2'-(6,6'-bis(octyloxy)biphenyl-3,3'-diyl)bis(ethene-2,1-diyl)bis(2-bromothiophene) (**M2**) were synthesized and characterized and are described in Section 5.2.1. Figure 5.9 (A & B) shows normalized UV-Vis absorption spectra and PL spectra of monomer **M1** and **M2** in dichloromethane. Monomer **M1** shows absorption at 343nm and the corresponding band gap was determined as 3.11eV and **M2** shows absorption at 347nm and its band gap is estimated at 3.19eV. Major emission peak appears at 428 nm for **M1** and 419nm for **M2**. Therefore monomers show their emission at UV-Vis wavelength region.

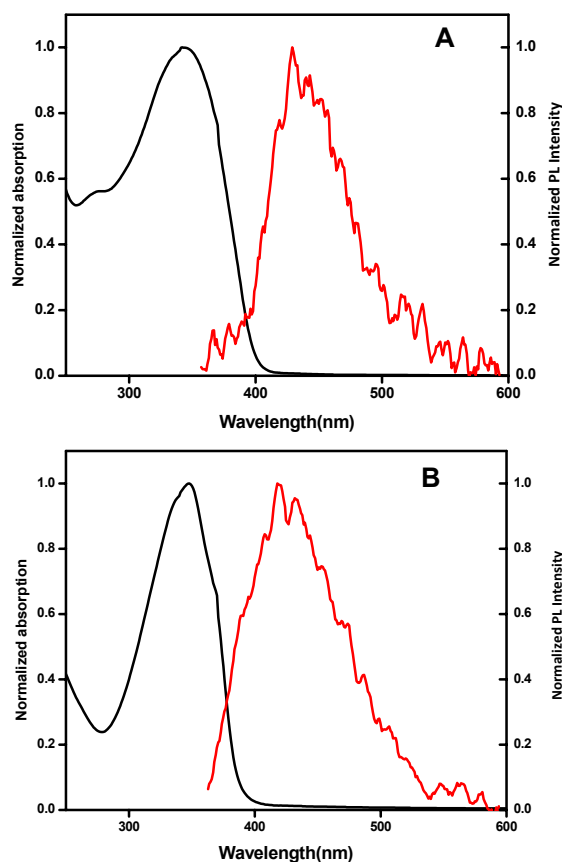


Figure 5.9 (A) absorption spectra and PL spectra of monomer **M1** (B) absorption spectra and PL spectra of monomer **M2**

5.2.6.2 Absorption and photoluminescence (PL) studies of polymers

The UV-Vis absorption spectra and PL spectra provide information on the electronic structures of the synthesized polymers. The absorption and photoluminescence (PL) spectra of the polymers **TBPV1** and **TBPV2** in dichloromethane solution and spin casted film are depicted in Figure 5.10. In solution state, the absorption peaks of **TBPV1** and **TBPV2** appear at 444nm and 442nm respectively which can be attributed to π - π^* transitions. The optical band-gap energies of **TBPV1** and **TBPV2** solutions calculated from the onset of the UV-Vis absorption spectra are 2.31eV and 2.32eV respectively. The longest wavelength absorption peaks of **TBPV1** and **TBPV2** films were 456nm and 455nm respectively. Compared to the corresponding monomers we have observed

a red-shift of about 12nm and 13nm in **TBPV1** and **TBPV2** polymers. Therefore, it can be assumed that the ground state interaction such as aggregation between the chains in the polymers is very low and does not interfere with the electronic properties of these polymers. Polymers with long octyloxy chains were selected in order to decrease the interchain interactions between the polymer backbones and to enhance the quantum efficiencies.

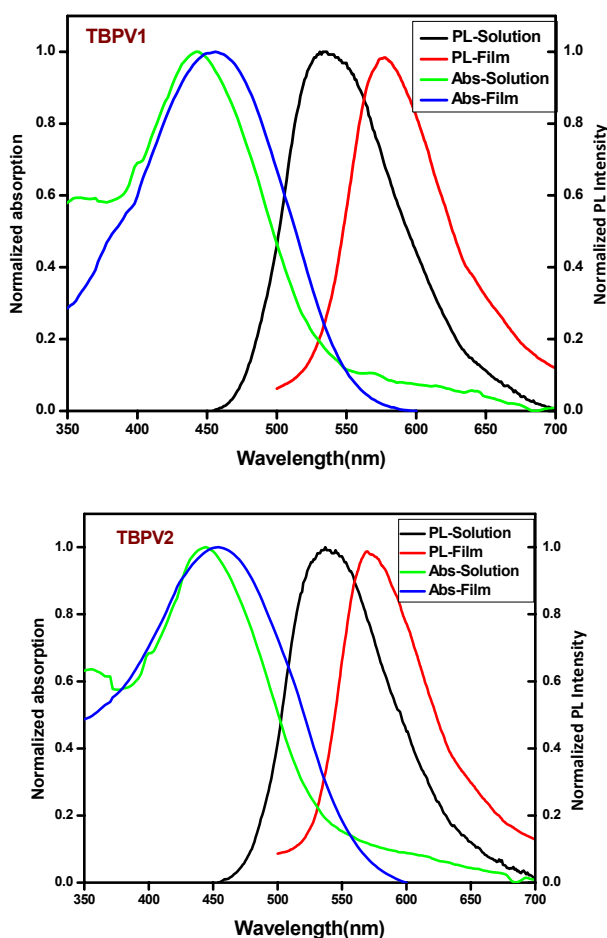


Figure 5.10 Normalized UV-Vis absorption spectra (UV) and photoluminescence (PL) of **TBPV1** and **TBPV2** in dichloromethane solution and in the solid state (film).

The PL maxima of **TBPV1** and **TBPV2** in dilute dichloromethane solutions appeared at 536nm and 538nm on excitation at 444nm and 442nm respectively. In **TBPV1** and **TBPV2** films, the PL maxima appear at 576nm and

571nm respectively. This small variation of emission wavelength of these polymers may be due to the difference of positional substitution of long octyloxy side chains present in the biphenylenevinylene backbone. Absorption maxima of copolymers in the film state bathochromically shifted with respect to their spectra in the solution state. Figure 5.11 shows that the light emissions of **TBPV1** and **TBPV2** under UV irradiation at 365nm. Both polymers show powerful green emission in their solution state as well as in their film forms. Previous section revealed that monomer **M1** and **M2** have emission in blue region but after polymerization of these monomers its emission spectrum shifted from blue to green region. In the case of both polymers their emission wavelength have shifted to higher wavelength region due to increased number of attached thienylene units present in the biphenylenevinylene backbone which leads to decrease in band gap.

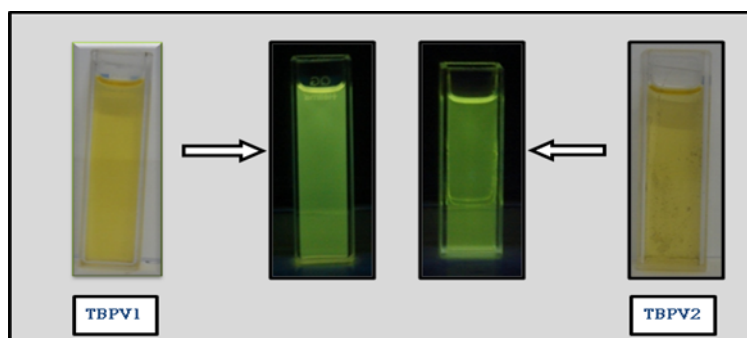


Figure 5.11 Light emissions of **TBPV1** and **TBPV2** under UV irradiation with light at 365nm

5.2.6.3 Fluorescence quantum yield of polymers

Photophysical data of **TBPV1** and **TBPV2** are shown in Table 5.2. Method for estimating fluorescence quantum yield (Φ_F)³⁴ is described elsewhere in this thesis (Section 3.2.6.1 in Chapter 3). The comparative fluorescence quantum yield for polymers **TBPV1** and **TBPV2** was determined by using fluorescein as the standard. Fluorescein has remarkably good photostability and high quantum yield of 0.79 in ethanol having excitation wavelength was used as 453nm (Kellogg, 1964).³⁵ The fluorescence quantum yield (Φ_F) of **TBPV1** was found to be 0.93 and **TBPV2** was obtained as 0.39 in dichloromethane solution.

Polymer **TBPV1** has higher fluorescence quantum yield than fluorescein. But **TBPV2** shows lower quantum yield due to the steric strain induced by 2,2' linked substitution present in its polymer backbone. We attribute the sharp decrease in quantum yield to geometric constraints imposed by substituents at 2,2'-positions in the biphenyl residue that is likely to tilt the two aryl rings out of planarity whereby effective conjugation is decreased. The fluorescence quantum yield (Φ_F) of **TBPV1** and **TBPV2** indicates that both the polymers are very attractive for application in optoelectronics.

Copolymer	UV-Vis (nm)		PL (nm)		E_g^{OP} (eV)	Fluorescence Quantum Yield (Φ_F)
	Solution	Film	Solution	Film		
TBPV1	444	456	536	576	2.31	0.93
TBPV2	442	455	538	571	2.32	0.39

Table 5.2 Photophysical data of **TBPV1** and **TBPV2**

5.2.7 Electrochemical studies

Redox potentials of the polymers were recorded using a BAS CV50W voltammetric analyzer. Figure 5.12 shows the current-voltage curve for **TBPV1** and **TBPV2** from the cyclic voltammetry measurements. Polymers were dissolved in dichloromethane containing 0.1M tetra-*n*-butyl ammonium hexafluoro-phosphate as supporting electrolyte. A platinum disc electrode was used as working electrode and a platinum wire was used as counter electrode and the potentials were referred to Ag/AgCl (calibrated against the FC/FC⁺ redox system) was 4.8eV below vacuum levels. Ferrocene was used as external standard. The estimations were done with the empirical relation was used:³⁶

$$E_{HOMO} = (IP) \text{ eV} = -e (E_{ox, on} - E_{foc}) - 4.8$$

$$E_{LUMO} = (EA) \text{ eV} = -e (E_{re, on} - E_{foc}) - 4.8$$

The *p-doping* and *n-doping* processes occur under the anodic and cathodic scans. Electrochemical data of **TBPV1** and **TBPV2** are displayed in Table 3. On sweeping **TBPV1** and **TBPV2** in anodic direction, onset oxidation potentials ($E_{\text{ox,on}}$) are 0.52V for **TBPV1**, 0.50V for **TBPV2** or in cathodic direction, onset reduction potentials ($E_{\text{re,on}}$) are -1.49V for **TBPV1**, -1.72V for **TBPV2** respectively. On the base of the measured oxidation potentials, HOMO (IP) levels of **TBPV1** and **TBPV2** have been estimated to be -4.869eV, -4.844eV. Similarly, the LUMO (EA) levels of **TBPV1** and **TBPV2** have been calculated to be -2.841eV, -2.619eV, respectively. From the equation $E_{\text{g}}^{\text{EC}} = e(E_{\text{ox,on}} - E_{\text{re,on}})$ the electrochemical band gaps were also calculated to be 2.21eV and 2.22eV for **TBPV1** and **TBPV2**. The positional difference of the 2,2' or 4,4' linked long octyloxy side chain substitution is the main reason for the small difference of band gap energies of the two polymers. Ding et al have reported that, alkoxy-substituted biphenyl compounds have band gap above 2.91eV.³⁷ The band-gap of **TBPV1** and **TBPV2** was engineered to the green region by the incorporating thienylene units into the biphenylenevinylene backbone. The optical band gap and electrochemical band gap calculated from the HOMO and LUMO are within the range of 0.2-0.5 eV.³⁸

Copolymer	$E_{\text{ox, on}}$ (V)	$E_{\text{re, on}}$ (V)	HOMO (eV)	LUMO (eV)	E_{g}^{EC} (eV)
TBPV1	0.52	-1.49	-4.86	-2.84	2.21
TBPV2	0.50	-1.72	-4.84	-2.61	2.22

Table 5.3 Electrochemical data of **TBPV1** and **TBPV2**

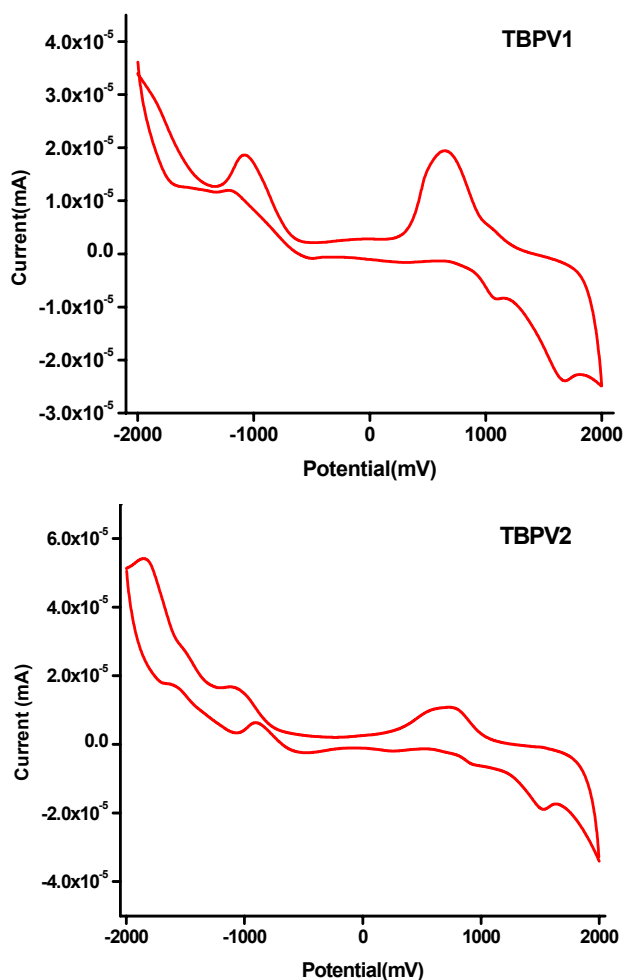


Figure 5.12 Cyclic voltammograms of **TBPV1** and **TBPV2** with solution of 0.1M tetra-*n*-butyl ammonium hexafluoro-phosphate as supporting electrolyte in dichloromethane at the scan rate of 10mV/s

*5.2.8 Measurement of Schottky diode characteristics

Schottky diode (metal-semiconductor) junction has been constructed from currently synthesized polymers **TBPV1** and **TBPV2**.³⁹ The device fabrication is simple because of direct casting of the polymers from the dichloromethane solution. Figure 5.13 shows three dimensional atomic Force Microscopy (AFM) image of the spin coated film of polymers **TBPV1** and **TBPV2** from

* The device fabrication and related characterizations are carried out in collaboration with Department of Physics, Cochin University of Science and Technology

dichloromethane solution.³⁹ The thickness of the films thus obtained was measured using Dektak 6M stylus profilometer and films with thickness 50nm (± 5 nm). AFM analysis reveals that polymers have smooth surface with the root mean square (RMS) value of **TBPV1** gives 1.53nm and **TBPV2** gives 1.80nm.

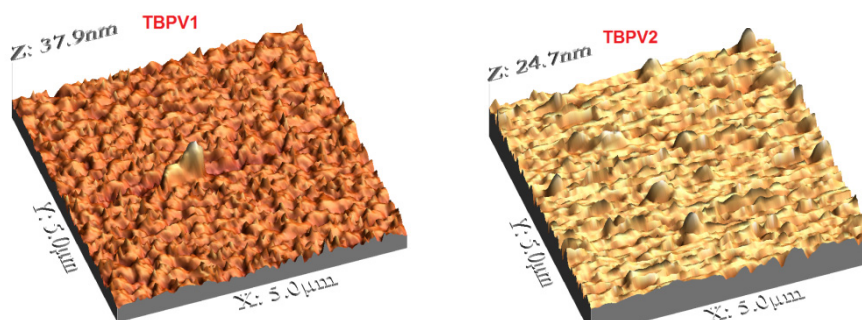


Figure 5.13 Three dimensional atomic force microscopy image of the spin coated film of **TBPV1** and **TBPV2**

Thin films of **TBPV1** and **TBPV2** made from dichloromethane were spin cast (SPS Spin wafer 150, 2000 rpm, 30s) from solutions on top of Indium Tin Oxide coated glass plates which is the anode. Aluminium contacts (top-electrode as cathode) were made on top of the spin coated polymer layers by thermal evaporation to form a Schottky junction. The current-voltage characteristics were analyzed using Keithley 2400 source meter (2-point probe method) for the two diode configurations to confirm the formation of metal-semiconductor junction which is mandatory for the fabrication of polymer light emitting diodes (PLEDs) as well as polymer photovoltaic devices. Figure 5.14 shows the Current Vs Voltage graph of **TBPV1** and **TBPV2** polymers respectively. From the two graphs, one can easily confirm that the polymers **TBPV1** and **TBPV2** show the formation of schottky diode. Both of the polymers exhibit very low onset voltage i.e. **TBPV1** shows 1.93V and **TBPV2** gives 2.38V. This indicates that **TBPV1** and **TBPV2** are very attractive for polymer light emitting diode applications.

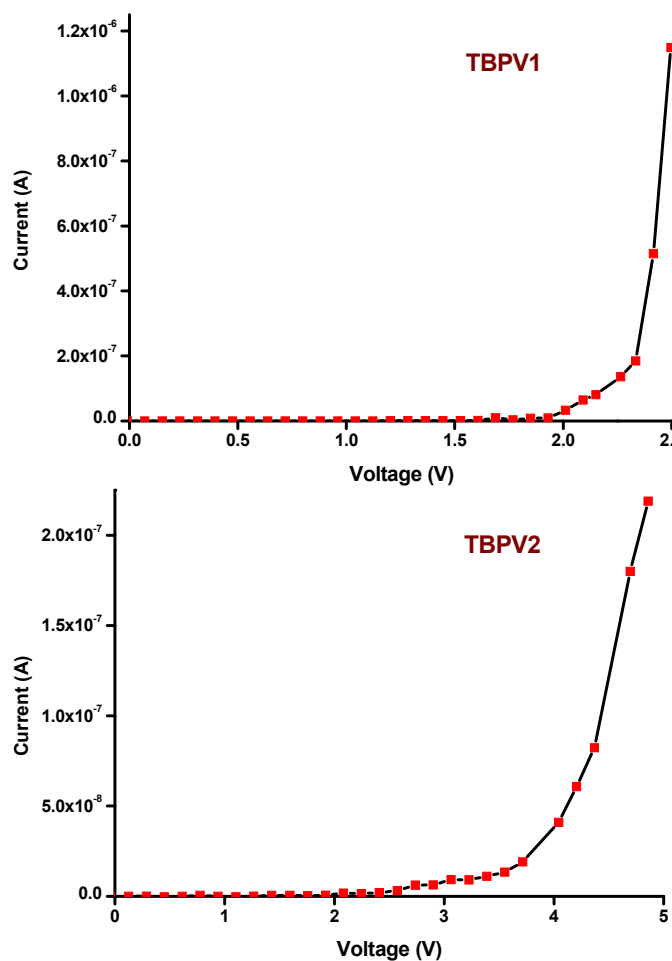


Figure 5.14 I-V characteristics of ITO /polymer/Al devices of **TBPV1** and **TBPV2**

The energy band diagrams of ITO/polymer/Al device configuration by using **TBPV1** and **TBPV2** are shown in Figure 5.15. The barrier heights of the polymers were found to be 0.16eV and 0.14eV at the interface of ITO (4.7eV)/HOMO state for holes and 1.35eV and 1.58eV at the interface of Al (4.2eV)/LUMO for electrons. The HOMO level of both polymers is very close to the work function of ITO which enables the effective supply of holes through ITO. Hence an intermediate layer between the emissive polymer and ITO can also be avoided. From the energy band diagram, one can assume that both polymers easily injected holes from the ITO electrode than of electron from the Al electrode. We can conclude that the required energy levels, excellent film

smoothness, high thermal stability of these two polymers are fulfilled for fabricating polymer light emitting diodes.

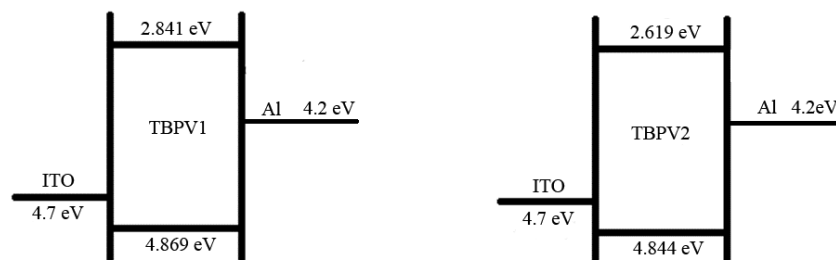


Figure 5.15 Energy band diagram of **TBPV1** and **TBPV2**

5.3 Conclusions

Two novel, highly soluble, thermally stable, highly luminescent, intense green-light emitting thienylene-biphenylenevinylene hybrid polymers synthesized using Stille coupling polymerization reaction. The Stille coupling reaction is superior to the conventional cross-coupling reactions like Suzuki and Kumada polycondensation reactions because of its simpler reaction conditions. The introduction of thienylene groups to the biphenylenevinylene backbone alters the emission spectrum of the polymers from lower wavelength region to higher wavelength region. Changing the substituent positions of the long chain octyloxy groups attached to the polymer backbone leads to some structural changes in both of the polymers. **TBPV1** is structurally more planar compared to **TBPV2** due to its 4,4' linkage of the substituent groups present in the biphenylenevinylene backbone. Photophysical studies confirm that both polymers give intense green emission in their solution state. Both polymers show excellent fluorescence quantum yield (Φ_F) in dichloromethane solution. The polymers show π -stacked structure in their solid state, which was confirmed by XRD analysis. The electrochemical band gap (E_g^{EC}) of the polymers analyzed by cyclic voltammetry analysis. Schottky diode formation has been confirmed from the I-V characteristics of the two polymers. Both of the hybrid polymers find prospects of application in the field of optoelectronics, mainly for Polymer LEDs.

5.4 Experimental Section

5.4.1 General Techniques

All reactions were performed in oven-dried glassware under a nitrogen atmosphere with magnetic stirring unless otherwise noted. Reagents and solvents were purchased from commercial suppliers and were used without further purification. Solvents used for experiments were distilled and dried according to procedures given in standard manuals. For all palladium-catalyzed reactions, the solvents were carefully degassed. All reactions were followed by TLC to completion. TLC analysis was performed by illumination with a UV lamp (254nm) or staining with Iodine. All Column chromatography was performed with 60-120 mesh silica gel purchased from SD Fine-Chem. limited, as the stationary phase. ¹H NMR spectra were measured on a Bruker Avance III 400 MHz instrument in CDCl₃, and chemical shifts were measured relative to residual solvent peak (δ 7.26). The following abbreviations were used to describe coupling: s = singlet, d = doublet, t = triplet, q = quartet, m = multiplet. ¹³C NMR spectra were measured on Bruker Avance III instruments at 100MHz with chemical shifts relative to residual solvent peak (δ 77.0). FTIR spectra were recorded using KBr pellet technique on a Thermo Nicolet, Avatar 370spectrometer. Melting points were recorded on a Fisher-Johns melting point apparatus. The percentage of elements C, H, S was analyzed by Elementar Vario EL III analyzer. The absorption and fluorescence spectra were recorded using UV-Visible spectrophotometer (JASCO V-570) and fluoromax-3fluorimeter was used to record the fluorescence spectra of the samples, respectively. The electrochemical cyclic voltammetry (CV) was conducted on a BAS CV50W voltammetric analyzer. Polymers were dissolved in dichloromethane containing 0.1M tetra-n- butyl ammonium hexafluoro-phosphate as supporting electrolyte, at a scanning rate of 10 mV/s at room temperature under the protection of argon. The Powder X-ray diffraction (XRD) patterns were obtained using a (Rigaku X-ray diffractometer with Cu K α radiation (1.542Å). The molecular weight of the

synthesized polymers was determined by GPC, (Waters 2414) using a column packed with polystyrene gel beads. The polymer was analyzed using toluene as eluent, at a flow rate of 0.5 mL/min at 25⁰C. The molecular weight was calibrated using polystyrene standards. Glass transition temperature was determined from differential scanning calorimeter (DSC), (Q-100, TA Instruments) under nitrogen at heating rate of 10⁰C/min. Thermal stability was determined from thermo gravimetric analyzer (TGA), (Q-50, TA Instruments) under nitrogen at a heating rate of 10⁰C/min. Homogeneous and good quality thin films in nanometer thickness scales were obtained by spin coating (SPS Spin wafer 150) the solution at different spin speeds in different durations on ultra-sonically cleaned glass substrates. The thickness of the films was measured using Dektak 6M stylus profiler. The morphology of the polymers was determined by scanning electron microscopy Scanning Electron Microscopy (SEM) (Hitachi FESEM SU6600). Atomic force microscopy image of copolymer film was analyzed by Park systems XEI 100 AFM. The current-voltage characteristics were analyzed using Keithley 2400 source meter (2-point probe method).

5.4.2 Materials

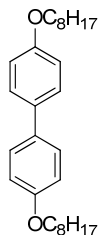
Compounds such as 4,4'-dihydroxy-1,1'-biphenyl, 1-bromooctane, Pd(PPh)₃, 2,5-bis(tributylstannyl)thiophene, 2,2'-dihydroxy-1,1'-biphenyl, and 5-bromothiophene-2-carboxaldehyde, were purchased from Sigma-Aldrich and used as received. HBr (31%) in glacial acetic acid, triethylphosphite and potassium *tert*-butoxide were purchased from Merck. Solvents were distilled and used in the reaction. Toluene used in the Stille coupling polymerization was dried using calcium chloride followed by distillation over sodium wire.

5.4.3 Synthesis of monomers M1 and M2

5.4.3.1: Synthesis of 4,4'-Dioctyloxy -1,1'-biphenyl (1a)

To a solution of 4,4'-dihydroxy-1,1'-biphenyl (2g, 10mmol) in 25mL of dry acetone was added anhydrous potassium carbonate (6g, 43mmol), 1-

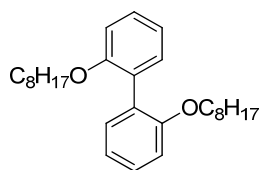
bromooctane (5mL, 25mmol), and a catalytic amount of sodium iodide. The mixture was refluxed for 48h under nitrogen atmosphere. The reaction mixture was poured into ice water. The product was filtered, washed with water, and dried. After recrystallization from acetone, product **1a** was obtained as white crystalline plates (yield: 90%).



¹H-NMR (400MHz, CDCl₃): δ 7.46-7.40 (4H, d), 6.95-6.92 (4H, d), 3.99-3.96 (4H, t), 1.81-1.77 (4H, t), 1.48- 1.29 (20H, m), 0.90 (6H, s).

5.4.3.2: Synthesis of 2,2'-Dioctyloxy-1,1'-biphenyl (2a)

To a solution of 2,2'-dihydroxy-1,1'-biphenyl (2g, 10mmol) in 50mL of dry acetonitrile was added anhydrous potassium carbonate (6g, 43mmol), 1-bromooctane (5mL, 25mmol), and a catalytic amount of sodium iodide. The mixture was refluxed for 72h under nitrogen atmosphere. The reaction mixture was cooled to room temperature and filtered. Solvent was evaporated under vacuum. The liquid product was purified by silica gel column chromatography (elution with hexane/dichloromethane). Compound **2a** was obtained as clear colourless oil. (Yield: 85%).

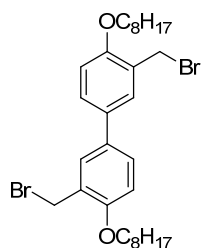


¹H-NMR (400MHz, CDCl₃): δ 7.32-7.28 (4H, m), 7.02-6.95 (4H, m), 3.94-3.91 (4H, t), 1.68-1.61 (4H, m), 1.32-1.26 (22H, m), 0.94-0.92 (6H, t).

5.4.3.3: Synthesis of 3,3'-bis(bromomethyl)-4,4'-di(octyloxy)-1,1'-biphenyl (1b)

To a suspension of 4,4'-dioctyloxy-1,1'-biphenyl (2g, 4mmol) and paraformaldehyde (0.5g, 15mmol) in 30mL of acetic acid was added 7mL of 31% HBr in glacial acetic acid in one portion at 80 °C under nitrogen atmosphere. The reaction mixture became clear immediately. The mixture was stirred for 4h at this temperature. It was then cooled to room temperature. The solid product was

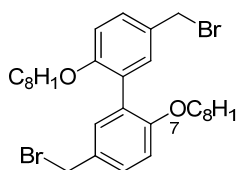
filtered and washed with water. The organic layer was taken in dichloromethane, neutralized with aqueous sodium bicarbonate solution, and dried. Solvent was evaporated and the residue recrystallized from acetone/hexane. The product was obtained as white crystals (yield: 80%).



$^1\text{H-NMR}$ (400MHz, CDCl_3): δ 7.50- 7.41 (4H, m), 6.91-6.89 (2H, d), 4.61 (4H, s), 4.06- 4.04 (4H, t), 1.87-1.81 (4H, m), 1.36-1.30 (20H, m), 0.92-0.82 (6H, t).

5.4.3.4: Synthesis of 5,5'-bis(bromomethyl)-2,2'-di(octyloxy)-1,1'-biphenyl (2b)

To a mixture of 4,4'-dioctyloxy-1,1'-biphenyl (3g, 7mmol) and paraformaldehyde (1g, 31mmol) in 30mL of acetic acid was added 7mL of 31% HBr in glacial acetic acid in one portion at 80 °C. The mixture was heated at this temperature for 4h under nitrogen atmosphere. It was then cooled to room temperature, and 100mL of cold water was added with constant stirring. The precipitate was filtered and washed with water. The solid was dissolved in dichloromethane, neutralized with aqueous sodium bicarbonate solution, and finally washed with brine. After drying over magnesium sulphate, solvent was evaporated from the organic layer. After recrystallization from dichloromethane, the product was obtained as a white solid (yield: 70%).

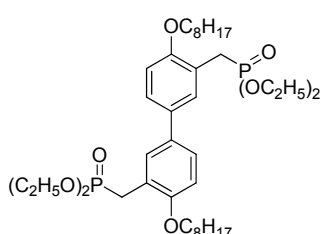


$^1\text{H-NMR}$ (400MHz, CDCl_3): δ 7.32-7.29 (4H, m), 6.89-6.86 (2H, d), 4.52 (4H, s), 3.91-3.88 (4H, t), 1.66-1.59 (4H, m), 1.27-1.22 (22H, t), 0.88-0.85 (6H, t).

5.4.3.5: Synthesis of 3,3'-bis(diethylphosphonate)-4,4'-di(octyloxy)-1,1'-biphenyl (1c)

A mixture of 3,3'-bis(bromomethyl)-4,4'-dioctyloxy-1,1'-biphenyl (1.0g, 1.68mmol) and triethylphosphite (1mL, 6mmol) was heated to 90°C for 2h under nitrogen atmosphere. Excess triethylphosphite was separated by vacuum

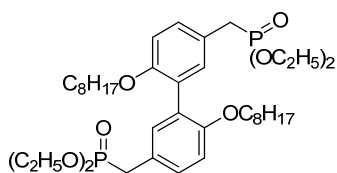
distillation. The product **1c** was obtained as thick oil (90%). It was used without further purification.



¹H-NMR (400MHz, CDCl₃): δ 7.53-7.36 (4H, m), 6.88-6.86 (2H, m), 4.13-3.97 (8H, m), 3.33-3.27 (4H, d), 1.83-1.7 (4H, t), 1.48-1.46 (4H, d), 1.34- 1.30 (m, 16H), 1.24-0.87 (12H, m).

5.4.3.6: Synthesis of 5,5'-bis(diethyl phosphonate)-2,2'-(dioctyloxy)-1,1'-biphenyl (**2c**)

A mixture of 5,5'-bis(bromomethyl)-2,2'-dioctyloxy-1,1'-biphenyl (3.0g, 5.75mmol) and triethylphosphate (12mL, 72mmol) was heated to 90°C for 2h under nitrogen atmosphere. Excess triethylphosphite was separated by vacuum distillation. The product **2c** was obtained as thick oil (82%). It was used without further purification.



¹H-NMR (400MHz, CDCl₃): δ 6.94-6.55 (6H, m), 3.84- 3.55 (12H, m), 2.83-2.77 (4H, m), 1.50-1.34 (20H, m), 1.26-1 (12H, m), 0.60-0.56 (6H, t).

5.4.3.7: Synthesis of monomer 5,5'-(1E,1'E)-2,2'-(4,4'-bis(octyloxy)biphenyl-3,3'-diyl)bis(ethene- 2,1- diyl)bis(2-bromothiophene) (**M1**)

To a stirred solution of **1c** (5.5g, 7mmol) in dry DMF (15mL) was added to 5-bromothiophene-2-carboxaldehyde (2.5g, 13mmol) at room temperature under nitrogen atmosphere. After stirring for 10 minutes, 3 eqv of powdered potassium *tert*-butoxide (2.35g, 21mmol) was added slowly. The reaction was carried out at 48h after which the resultant mixture was poured into water and extracted with dichloromethane. Solvent was evaporated under reduced pressure to obtain the product as yellow waxy liquid. It was further purified by column chromatography

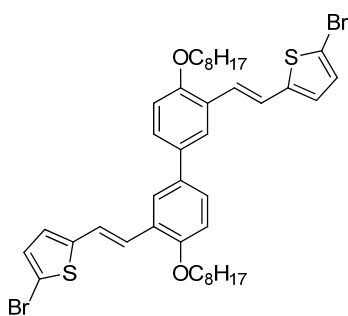
over silica gel using CH₂Cl₂ in hexane (1:19) as eluent. Solvent was evaporated to obtain the product as bright yellow crystals. Yield: 35%. mp: 65°C.

¹H-NMR (400MHz, CDCl₃): δ 7.64-6.70(14H, m), 4.07(4H, t), 1.89-1.85(2H, t), 1.33-1.25(19H, m), 0.89-0.85(9H, m).

¹³C-NMR (100MHz, CDCl₃): δ 154.8, 144.4, 132.3, 129.3, 126.1, 124.8, 124.8, 124.0, 123.2, 120.9, 111.4, 109.7, 67.7, 30.9, 30.8, 28.6, 28.2, 25.2, 21.6, 13.0;

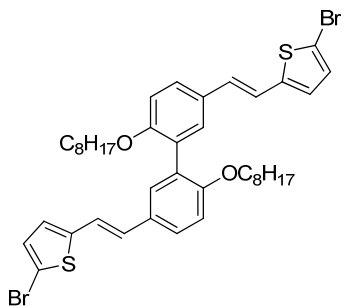
IR (KBr) ν 3028, 2920, 2949, 1603, 1519, 1427, 1376, 1304, 1236, 1127, 1062, 1004, 952, 832, 788, 715, 653, 614 cm⁻¹;

Anal. Calcd. For C₄₀H₄₈Br₂O₂S₂: C 61.22, H 6.17, Br 20.36, O 4.08, S 8.17; Found: C 60.88, S 7.69, H 6.10.



5.4.3.8: Synthesis of monomer 5,5'-(1E,1'E)-2,2'-(6,6'-bis(octyloxy)biphenyl-3,3'-diyl)bis(ethane-2,1-diyl)bis(2-bromothiophene)(M2)

To a stirred solution of **1c** (4g, 5mmol) in dry DMF (10mL) was added 5-bromothiophene-2-carboxaldehyde (2.2g, 11mmol) at room temperature under nitrogen atmosphere. After 10 minutes for stirring 3 eqv of powdered potassium *tert*-butoxide (1.68g, 15mmol) was added slowly. The reaction was carried out at 48h; the resultant mixture was poured into water, extracted with dichloromethane. The solvent was evaporated under reduced pressure to obtain the product as brown waxy liquid. It was further purified by column chromatography over silica gel using CH₂Cl₂ in hexane (1:19) as eluent. Solvent was evaporated to obtain the product as light brown crystals. Yield: 22%. mp: 85°C.



¹H-NMR (400MHz, CDCl₃): δ 7.39-6.71(14H, m), 3.93-3.90(4H, t), 1.63-1.60(3H, t), 1.25-1.19(16H, m), 0.86-0.85(5H, d).

¹³C-NMR (100MHz, CDCl₃): δ 155.6, 144.0, 129.3, 128.2, 127.6, 127.5, 127.2, 125.9, 124.2, 117.9, 111.1, 109.1, 67.5, 30.7, 28.3, 28.2, 28.2, 25.0, 21.6, 13.0;

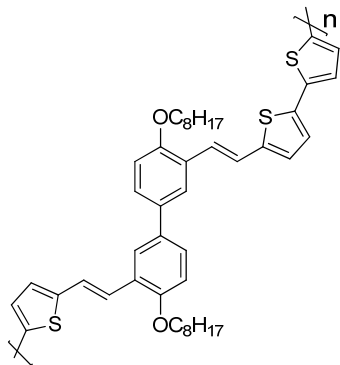
IR (KBr) ν 2952, 2922, 2848, 1604, 1468, 1432, 1385, 1259, 1150, 1051, 1014, 947, 806 cm⁻¹;

Anal. Calcd. For C₄₀H₄₈Br₂O₂S₂: C 61.22, H 6.17, Br 20.36, O 4.08, S 8.17; Found: C 60.12, S 7.21, H 5.81.

5.4.4 Synthesis of polymers Using Stille Coupling Reaction

5.4.4.1 Synthesis of polymer TBPV1

Pd(PPh)₃ (50mg, 0.043mmol), monomer **M1** (0.15g, 0.19mmol), and 2,5-bis(tributylstannyl)thiophene (0.12g, 0.18mmol) were taken in a three-necked flask. The mixture was flushed with nitrogen for 10min, and then 5mL of freshly distilled toluene was added. Under a positive pressure of nitrogen, the reactants were heated to reflux until the black metallic palladium precipitated. The mixture was then cooled to room temperature and poured into 50mL methanol and filtered into a thimble to remove metallic palladium. Sequential extraction was performed with methanol, hexane and THF. The polymer was recovered from the THF fraction by rotary evaporation. The resultant reddish brown solid was dried under vacuum over night. Yield: 0.22g (87%).



$^1\text{H-NMR}$ (400MHz, CDCl_3): δ 7.61-6.85(16H, m), 3.99-3.98(4H, d), 1.82-1.80(8H, d), 1.48-1.29(16H, m), 0.81(6H, s).

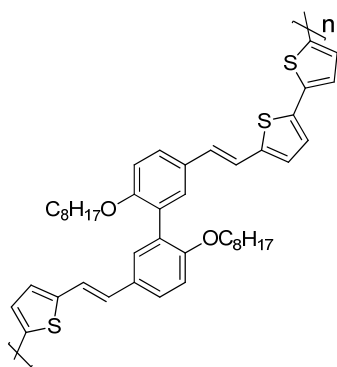
$^{13}\text{C-NMR}$ (100MHz, CDCl_3): δ 154.84, 142.86, 135.42, 132.42, 126.51, 125.89, 125.22, 124.65, 124.12, 123.26, 123.04, 122.83, 121.58, 121.37, 111.54, 67.80, 30.85, 28.43, 28.34, 25.30, 25.25, 21.69, 13.10.

IR (KBr) ν 2923, 2853, 1616, 1486, 1464, 1384, 1243, 1113, 1023, 954, 793, 692 cm^{-1}

Anal. Calcd. For $\text{C}_{44}\text{H}_{50}\text{O}_2\text{S}_3$: C 74.80, S 13.61, H 7.07; Found: C 73.44, S 13.24, H 6.37.

5.4.4.2 Synthesis of polymer TBPV2

$\text{Pd}(\text{PPh}_3)_3$ (50mg, 0.043mmol), monomer **M2** (0.3g, 0.38mmol), and 2,5-bis(tributylstannyl)thiophene (0.21g, 0.32mmol), were taken in a three-necked flask. The mixture was flushed with nitrogen for 10min, and then 5mL of freshly distilled toluene was added. Under nitrogen atmosphere, the reactants were heated to reflux until the black metallic palladium precipitated. The mixture was then cooled to room temperature and poured into 80mL methanol and filtered into a thimble to remove the metallic palladium. Sequential extraction was performed with methanol, hexane and THF. The polymer was recovered from the THF fraction by rotary evaporation. The resultant dark brown solid was dried under vacuum over night. Yield: 0.21g (77%).



¹H-NMR (400MHz, CDCl₃): δ 7.61-6.83(17H, m), 4.01-4.00(4H, m), 1.83-1.81(2H, d), 1.50-1.13(24H, m), 0.82-0.75(8H, m).

¹³C-NMR (100MHz, CDCl₃): δ 154.85, 126.85, 125.96, 125.20, 124.68, 124.13, 123.41, 123.23, 123.06, 122.51, 121.61, 121.44, 111.55, 111.24, 110.34, 67.81, 67.55, 30.85, 29.87, 28.43, 28.34, 28.27, 25.30, 25.05, 21.69, 13.09;

IR (KBr) ν 2924, 2853, 1599, 1550, 1487, 1465, 1383, 1244, 1119, 1022, 952, 793, 723, 692 cm⁻¹

Anal. Calcd. For C₄₄H₅₀O₂S₃ : C 74.80, S 13.61, H 7.07; Found: C 73.32, S 13.02, H 6.03.

5.5 References

1. Moliton, A.; Hiorns R. C. *Polym. Int.* **2004**, *53*, 1397.
2. Heeger, A. J. *Solid State Communications* **1998**, *107*, 673.
3. Friend, R. H.; Gymer, R. W.; Holmes, A. B.; Burroughes, J. H.; Marks, R. N.; Taliani, C.; Bradley, D. D. C.; Dos Santos, D. A.; Brédas, J. L.; Lögdlund, M.; Salaneck, W. R. *Nature* **1999**, *397*, 121.
4. Bernius, M. T.; Inbasekaran, M.; O'Brien, J.; Wu W. *Adv. Mater.* **2000**, *12*, 1737.
5. Amrutha, S. R.; Jayakannan, M. *J. Phys. Chem. B.* **2006**, *110*, 4083.
6. Wang, H.; Tao, X.; Newton, E. *Polym Int.* **2004**, *53*, 20.
7. Fahlman, M.; Lögdlund, M.; Stafström, S.; Salaneck, W. R.; Friend, R. H.; Burn, P. L.; Holmes, A. B.; Kaeriyama, K.; Sonoda, Y.; Lhost, O.; Meyers, F.; Brédas, J. L. *Macromolecules* **1995**, *28*, 1959.

8. Hwang, D. H.; Kang, I. N.; Jang, M. S.; Shim, H. K. *Bull. Korean Chem. Soc.* **1995**, *16*, 135.
9. Wan, W. C.; Antoniadis, H.; Choong, V. E.; Razafitrimo, H.; Gao, Y.; Feld, W. A.; Hsieh, B. R. *Macromolecules* **1997**, *30*, 6567.
10. Chang, C. P.; Wang, C. C.; Chao, C. Y.; Lin, M. S. *Journal of Polymer Research* **2005**, *12*, 1.
11. Choo, D. J.; Talaie, A.; Lee, Y. K.; Jang, J.; Park, S. H.; Huh, G.; Yoo, K. H.; Lee, J. Y. *Thin Solid Films* **2000**, *363*, 37.
12. Jeong, H. Y.; Lee, Y. K.; Talaie, A.; Kim, K. M.; Kwon, Y. D.; Jang, Y. R.; Yoo, K. H.; Choo, D. J.; Jang, J. *Thin Solid Films* **2002**, *417*, 171.
13. Wudl, F.; Sigurd, H. *United States Patent. 5679757*, **1997**.
14. Ahn, T.; Ko, S. W.; Lee, J.; Shim, H. K. *Macromolecules* **2002**, *35*, 3495.
15. Hohnholz, D.; Schweikart, K. H.; Subramanian, L. R.; Wedel, A.; Wischert, W.; Hanack, M. *Synthetic Metals* **2000**, *110*, 141.
16. Jin, Y. D.; Chen, H. Z.; Heremans, P. L.; Aleksandrak, K.; Geise, H. J.; Borghs, G.; Auweraer, V. *Synthetic Metals* **2002**, *127*, 155.
17. Sarker, A. M.; Ding, L.; Lahti, P. L.; Karasz, F. K. *Macromolecules* **2002**, *35*, 223.
18. Hou, J.; Yang, C.; Qiao, J.; Li, Y. *Synthetic Metals* **2005**, *150*, 297.
19. Egbe, D. A. M.; Roll, C. P.; Birckner, E.; Grummt, U. W.; Stockmann, R.; Klemm, E. *Macromolecules* **2002**, *35*, 3825.
20. Chu Q.; Pang Y.; Ding L.; Karasz F. E. *Macromolecules* **2003**, *36*, 3848.
21. Carsten, B.; He, F.; Son, H. J.; Xu, T.; Yu, L. *Chem. Rev.* **2011**, *111*, 1493.
22. Xia, Y.; Deng, X.; Wang, L.; Li, X.; Zhu, X.; Yong Cao, Y.; *Macromol. Rapid Commun.* **2006**, *27*, 1260.
23. Van der Made, A. W.; Van der Made, R. H. *J. Org. Chem.* **1993**, *58*, 1262.
24. Bhattacharya, A. K.; Thyagarajan, G. *Chem. Rev.* **1981**, *81*, 415.

25. Edmonds, M.; Abell, A. *Modern Carbonyl Olefination*, WILEY-VCH, Verlag, Weinheim, **2004**.
26. Hohnholz, D.; Wedel, A.; Hanack, M. *Synthetic Metals* **1999**, *101*, 626.
27. Huo, L.; Hou, J.; He, C.; Han, M.; Li, Y. *Synthetic Metals* **2006**, *156*, 276.
28. Gürel, E.E.; Pasco, S.T.; Karasz, F.E. *Polymer* **2000**, *41*, 6969.
29. Wu, S. H.; Chen, J. H.; Shen, C. H.; Hsu, C.C.; Tsiang, R. C. C. *J. Polym. Sci.: Part A: Polym. Chem.* **2004**, *42*, 6061.
30. Yamamoto, T.; Muramatsu, Y.; Lee, B. L.; Kokubo, H.; Sasaki, S.; Hasegawa, M.; Yagi, T.; Kubota, K. *Chem. Mater.* **2003**, *15*, 4384.
31. Resel, R.; Tertinek, B.; Tasch, S.; Davey, A.; Blau, W.; Hörhold, H. H.; Rost, H.; Leising, G. *Synthetic Metals* **1999**, *101*, 96.
32. Yamamoto, T.; Fang, Q.; Morikita, T. *Macromolecules* **2003**, *36*, 4262.
33. Li, Y.; Wu, Y.; Liu, P.; Birau, M.; Pan, H.; Ong, B.S. *Adv. Mater.* **2006**, *18*, 3029.
34. Williams, A. T. R.; Winfield, S. A.; Miller, J. N. *Analyst* **1983**, *108*, 1067.
35. Kellogg, R. E.; Bennett, R. G. *J. Chem. Phys.* **1964**, *41*, 3042.
36. Lu, C.; Wang, H.; Wang, X.; Li, Y.; Oiu, T.; He, L.; Li, X. *Journal of Applied Polymer Science* **2010**, *117*, 517.
37. Ding, X. B.; Zheng, J. G.; Jin, Y. D.; Aerts, G.; Peng, B. X.; Heremans, P. L.; Borghs, G.; Geise, H. J. *Synthetic Metals* **2004**, *142*, 267.
38. Zou, Y.; Liu, B.; Li, Y.; He, Y.; Zhou, K.; Pan, C. *J. Mater. Sci.* **2009**, *44*, 4174.
39. Sreekanth. J. Varma, *Ph D Thesis*, CUSAT, **2012**.

Chapter 6

Summary and Conclusion

Abstract

This chapter deals with the overall summary of the research work. The aim of the present work focuses the synthesis and characterization of new light emitting conjugated polymers based on poly(phenylenevinylene) and polythiophenes. Photophysical, electrochemical, thermal, structural and morphological properties of the synthesized polymers are also explained. The suitability of these polymers in the field of optoelectronic devices was also investigated.

In this work some of the light emitting conjugated polymers (LEPs) related to poly(phenylenevinylene)s and polythiophenes have been synthesized successfully. Three different categories of LEPs consisting of fully-conjugated PPV derivatives, segmented block PPV derivatives and light emitting hybrid polymers based on thienylene/biphenylenevinylene polymers were selected for studies. **MEH-PPV** was taken as the model material for fully conjugated PPV derivative. Three segmented block PPV derivatives (**P1**, **P2** & **P3**) were synthesized through Horner- Emmons condensation polymerization. Two novel green light emitting thienylene- biphenylenevinylene hybrid polymers (**TBPV1** & **TBPV2**) synthesized using Stille coupling reaction. The structure of the synthesized polymers was characterized by using different spectroscopic techniques such as ^1H NMR, ^{13}C NMR, FT-IR etc. All the synthesized six light emitting polymers are completely soluble in commonly used polar and non-polar organic solvents. Therefore synthesized polymers show excellent processability in both film state and solution state.

Foremost findings drawn from the thesis are,

- **Chapter 2** discusses synthesis, characterization and an amplified spontaneous emission (ASE) characteristic of MEH-PPV. Glich polymerization route used for the synthesis of MEH-PPV and purification

was done by sequential extraction method. Synthesized material has narrow molecular weight distribution and low molecular weight (below 60000). Therefore the material shows excellent fluorescent quantum yield in different organic solvents due to perfect structural regularity of the polymer. ASE studies disclose that laser emission characteristics strongly depend upon the concentration of the MEH-PPV solution.

- **Chapter 3** describes the synthesis and characterization of two segmented block PPV copolymers. These are long aliphatic chain (octyloxy) substituted Poly [1,6-hexanedioxy-(1,4-phenylene)-1,2ethenylene-(2,5-dioctyloxy-1,4phenylene)-1,2ethenylene-(1,4phenylene)] (**P1**) and rigid ring substituted Poly[1,6-hexanedioxy-(1,4phenylene)-1,2ethenylene-(2,5-dicyclohexylmethyloxy-1,4phenylene)-1,2ethenylene-(1,4phenylene)] (**P2**). The Horner-Emmons methodology gives relatively good yield and narrow polydispersities. Differential scanning calorimetric measurements and X-ray diffraction analysis enlighten the idea about the semicrystalline nature of the synthesized SBCs. Results show that structural modification alters the glass transition temperature and thermal stability of the copolymers. Therefore **P2** shows higher T_g than **P1**; polymers having higher T_g values are inevitable in optoelectronic device fabrications. Due to structural dissimilarities, both copolymers show different morphologies in their SEM pictures. Photoluminescence studies reveal that **P1** gives blue light emission and **P2** gives bluish-green emission. The emission characteristics also confirm the effective structural modifications were done in these copolymers. These copolymers show excellent fluorescence quantum yield (Φ_F) comparable to coumarin-481 dye. Cyclic voltammetry analysis gives the idea about the redox potentials of the copolymers. Simple Schottky diode device was fabricated consisting of ITO as anode Al as cathode. ITO/copolymer/Al sandwiched device shows well defined diode characteristics. Overall results consist of excellent solubility, semicrystalline nature, good thermal stability, high purity, low

polydispersity index, high fluorescence quantum yield, excellent film forming capacity and finally I-V characteristics of copolymers **P1** & **P2** confirms the suitability of these copolymers in the field of polymer based LEDs.

- **Chapter 4** explain the synthesis and optical studies of a new type of SBC. Based on **P2** core, another blue light emitting new segmented block copolymer poly[1,6-hexanedioxy-(2,6-dimethoxy-1,4-phenylene)-1,2-ethenylene-(2,5-dicyclohexylmethoxy-1,4-phenylene)-1,2ethenylene-(3,5-dimethoxy-1,4phenylene)] [**P3**] was synthesized by using Horner-Emmons reaction and characterized. We retained the basic structure of **P2** in tact while introducing electron releasing methoxy groups to fine tune photophysical and electrochemical properties. Due to the introduction of methoxy groups into the polymeric backbone helps to improvise the solubility of this copolymer. Like **P1** and **P2**, **P3** shows good solubility, high thermal stability, low molecular weight distribution, semicrystalline nature etc are same as **P1** & **P2**. Photophysical studies and schottky diode action from I-V data confirmed the suitability of **P3** as a good candidate for fabricating PLEDs.
- Hybrid light emitting polymer derivatives are rare in the field of light emitting polymers. **Chapter 5** describe the synthesis and characterization of novel class of intense green light emitting thienylene-biphenylenevinylene hybrid polymers (**TBPV1** and **TBPV2**) using Stille coupling polymerization. Stille coupling polymerization is commonly used for synthesizing highly luminescent thiophene related polymers, having superior characteristics. A new class of monomers **M1** & **M2** were synthesized using Wittig- Horner reaction. These two monomers show blue light emission. Two hybrid polymers contain thienylene and biphenylenevinylene combination gives excellent thermal stability, high solubility, good film forming property and low molecular weight distribution. Biphenylenevinylene backbone was structurally modified

with thienylene units leads to alter the emission characteristics of the synthesized polymers. Photoluminescence studies show that both polymers give excellent green light emission. The comparative fluorescence quantum yield (Φ_F) studies show that fluorescence quantum yield of **TBPV1** has higher than **TBPV2** apparently due to steric strain inducing 2,2'-substitution on the biphenylene unit present in its polymer backbone. Electrochemical studies give the HOMO- LUMO values of these hybrids. Optical band gap and electrochemical band gap are almost comparable in both of the polymers. Schottky diode formation has been confirmed from the I-V characteristics of the two hybrid polymers. All the above mentioned characteristics of the hybrid polymers demonstrated that these new polymers can be used for the fabrication of light emitting polymer based devices such as PLEDs, photovoltaic cells etc.

- In collaboration with the Department of Physics, Cochin University of Science and Technology, we demonstrated LED activity of a few polymers such as **P1**, **P2**, **P3**, **TBPV1** and **TBPV2**. Details of device fabrication and demonstration of LED activity is available elsewhere.¹

Our overall research findings show that there exist plentiful scope for the synthesis and structural modification of light emitting polymers to improve their processability and optoelectronic properties.

References

1. Sreekanth. J. Varma. *Ph.D Thesis*, CUSAT, **2012**.

Publications

- “Novel, highly Soluble, intense green light emitting hybrid thienylene-biphenylenevinylene polymers: synthesis, characterization, molecular assembly and photophysical studies” **Vidya.G**, Sreekanth J. Varma, S. Prathapan, S. Jayalekshmi and Rani Joseph, *under preparation*.
- “Substituent effects on light-emitting segmented block PPV copolymers: synthesis, characterization and photophysical studies” **Vidya. G**, Sreekanth J. Varma, S. Prathapan, S. Jayalekshmi and Rani Joseph, *under preparation*.
- “Synthesis and characterization of new intense blue-light emitting ring substituted- semicrystalline segmented PPV block copolymer” **Vidya. G**, Sreekanth J. Varma, S. Prathapan, S. Jayalekshmi and Rani Joseph, *under preparation*.
- “Laser resonant modes from MEH-PPV dissolved in tetrahydrofuran.” Sreelekha, G.; **Vidya, G.**; Geetha, K.; Joseph, R.; Prathapan, S.; Radhakrishnan, P.; Vallabhan, C. P. G.; Nampoori, V. P. N. *International Journal of Photonics* 2011, 3, 31.
- “Characteristics of Dual Amplified Spontaneous Emission from MEH-PPV solutions” G.Sreelekha, **G. Vidya**, K. Geetha, Rani Joseph ,S. Prathapan , P. Radhakrishnan , C.P.G. Vallabhan and V.P.N. Nampoori, *Accepted in International journal of Optics and Photonics*.
- “Evaluation of absolute fluorescence quantum yield of MEH-PPV using laser induced thermal lens technique” G.Sreelekha, **G. Vidya**, Rani Joseph, S. Prathapan , P. Radhakrishnan, C.P.G. Vallabhan and V.P.N. Nampoori, *Accepted in Asian journal of Spectroscopy*.

Publications in Conferences

- **G.Vidya**, G.Sreelekha, S. Prathapan, V. P. N. Nampoori, C.P.G.Vallabhan, Rani Joseph, International Conference on Advances in Polymer Technology, APT'10, Feb 26-27, 2010, Cochin. India. "Synthesis and photo physical investigations of Poly [2-methoxy-5-(2'-ethyl-hexyloxy) -1, 4-phenylenevinylene] (MEH-PPV)"
- **G.Vidya**, G.Sreelekha, S. Prathapan, V. P. N. Nampoori, C.P.G.Vallabhan, Rani Joseph, International Conference on Advancements in Polymeric Materials, APM'11, March 25-27, 2011, CIPET, Chennai, India. "Synthesis and Characterization of Two Novel Thiophene-Phenylenevinylene Hybrid Monomers".
- "Photoluminescence of MEH-PPV/PS based planar waveguide structure" G.Sreelekha, **G. Vidya**, K. Geetha, M.S. Ebin, Rani Joseph ,S. Prathapan, P. Radhakrishnan ,C.P.G. Vallabhan and V.P.N. Nampoori ,International Conference on Recent Trends in Materials Science and Technology(ICMST) October 29-31, 2010 at Thiruvananthapuram, Kerala.
- "Two photon fluorescence spectra of MEH-PPV/PS blend films under femtosecond irradiation" M S Ebin, G Sreelekha, S Sreeja, P Radhakrishnan, V P N Nampoori ,C P G Vallabhan ,K Geetha ,**G Vidya**, Rani Joseph and S Prathapan, International Conference on Recent Trends in Materials Science and Technology (ICMST) October 29-31, 2010 at Thiruvananthapuram.
- "Laser emission from MEH-PPV/PS based planar waveguide structure" G.Sreelekha, **G. Vidya**, M.S. Ebin, K. Geetha, Rani Joseph ,S. Prathapan , P. Radhakrishnan ,C.P.G. Vallabhan and V.P.N. Nampoori. International Conference on Fiber Optics and Photonics 2010 at Indian Institute of Technology, Guwahati, during December 11-15, 2010.
- "Thickness effects on the fluorescence spectra of MEH:PPV/PMMA thin film waveguides" Geetha K, Sreelekha G, **Vidya G**, Rani Joseph, C P G

Vallabhan, P Radhakrishnan and V.P.N Nampoori EIGHTH DAE-BRNS NATIONAL LASER SYMPOSIUM- NLS-08 , January 7-10, 2009

- “Dual wavelength Amplified Spontaneous Emission from MEH-PPV” G. Sreelekha, **G. Vidya**, K. Geetha, P. Radhakrishnan, Rani Joseph, S. Prathapan ,C.P.G. Vallabhan and V.P.N. Nampoori Nineth DAE-BRNS National Laser Symposium 13th-16th January, 2010 Organized at BARC, Mumbai
- “Multimode emission from MEH-PPV dissolved in tetrahydrofuran” G.Sreelekha, **G. Vidya** ,K. Geetha, P. Radhakrishnan , Rani Joseph, S. Prathapan ,C.P.G. Vallabhan and V.P.N. Nampoori "DAE-BRNS National Laser Symposium" at RRCAT, Indore from Dec.1-4, 2010
- “Measurement of the absolute fluorescence quantum yield of MEH-PPV solution using a dual-beam thermal lens technique” G.Sreelekha, **G. Vidya**, A. Santhi, K. Geetha, Rani Joseph ,S. Prathapan , P. Radhakrishnan, C.P.G. Vallabhan and V.P.N. Nampoori, Kerala Women’s Science Congress 2010, at St. Teresa’s College, Ernakulam on August 10- 12, 2010

